FIBROBLAST GROWTH FACTOR SIGNALING IN PROSTATE STEM CELLS AND PROSTATE CANCER

A Dissertation

by

YANQING HUANG

Submitted to the Office of Graduate and Professional Studies of
Texas A&M University
in partial fulfillment of the requirements for the degree of

DOCTOR OF PHILOSOPHY

Chair of Committee,	Fen Wang
Co-Chair of Committee,	Wallace L. McKeehan
Committee Members,	Nora M. Navone
	David R. Rowley
	Michael M. Ittmann
Head of Department,	Fen Wang

August 2015

Major Subject: Medical Sciences

ABSTRACT

The prostate is an androgen-dependent male reproductive organ that is comprised of epithelial and stromal compartments. The epithelial compartment contains basal, luminal, and neuroendocrine cells. Two types of prostate epithelial stem cells (P-SCs), basal stem cells and luminal stem cells, have been identified in both human and mouse adult prostates based on tissue recombination models, cell lineage tracing, and *in vitro* prostasphere or organoid cultures. Using lineage-tracing with *P63*^{CreERT2} and prostasphere culture, we show here that the sphere-forming P-SCs are P63-expressing cells and reside in the basal compartment. Therefore we designate them as basal P-SCs (P-bSCs). P-bSCs are capable of differentiating into AR^{+} and CK18^{+} organoid cells, but not vice versa. We also report that prostaspheres contain quiescent stem cells, which possess more potent self-renewal capacity. Distinct from other tissue stem cells, P-bSCs do not contain Lgr5^{+} cells.

The fibroblast growth factor signaling axis regulates embryonic stem cell development as well as tissue specific stem cell maintenance and differentiation. However, the role of FGF signaling in P-SC self-renewal and differentiation is still elusive. We show that the type 2 FGF receptor (FGFR2) signaling axis is crucial for preserving self-renewal and preventing the differentiation of P-bSCs. FGFR2 signaling mediated by FGFR substrate 2α (FRS2α) is indispensable for formation and maintenance of prostaspheres derived from P63^{+} P-bSCs.

Ablation of *Fgfr2 in vivo* reduces P63-expressing basal cells, and promotes basal-to-luminal differentiation. In addition, ablation of *Fgfr2* in $P63^{+}$ cells disrupts postnatal development of the prostate.

Accumulating evidence has also shown that prostate cancer (PCa) progression is frequently associated with dysregulation of FGF signaling. Herein, we report that forced expression of FGF9 in prostate epithelial cells leads to high grade prostatic intraepithelial neoplasia (PIN). Overexpression of FGF9 in TRAMP mice induces more malignant PCa and higher frequency of metastasis. Hyperproliferative stromal cells are shown in the F9TG and F9TRAMP mouse prostates. Reactive stroma which upregulates TGF-β1, was observed in F9TG and F9TRAMP prostates. We also show that transcription factor c-Jun is a mediator in the FGF9-TGFβ1 axis.

Collectively, our study provides new insights into prostate stem cells and prostate cancer. Upset of the intricate balance of FGF signaling in the prostate disrupts stem cell homeostastasis and prostate development, and initiates prostate tumorigenesis.

ACKNOWLEDGEMENTS

Appreciation and deepest gratitude goes to the following persons who in one way or another have made this study possible.

Dr. Fen Wang gave me the opportunity to conduct my research in his lab. Thanks for his continuous support and guidance throughout the last seven years. He offered me freedom and responsibility for executing the work and trained me to think independently, which will be my greatest assets in my future academic pursuit.

Dr. Wallace McKeehan posed intriguing and incisive questions, which made me to think deeper in a wider scope. He also urged me to put myself out there and speak confidently in public.

Dr. Nora Navone offered generous advice and suggestions. The collaboration between our two labs broadened my perspective in prostate cancer bone metastasis.

Dr. David Rowley gave me insightful advice on reactive stroma. He also generously shared HPS-19I human prostate stromal cells.

Dr. Michael Ittmann's questions always made to think beyond my own research and prompted me to be more knowledgeable about prostate research in general.

Dr. Stefan Siwko helped me with the proofreading of my manuscripts and other writings. He offered informative, interesting and inspiring advice

Alon Arezon helped me with FACS cell sorting and data analysis. Dr. Chengliu Jin generated FGF9 transgenic mice; Dr. Michael Shen shared the *Nkx3.1*^{cre} knock-in mice; Dr. Jianming Xu shared the *P63*^{CreERT2} knock-in mice; Dr. Juha Patanen shared the *Fgfr1*^{floxed} mice; Dr. David Ornitz shared the *Fgfr2*^{floxed} mice; Dr. Elaine Fuchs shared the *K5*$^{H2B/GFP}$ mice; Dr. Hans Clevers shared the *Lgr5*$^{EGFP\text{-}CreERT2}$ mice.

I thank my family for their long-time support and unconditional love. Special thanks goes to my best friend and my favorite person Corey Paulson.

Thanks go to my friends and colleagues, Junchen Liu, Lei An, Yi Liang, Jia Zeng, Li Zeng, Fei Yue, Wenjiao Li, Xiaojing Yue, Ji Jing, Haiyi Wang, Xianglai Xu, Yongshun Lin, Yongyou Zhang, Jue Zhang, Julia Chang, Xiang Lin, Cong Wang, Pan You, Tomoaki Hamana, Xiangfeng Zeng, Doug Huynh, Jean Tien, Xiao Li, and Jonathian Few.

Funding support: This work was supported by the NIH CA96824, DE023106, TAMU1400302, and CPRIT 110555 to FW, CA140388 to WLM, the Natural Science Foundation of Zhejiang Province of China Y2110492, and the National Natural Science Foundation of China 81101712, 31371470, and 81270761 to CW.

TABLE OF CONTENTS

Page

LIST OF FIGURES

Page

CHAPTER I

INTRODUCTION

The prostate is a compound tubuloalveolar exocrine gland of the male reproductive system whose secretion constitutes roughly 30% of the volume of the semen. The human male prostate surrounds the urethra below the urinary bladder. Human prostate is an acorn-shaped organ that can be divided into three histologically distinct regions: the peripheral zone (PZ), central zone (CZ), and transition zone (TZ)(1) . Around 70-80% of prostatic cancers originate from the peripheral zone, while benign prostatic hyperplasia (BPH) occurs mainly in the transition zone (2,3). Unlike the human prostate, the mouse prostate consists of four different pairs of lobes, designated as the anterior lobes (AP), dorsal lobes (DP), lateral lobes (LP), and ventral lobes (VP). The dorsal and lateral lobes are frequently referred to the dorsolateral lobes (DLP). These lobes are arranged circumferentially around the urethra (4).

In spite of the anatomical distinctions, both the human and mouse prostates exhibit similar glandular morphology and are composed of epithelial and stromal compartments separated by basement membranes. Both the human and mouse prostates contain three epithelial cell types. The majority of the epithelial cells is luminal cells, which are column-shaped secretory cells. Between the luminal cells and the underlying basement membrane are spindle-shaped basal cells and rare neuroendocrine cells with unidentified function. The luminal cells are

characterized by expression of the androgen receptor (AR), cytokeratin 8 and 18, Nkx3.1, and prostate specific antigen (PSA) in human prostates. Basal cells are characterized by the expression of p63, cytokeratin 5, and cytokeratin 14. Neuroendocrine cells can be specified by the expression of synaptophysin and chromogranin A.

The histological difference between human and mouse prostates lies in the stromal cell density. In mouse prostates, stromal cells have almost the same cell number as epithelial cells, while in human prostates, stromal to epithelial cell ratio is around 5:1. Both the mouse and the human prostate stroma is largely composed of smooth muscle cells (SMC), fibroblasts, extracellular matrix, blood vessels, nerves, and immune cells. The SMC cells, which express α-smooth muscle actin, tightly adheres to basement membrane and surround the luminal epithelial cells. Adult prostate stroma normally consists mainly of smooth muscle cells. SMC cells number is considerably reduced and replaced by fibroblasts and become less differentiated during progression to malignancy (5). The fibroblast and other stromal cells are loosely associated with epithelial cells and dispersed within the stromal matrix. During wound healing and in the reactive stroma, both SMC and fibroblast undergo extensive phenotypical switch, which will be discussed in Chapter IV.

The mouse prostate development starts at embryonic day 17 (E17) when the urogenital sinus epithelial cells (UGE) grow into surrounding urogenital sinus mesenchyme (UGM) in anterior, ventral, dorsal, and lateral directions, which

subsequently form the four prostate lobes, respectively. This process requires interactions between UGE and UGM. Androgen receptor (AR) positive cells in the stroma regulate epithelial cell growth, death and differentiation via stroma-produced “andromedins”, which includes fibroblast growth factor (FGF), insulin-like growth factor (IGF), epidermal growth factor (EGF), Wnt and hepatocyte growth factor (HGF). In the classic *in vivo* recombination assay, isolated single epithelial cells are combined with rat UGM and grafted under the renal capsule. UGM is informative in directing the growth and differentiation of epithelial cells.

Prostate development and tissue homeostasis are both finely regulated process. It is believed that stem cells sit at the top of the lineage hierarchy of the cellular organization. Stem cells contribute to all cell lineages of the prostate and maintain homeostasis. Evidence also supports the hypothesis that prostate cancer arises from malignant transformation of stem cells. Stem cells acquire epigenetic modifications and genetic mutations through exposure to insults, resulting in the dysregulation of normal stem cell functions and even worse outcome: cancer (6,7). Therefore, to understand the cellular composition of the prostate stem cells provide insights into the cells of origin for cancer. To identify the signaling pathways that regulate stem cell functions may lead to effective therapies for prostate cancer treatment.

Prostate cancer is the most common cancer in American men other than skin cancer, and second leading cause of cancer death only after lung cancer. The American Cancer Society’s estimates for prostate cancer in the United States for

2015 are about 220,800 new cases of prostate cancer and 27,540 deaths from prostate cancer. About 1 man in 7 will be diagnosed with prostate cancer during his lifetime, and around 1 man in 38 will die of prostate cancer.

As described, there are three histologically distinct regions in the human prostate: the peripheral zone (PZ), central zone (CZ), and transition zone (TZ). Benign prostatic hyperplasia (BPH), a non-cancerous overgrowth in aging men, occurs mainly in the transition zone, while prostate cancer arises primarily in the peripheral zone. >95% of prostate cancers are classified pathologically as adenocarcinoma, while the other rare types include sarcomas, small cell carcinomas, neuroendocrine tumors (other than small cell carcinomas), and transitional cell carcinomas.

Histopathological studies of prostate cancer tissue have suggested that prostate cancer starts out as a pre-cancerous condition, although this is not certain yet. Two types of pre-malignant lesions were shown, proliferative inflammatory atrophy (PIA), and prostatic intraepithelial neoplasia (PIN). PIA belongs to the atrophic lesions that is common in the prostate. It has been shown that the location of PIA in the periphery of the gland is close to prostate carcinoma, and is capable of directly transforming to malignant or pre-malignant epithelia (8). PIN is recognized as a continuum between low-grade (LGPIN) and high-grade (HGPIN) form. While HGPIN is considered to be precancerous lesions of the prostate, most cases of LGPIN do not progress, thus it has different clinical outcomes than does HGPIN. HGPIN is generally characterized by the

appearance of luminal epithelial hyperplasia, reduction in basal cells, enlargement of nuclei, cytoplasmic hyperchromasia, and nuclear atypia. HGPIN is thought to represent the immediate precursor of early invasive adenocarcinoma, which can be classified into four architectural patterns: tufting, micropapillary, cribriform, and flat.

The progression of PCa is a multiple-step process of orderly events, complicated by its heterogeneity and driven by various genetic abnormalities. PCa almost invariably metastasizes to the bone, which accounts for most of the morbidity and mortality of PCa patients (9). At early stages, PCa is androgen responsive; androgen deprivation is a common treatment that generally causes PCa to regress. However, most PCa eventually recurs, becomes castration-resistant, and eventually develops metastases (10).

A number of tumor suppressor genes and proto-oncogenes are involved in the development and progression of PCa (10), such as *NKX3.1, PTEN, MYC, NOTCH-1.* In approximately 40% of the primary prostate tumors, a recurrent translocation of an ETS transcription factor *ERG* to the *TMPRSS2* promoter region occur, which results in constitutively active from of the TMPRSS2-ERG fusion protein (11-13).

A series of genetically engineered mouse models have been generated to recapitulate the pathological and physiologic characteristics of human PCa (14). Viral oncogene driven model, TRAMP (transgenic adenocarcinoma of mouse

prostate) model, is a transgenic line contains a minimal probasin promoter that express SV40 large T and small t tumor antigens, both of which serve as oncoproteins(15)(15). The TRAMP mice characteristically develop distinct high-grade PIN and/or PCa in the epithelium by 10 weeks of age. Distant site metastases are readily detectable as early as 12 weeks of age, primarily to the lungs, liver and lymph nodes and less often to bone, kidneys and adrenal gland. Androgen-depletion by castration doesn't delay the overall progression to poorly differentiated and metastatic disease (16-18). Although this model exhibits neuroendocrine phenotype at late stages, it is still a useful model in studying metastatic spread. Moreover, neuroendocrine phenotype is emerging to be important in the prognosis, evolution and progression of castration-resistant human prostate cancer.

PTEN is a second generation of PCa model which has used loss-of-function mutations in PTEN (phosphatase and tensin homolog deleted from chromosome 10). PTEN is a negative regulator of AKT, and most oncogenic phenotypes of PTEN loss are attributed to AKT activation (19,20). In human, PTEN deletions and/or mutations are found in 30% of primary prostate cancers and 63% of metastatic prostate cancers.

Aside from the genetic or epigenetic modifications in prostate epithelial cells, stromal cells are equally critical in tumorigenesis. A stromal reaction in cancers seems similar, if not identical, to a generic wound repair response. In the wake of reactive stroma, extracellular matrix production deposition is elevated, and

growth factors and matrix remodeling enzymes are overwhelmed to create a growth-promoting microenvironment. Meanwhile, stimulated angiogenesis and influx of tumor associated macrophages (TAM) enhance tumor progression (21). Given the magnitude of stromal changes are related to tumor aggressiveness and patient outcome, the tumor stroma has emerged to be a valid target for therapy. Stroma factors has gradually been used a prognostic and treatment predictive markers, in conjunction with other conventional epithelial cell markers. New clinical diagnosis and treatment for prostate cancer is on the rise. Prostate-specific antigen, or PSA, is a protein produced by cells of the prostate gland. The PSA test has been widely used to screen men for prostate cancer, in conjunction with urine test to look at the level of prostate cancer antigen 3 or an *TMPRSS2:ERG* after a digital rectal exam (DRE). Prostate cancer therapy includes radical prostatectomy, radiation therapy, hormonal therapy, and immunotherapy. Since prostate cancer is largely dependent on androgen receptor signaling in its early development, targeting androgen receptor (AR) axis signaling or to lower testosterone levels is the first-line therapy for prostate cancer. There are different types of drugs on the market: (1) Luteinising hormone (LH) blockers, (2) Gonadotrophin releasing hormone (GnRH) blockers, (3) Anti androgens (4) Abiraterone (Zytiga) and Enzalutamide (Xtandi). A more potent AR inhibitor, ARN-509 (Aragon) is in clinical trial and is purportedly more efficacious than enzalutamide. However, the androgen therapy is palliative, as recurrence of the tumor is almost inevitable at some time after the androgen

therapy. The recurrent tumors are then generally androgen independent and highly malignant. Unfortunately, so far, there are still no effective drugs for recurring prostate cancer. The only cell-based cancer immunotherapy currently approved for treatment of prostate cancer is Dendreon's Provenge. FGFR inhibitors have also shown encouraging clinical outcomes in prostate cancer, however, some challenges of FGFR inhibitor development remain, for example, FGFR-mediated recurrence or resistance. Thus, new drug discovery is in urgent need.

CHAPTER II

PROSTASPHERE-FORMING STEM CELLS ARE DERIVED FROM THE P63-EXPRESSING BASAL COMPARTMENT

Introduction

The prostate is an androgen-dependent organ. Androgen-deprivation results in massive apoptosis of the epithelial cells and prostate atrophy. During the regressed state, 90% of the luminal cells undergo apoptosis while most of the basal cells survive. However after androgen replenishment, the surviving epithelial cells actively proliferate and the prostate regenerates back to the normal size in 14 days. This regression/regeneration cycle can be repeated for at least 15 rounds, providing the first clue that there is a type of castration resistant prostate stem cells that contribute to prostate regeneration (22-24). It has been suggested that prostate stem cells may reside in the proximal region of the mouse prostate (25,26). Prostate stem cells are slow cycling cells which are capable of existing its dormancy and reentering cell cycle *in vitro*. Together with urogenital mesenchyme, prostate stem cells have the ability to reconstitute prostate structures in renal capsule.

Emerging evidence indicate that P-SCs reside in both basal and luminal cell compartments of the human and mouse prostate under different circumstances. *In vitro* sphere/organoid culture, *in vivo* renal capsule implantation, FACS

analysis, and *in vivo* lineage tracing assays have shown that basal stem cells have self-renewal and multi-lineage differentiation capacities (27-33). Specifically, CK5, CK14-positive basal cells have been shown to give rise to basal, luminal and neuroendocrine cells during postnatal development (32). On the other hand, a subtype of luminal cells that express Nkx3.1 during castration can give rise to both basal and luminal cells both in *in vitro* organoid culture and *in vivo* (34,35). However, other studies also imply that during tissue homeostasis and regression/regeneration, both basal stem cells and luminal stem cells are mostly self-sustained (36,37). Interestingly, it has been reported that in developing prostatic epithelia, basal cells display both symmetric and asymmetric divisions leading to different cell fates, while luminal cells only exhibit symmetrical divisions (33). Although the hierarchy of P-SCs in basal (P-bSCs) and luminal (P-lSCs) compartments and their relative importance in prostate biology and pathology are still not fully certain, both lineages of cells have been shown capable of, although with different plasticity, developing prostate cancers with distinct aggressiveness and molecular signatures upon loss of Pten function (15,36,38-40).

Prostasphere cell cultures have been extensively used for *in vitro* P-SCs propagation. Prostasphere cells express basal cell cytokeratins and P63, and are capable of self-renewal and multi-lineage differentiation. However, the cell lineage of prostaspheres is not clear. Moreover, whether the prostasphere forming cells represent P-SCs is still controversial. *In vitro* growth of luminal-

resident P-SCs remained problematic until two groups developed distinct culture systems recently (34,41). One group shows that both CARNs and normal prostate luminal epithelial cells can form prostate organoids and exhibit functional androgen receptor (AR) activity in culture. The other group shows that a 3D culture system supports expansion of primary mouse and human prostate organoids, which are composed of fully differentiated CK5+ basal and CK8+ luminal cells and preserve androgen responsiveness. Although both basal and luminal cells give rise to organoids, luminal cells-derived organoids more closely resemble prostate glands (41).

Herein we report that prostaspheres were derived from P63-expressing basal cells. The cells were designated as basal prostate stem cells (P-bSCs) to be distinguished from luminal P-SCs (P-lSCs). In addition, prostaspheres were capable of forming organoids with functional differentiation markers AR and CK18. However, organoids-derived cells could not form prostaspheres. The results suggest that P-bSCs represent more primitive P-SCs than P-lSCs. We also showed that both the prostate and prostaspheres had a reservoir of quiescent stem cells, which possessed a high self-renewal capacity. Different from other rapid-turnover organs and cells, the prostate and prostaspheres did not contain Lgr5+ cells.

Materials and Methods

Animals

Mice were housed under the Program of Animal Resources of the Institute of Biosciences and Technology, Texas A&M Health Science Center in accordance with the principles and procedure of the Guide for the Care and Use of Laboratory Animals. All animal procedures were approved by the Institutional Animal Care and Use Committee. Mice carrying the *Nkx3.1*^{cre}, *P63*^{CreERT2}, *K5*$^{H2B/GFP}$, *Lgr5*$^{EGFP\text{-}CreERT2}$, and *ROSA26*^{LacZ} reporter alleles were bred and genotyped as previously described (42-46). Prostates were harvested immediately after the animals were euthanized by CO_2 asphyxiation.

For inducible gene activation, mice bearing *P63*^{CreERT2} and the reporter alleles, as well as their wildtype littermates were i.p. injected of 20 mg/ml tamoxifen (Sigma; diluted in corn oil) at a dosage of 100 mg/kg. For *in vitro* ablation, the cells were treated with 5 mM 4-hydroxytamoxifen (Sigma, in ethanol) at a final concentration of 500 nM.

Prostaspheres and organoid cultures

The conditions for preparing, culturing, and passaging prostate spheres were developed based on published protocols (29). Prostates were dissected from 6- to 8-week-old male mice immediately after euthanasia, minced with a pair of steel scissors. The minced tissues were then incubated with 10 ml DMEM with 10% FBS containing 1 mg/ml collagenase (Sigma) at 37°C for 90 minutes. The

cells were then washed with PBS, and incubated with 0.25% trypsin/EDTA for 10 minutes at 37°C, followed by passing through a 25-gauge syringe several times. After adding FBS to the cell suspension to inactivate trypsin, the cells were passed through a 40-μm cell strainer, washed with DPBS (Sigma), and counted. Prostate cells were suspended with 50 μl of the prostate epithelial growth medium (PrEGM, Lonza, Walersville) at a density of $6x10^5$/ml and then mixed with Matrigel (BD Biosciences) at a ratio of 1:1. The mixtures (100 μl) were plated around the rim of wells in a 12-well plate. After incubation at 37°C for 30 minutes or until the Matrigel solidified, 1 ml of PrEGM was added to each well, and the plates were transferred to a 5% CO_2 tissue culture incubator. The cells were then cultured at 37°C for 8-10 days with the medium replenished every other day, until the spheres reached the size over 60 μm in diameters. The Matrigel was then digested by incubation in 1 ml of 1 mg/ml dispase solution (Life Technologies, Grand Island, NY) at 37°C for 30 minutes. The spheres were harvested for analyses or subcultures by centrifugation. For subculturing, the pellets were digested with 1 ml of 0.05% trypsin/EDTA (Invitrogen) for 5 minutes at 37°C, followed by inactivation of trypsin by FBS. The cells were passed through a 40-μm cell strainer, counted, and replated.

For organoid culture in hepatocyte medium as described (34), the cells were resuspended in hepatocyte culture medium (designated as Medium H), consisting of: hepatocyte medium supplemented with 10 ng/ml EGF (Peprotech), 10 μm Fasudil (Tocris), 1X Glutamax (Gibco), 5% Matrigel (Corning), and 5%

charcoal-stripped FBS (Gibco) that had been heat-inactivated at 55^{o}C for 1 hour. 10,000 dissociated cells were resuspended in Medium H and plated in ultralow-attachment 96-well plates (Corning) in the presence of 100 nM DHT. 100 µl of fresh Medium H was added to the wells every other day. The cells were incubated at a 37^{o}C for 8-10 days. The organoids were dissociated for subcultures by incubation in trypsin/EDTA with the addition of 10 µM Fasudil for 5 minutes at 37^{o}C.

For organoid culture in the DMEM/F12 medium (41), prostate cells ($3x10^{4}$) isolated as above were suspended in 50 µl of the DMEM/F12 medium (designated as Medium DF), which was supplemented 1X B27 (Life technologies), 10 mM HEPES, Glutamax (Life technologies), Penicillin/Streptomycin, 10 ng/ml EGF, 500 ng/ml recombinant R-spondin1, and 100 ng/ml recombinant Noggin (Peprotech), the TGF-β/Alk inhibitor A83-01 (Tocris), and 1 nM dihydrotestosterone (Sigma). The cell suspension was mixed with Matrigel (1:1) and plated around the rim of the wells in a 12-well plate. After incubation at 37^{o}C for 30 minutes for solidification, 1 ml of Medium DF was added to each well. The cells were incubated at 37^{o}C for 8-10 days with a half of the medium was replenished every other day. The organoids were dissociated for passaging by trypsinization with trypsin/EDTA with the addition of 10 µM Fasudil for 5 minutes at 37^{o}C.

BrdU labeling

For BrdU incorporation assay, BrdU (Sigma Co, Saint Louis, MO) was added to the culture medium at a final concentration of 2.5 μM. After incubation at 37°C for 40 hours, the spheres were harvested as described and BrdU positive cells were identified by immunostaining. For long-term BrdU retention, 24 hours after labeling, the medium was aspirated and the culture were washed 3 times with fresh medium to remove free BrdU. The cells were cultured in fresh medium for another 7 days prior to being harvested for analyses. Immunostaining with anti-BrdU antibody (1:500 dilution; Sigma Co, Saint Louis, MO) was used to detect BrdU labeled cells.

Flow cytometry and cell sorting

Dissociated single prostate cells were incubated with FITC-conjugated anti CD31, CD45, Ter119 antibodies, and PE-conjugated anti-Sca-1 antibody (eBioscience), or Alexa 647-conjugated anti CD49f antibody (Biolegend) diluted in the cell sorting buffer (2% FBS in PBS). Primary antibody labeling was conducted by incubation for 20 minutes in ice-cold conditions with antibody dilution according to manufacturer's suggestions in a volume of 100 μl per 10^5-10^8 cells. The cells were then washed in 1 ml ice-cold cell sorting buffer to remove unbound antibodies, resuspended in 0.5 ml cell sorting buffer, followed by resuspension in the cell sorting buffer for fluorescence-activated cell sorting

on a BD FACSAria I SORP. The sorted cells were collected in DMEM medium containing 20% FBS.

Histology

Prostaspheres or cells were fixed with 4% paraformaldehyde-PBS solution for 30 minutes at room temperature. The spheres were pelleted and suspended in Histogel. After solidifying at room temperature, the pellets were ethanol dehydrated, paraffin embedded in paraffin, and sectioned at 5 μm thickness as described (29). For histology analyses, sections were re-hydrated for H&E staining. For immunostaining, the slides were incubated in boiling citrate buffer (pH 8.0) for 20 minutes for antigen retrieval. The source and concentration of primary antibodies are: anti-cytokeratin 8 (1:15 dilution) and anti-cytokeratin 5 (1:500 dilution) from Fitzgerald Industries International (Concord, MA); anti-cytokeratin 18 (1:200 dilution) and anti-androgen receptor (1:200 dilution) from Abcam; mouse anti-BrdU (1:500 dilution) from Sigma (St Louis, MO); mouse anti-cytokeratin 14 (1:100 dilution) and anti-p63 (1:150 dilution) from Santa Cruz (Santa Cruz, CA), rabbit anti-β-Catenin (1:200 dilution), and anti-cleaved-Caspase 3 (1:200 dilution) from Cell Signaling Technology. After washing, the specifically bound antibodies were detected with and fluorescence-conjugated secondary antibodies (Invitrogen) or the ExtraAvidin Peroxidase System (Sigma). For the immunofluorescence staining, the nuclei were counter stained with To-Pro 3 before being observed under a confocal microscope (Zeiss LSM

510). For LacZ staining, the prostates or prostaspheres were lightly fixed with 0.2% glutaraldehyde for 1 hour at room temperature, and then incubated overnight with 1 mg/ml X-Gal at room temperature. After washing with PBS, the tissues or prostaspheres were post-fixed with 4% PFA for 1 h, ethanol dehydrated, paraffin-embedded, and sectioned for subsequent analyses.

Western blotting

The prostate spheres were pelleted by centrifugation, resuspended in RIPA buffer (50 mM Tris-HCl buffer pH 7.4, 1% NP40, 150 mM NaCl, 0.25% Na-deoxycholate, 1 mM EGTA, 1 mM PMSF), and homogenized with a tissue homogenizer. The protein extracts were harvested by centrifugation. Samples containing 30 μg proteins were separated by SDS-PAGE and electroblotted onto PVDF membranes. The membranes were then incubated with the indicated antibodies at 4°C overnight. The dilutions and the sources of the antibodies are: anti-phosphorylated ERK1/2, 1:1000; anti-phosphorylated AKT, 1:1000; anti-ERK1/2, 1:1000; and anti-AKT, 1:1000 (Cell Signaling Technology). After being washed with the TBST buffer for three times to remove nonspecific antibodies, the membranes were then incubated with the horseradish peroxidase conjugated secondary antibody at room temperature for 1 hour, followed by washed with the TBST buffer for three times to remove the unbound antibodies. The specifically bound antibodies were visualized by using the ECL-Plus

chemoluminescent reagents. The films were scanned with a densitometer for quantitation.

RNA expression

Total RNA was isolated from prostaspheres using TRIzol RNA isolation reagents (Life Technologies). The SuperScript III reverse transcriptase (Invitrogen, Carlsbad, CA) and random primers were used for first-strand cDNAs synthesis according to manufacturer's protocols. Real-time PCR analyses were carried out using the Fast SYBR Green Master Mix (Life Technologies). After normalization to the β-actin internal control, the relative abundance of mRNA was calculated using the comparative threshold (CT) cycle method. The mean ± sd from at least three individual experiments are shown.

Statistical analysis

Statistical analysis was performed using the two tailed t test, with significance set to $P<0.05$. Error bars indicate standard deviation.

Results

Prostaspheres originate from basal epithelial cells and maintain basal cell properties

To establish prostasphere cultures, single cell suspensions were prepared from adult prostate tissues and plated in Matrigel as described (29). The spheres follow a step-wise development. Small, solid spheres were visible at day 5 and two-layer spheres around day 7 to 10, which reached an average size of 100 μm or larger in diameter. The outermost layer of the spheres and the layers closely underneath were aligned concentrically around a central cavity filled with acellular substances (Fig. 2.1A). During development, the NKX3.1 homeobox protein is the earliest known marker for prostate epithelial precursor cells and prostate formation (47). Cell-lineage tracing with the *Nkx3.1*^{cre}-activated *ROSA26*^{LacZ} reporter demonstrated that cells in prostaspheres were of epithelial origin as illustrated by *LacZ* staining (Fig. 2.1B).

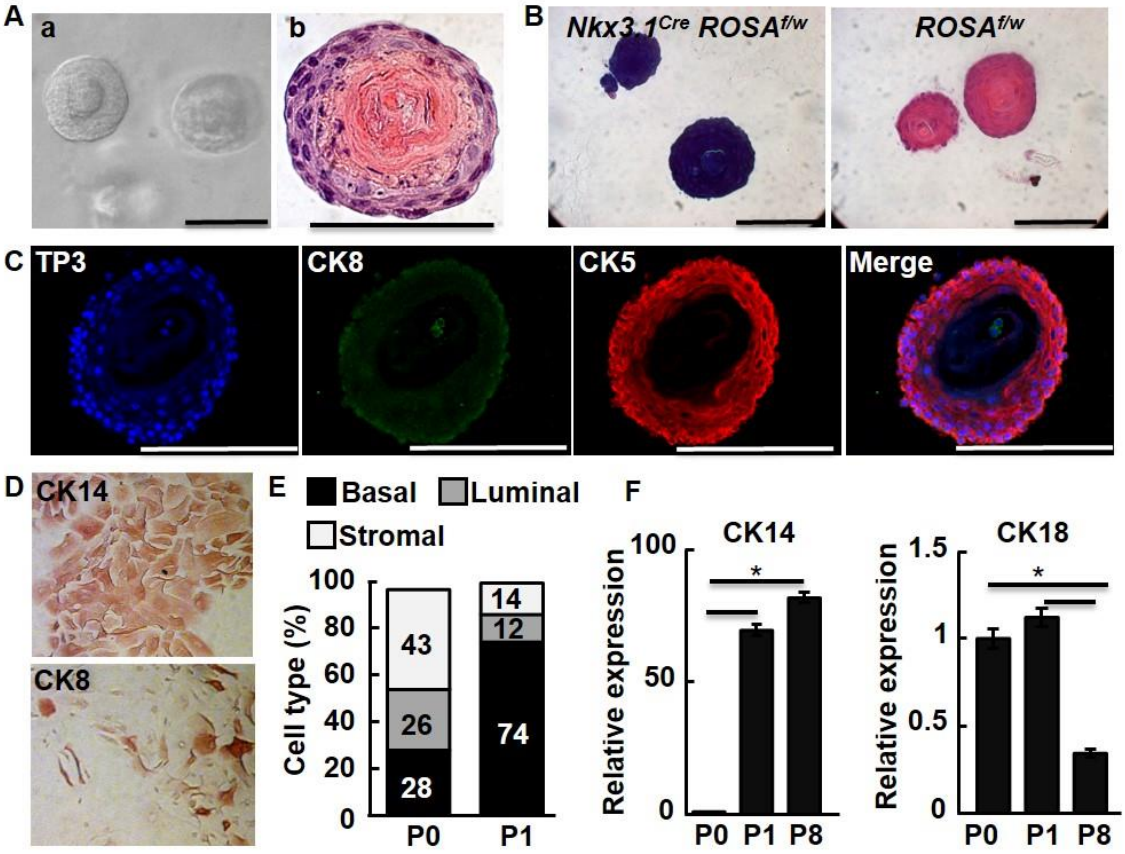

Fig. 2. 1. Prostaspheres are derived from basal cells and maintain basal cell properties.

A. Phase contrast image of representative prostaspheres in Matrigel (a) and H&E staining of a prostasphere section (b). **B**. X-gal staining of prostaspheres derived from the indicated mouse genotype. **C**. Immunostaining of prostaspheres with luminal cell-specific CK8 and basal cell-specific CK5. **D.** Disassociated prostasphere cells were cultured on tissue culture dishes for 3 days and stained with anit-CK14 or CK8 antibodies as indicated. **E&F.** FACS analysis of the primary and 1st generation prostaspheres. Numbers indicate percentages of indicated cell type (E). Real-time RT-PCR analyses of CK14 and CK18 expression in primary prostate cell suspensions (P0) and P1 or P8 prostaspheres (F). f, floxed; w, wildtype; CK5, cytokeratin 5; CK8, cytokeratin 8; CK14, cytokeratin 14; TP3, To-Pro3; *, P≤0.05.

Most cells in the spheres expressed basal cell-specific cytokeratin (CK) 5; only a few cells in the inner layers expressed luminal cell-specific CK8 (Fig. 2.1C). However, when the cells were transferred to regular 2-D culture conditions, a higher number of cells displayed luminal keratin ($CK8^+$) (Fig. 2.1D). FACS analysis revealed that in contrast to 28% $Sca\text{-}1^+/CD49f^+$ cells in primary prostates, 74% of the sphere cells were $Sca\text{-}1^+/CD49f^+$, indicating that the sphere culture enriched cells with basal cell properties (Fig. 2.1E). Real time RT-PCR analysis also showed an 80-fold increase of CK14 expression in the 1^{st} and 8^{th} generation of spheres and a significant reduction of CK18 expression in the 8^{th} generation sphere (Fig. 2.1F).

Prostaspheres are derived from P63-expressing basal stem cells

Even though prostaspheres were derived from the Nkx3.1-expressing progenitor cells, expression of Nkx3.1 in prostaspheres was below the detection limit of RT-PCR (Fig. 2.2A). Since Nkx3.1 is expressed in luminal epithelial cells of adult prostates (48), the data indicate that prostaspheres do not contain or only contain scanty terminal differentiated luminal epithelial cells, which is consistent with the rare CK8 staining in the prostaspheres (Fig. 2.1C).

P63 is expressed in prostate basal cells and is required for prostate development. $P63^{-/-}$ mice fail to form prostate (49-51). Lineage tracing with the $ROSA26^{LacZ}$ reporter activated by $P63^{CreERT2}$ at 2 weeks after birth showed that

LacZ positive progeny were distributed in both basal and luminal compartments (Fig. 2.2Ba). This indicated that P63-expressing cells gave rise to both luminal and basal cells as reported (52). To determine whether prostaspheres were derived from P63 expressing basal cells, the prostaspheres derived from $P63^{CreERT2}$-$ROSA26^{LacZ}$ mice were treated with 4-hydroxytamoxifen (4-OHT) at day 1 to activate the $ROSA26^{LacZ}$ reporter. X-Gal staining revealed that almost all prostaspheres were homogeneously $LacZ^{+}$ (Fig. 2.2Bb,c). Thus, the spheres were derived from P63-expressing basal stem cells. Immunofluorescence revealed that Ki67 was co-localized with P63 and only located at the outermost layer of the spheres. This indicated that most proliferating cells were P63-expressing cells (Fig. 2.2C). Sphere cultures of FACS-fractionated cells demonstrated that approximately 3.17% of basal cells formed spheres, while only 0.02% luminal and stromal cells formed spheres (Fig. 2.2D). Together, the data indicated that prostaspheres contain basal cells but not terminally differentiated luminal cells. And only basal cells, specifically P63-positive basal cells, have the highest capacity to self-renew in our culture system. The prostaspheres are derived from basal cells but not luminal cells, therefore the cells are designated as basal P-SCs (P-bSCs).

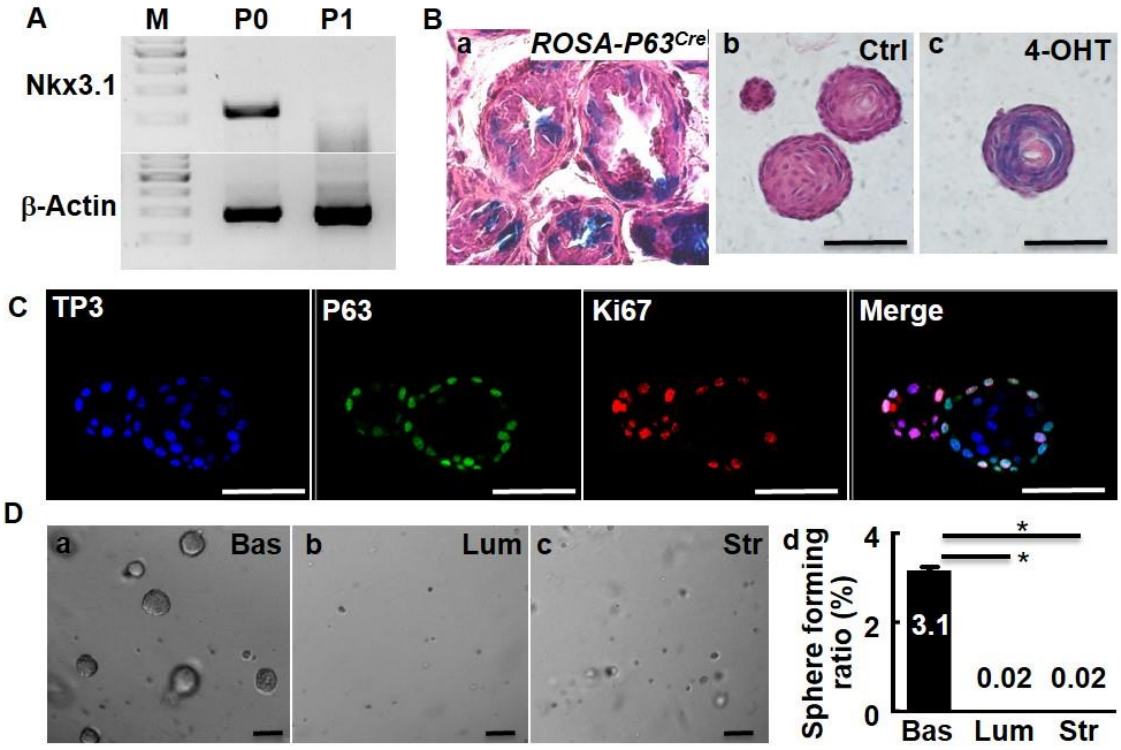

Fig. 2. 2. Prostaspheres are derived from P63-expressing basal cells.

A. RT-PCR analyses of *Nkx3.1* in primary (P0) and 1st generation prostaspheres (P1). **B.** X-Gal staining of prostate (a) or prostasphere (b,c) sections from the mice bearing *ROSA26*^{LacZ} and *P63*^{CreERT2} reporter alleles. Panel a, the mouse was injected i.p. with tamoxifen 2 weeks after birth and the prostates were harvested at 6 weeks.. Panels b&c, prostaspheres were treated with alcohol or 4-OHT at day 1 after the inoculation. **C.** Prostasphere sections were immunostained with anti-P63 and Ki67 antibodies. **D.** Prostasphere forming assays for FACS fractionated cells. P0, primary prostate cells; P1, 1st generation of prostaspheres; TP3, To-Pro 3 staining for nuclei; Ctrl, control; Bas, basal cells; Lum, luminal cells; Str: stromal Cells; *, P≤0.05.

The slow cycling cells in prostaspheres have high capacity to form prostaspheres

One of the characteristics of stem cells is long-term label retaining. To determine the existence of label-retaining, namely slow-cycling, cells in the prostaspheres, BrdU was used to label and trace the cells engaged in DNA synthesis. Approximately 90% of cells in the outer layer displayed BrdU forty hours after labeling (Fig. 2.3Aa). At seven days after labeling, a few $BrdU^+$ cells in the outer layer were still visible. This confirmed that the spheres contained rare long-term label retaining cells (Fig. 2.3Ab).

To further determine whether these slow cycling or prostasphere-forming cells were basal cells, the tetracycline-regulated K5H2B/GFP reporter allele was used as described (53). Over 80% of prostaspheres derived from the reporter-bearing prostate were GFP^+ in the absence of doxycycline (Fig. 2.3B), which further indicated that most of the prostaspheres were basal cells that expressed CK5. In contrast to the majority of GFP^+ prostasphere cells in its absence, the presence of doxycycline resulted in only 1 or 2 GFP^+ cells at the outer layer, which represented long-term label-retaining cells (Fig. 2.3Ca,b). These long-term label retaining GFP^+ cells showed four-fold higher capacity to form spheres than GFP^- cells (Fig. 2.3Cc).

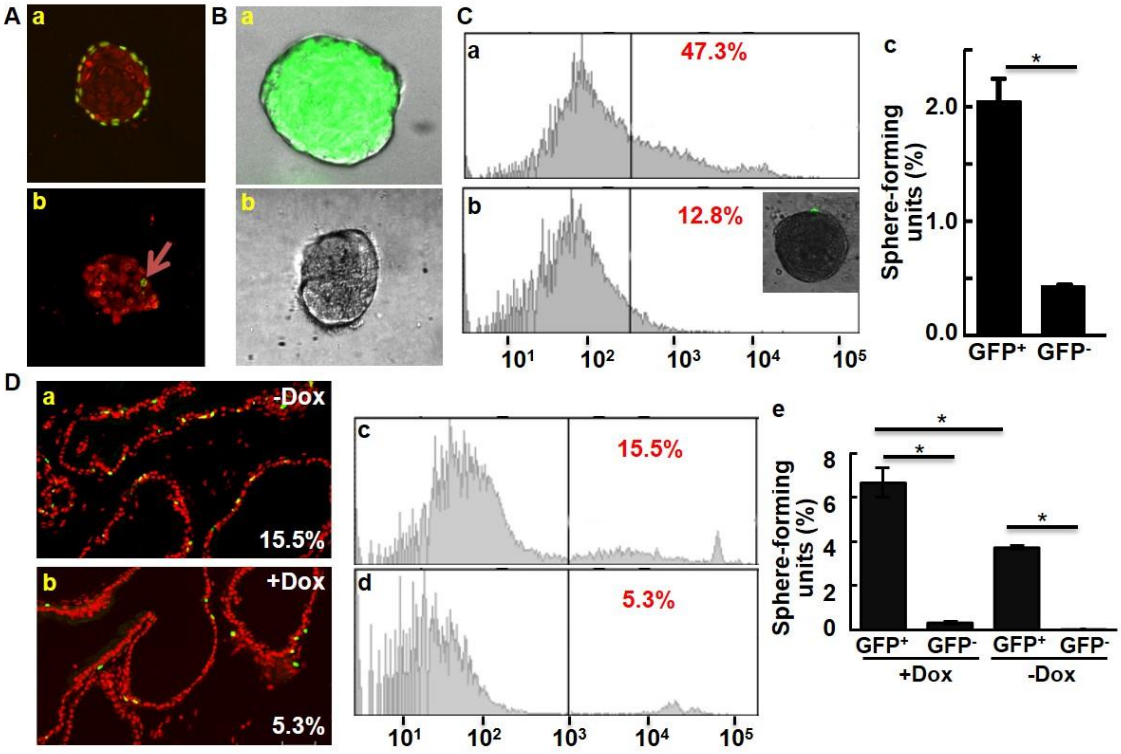

Fig. 2. 3. Prostaspheres contain slow-cycling P-bSCs.

A. Prostaspheres were labeled with BrdU for 40 hours (a), or a 24-hour pulse and 7-day chase (b). The labeled cells were detected by anti-BrdU immunostaining. Arrow indicates label-retaining cells. **B**. Merged images of phase contrast and fluorescent microscopy of prostaspheres bearing the *K5*$^{H2B/GFP}$ reporter showing GFP$^+$ prostaspheres (a) are derived from K5 expressing basal cells and GFP$^-$ prostaspheres (b). **C**. FACS analyses of primary prostate cells from mice carrying the *K5*$^{H2B/GFP}$ reporter in the absence or presence of doxycycline (a&b). Numbers indicate percent of GFP$^+$ cells. Insert, prostasphere derived from doxycycline treated *K5*$^{H2B/GFP}$ prostate. The FACS fractionated cells were cultured in Matrigel and the average sphere numbers derived from 100 cells were showed as mean ± sd (c). **D.** The prostates bearing the *K5*$^{H2B/GFP}$ reporter allele with or without doxycycline were sectioned and GFP was detected by confocal microscopy (panels a&b), or subjected to FACS analyses (panels c&d). The sphere forming activity of the 4 groups of cells was assessed and presented as numbers of spheres per 100 cells (e). Dox, doxycycline; *, P≤0.05.

Consistently, in the absence of doxycycline, the majority of prostate basal cells *in vivo* were GFP^+ (Fig. 2.3Da,c), which accounted for 15.5% of total prostate cells. However, one month after feeding with doxycycline to repress GFP expression, only 5.3% of the cells in the prostate were still GFP^+ (Fig. 2.3Db,d). Prostates with or without doxycycline treatment were then dissociated into single cells. The GFP^+ and GFP^- cells were separated by cell sorting and cultured in Matrigel to assess their sphere-forming capacity. The results showed that the GFP^+ cells from the doxycycline treated group, which represented the long-term label retaining cells in the prostates, had a higher capacity in forming prostaspheres than the general population of basal cells (Fig. 2.3De). None of the GFP^- cells formed spheres with a diameter larger than 50 µm. The results further demonstrate that label-retaining basal cells have a high capacity to form prostaspheres.

P-bSCs have the capacity to form organoids, but not vice versa

Two recent reports show that the luminal compartment contains P-SCs that form prostate-like organoids in two different *in vitro* conditions. To determine whether the organoid-forming P-SCs and P-bSCs were interchangeable and shared the same properties, P-bSCs were transferred to the two organoid-culture conditions, namely Medium H and Medium DF as described in Methods. Interestingly, P-bSCs formed organoid-like structures with a morphology similar

to reported earlier in both media (Fig. 2.4Aa,b). Immunostaining showed that the resulting organoids in Medium H contained cells expressing AR and luminal cell-specific CK18, but no longer P63 (Fig. 2.4Ac-e). The organoids generated in Medium DF contained cells expressing AR and CK18. Only a few cells located at the outer layer expressed P63 (Fig. 2.4Af-h). Thus, the results indicate that prostaspheres contain organoid-forming cells, which can differentiate into luminal cells under the organoid culture conditions.

To determine whether the organoids contained prostasphere-forming cells, primary prostate cells were first cultured in organoid conditions as reported. The organoids cells were then harvested and grew either in the organoid or sphere culture conditions. Although the cells continued to form organoids in the organoid culture conditions, none of them formed prostaspheres in the prostasphere culture condition (Fig. 2.4B). Therefore, it was unlikely that the organoids contained prostasphere-forming P-bSCs. Together with the data that prostasphere-forming P-bSCs were capable of forming organoids, the results indicate that P-bSCs sit in a higher hierarchy position than luminal resident organoid-forming P-SCs.

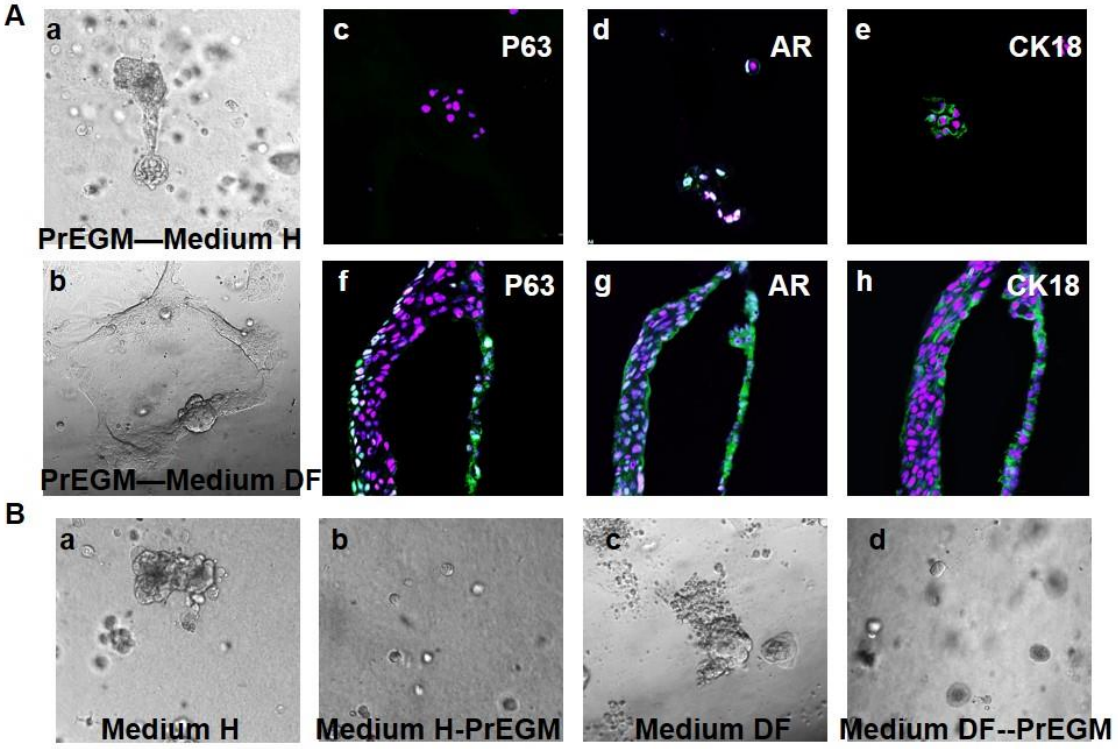

Fig. 2. 4. Prostasphere cells have the capacity to form prostate organoids, but not vice versa.

A. Prostaspheres cultured in Matrigel with prostasphere culture medium (PrEGM) were dissociated and inoculated in organoid culture with hepatocyte (Medium H) or DMEM/F12 (Medium D/F) as described. Panels a&b are phase contrast microscopy images. Panels c-e and f-h are immunostaining of organoid sections from Medium H or Medium DF with the indicated antibodies. **B**. Organoids cultured in the indicated medium were dissociated and inoculated in Matrigel-PrGEM. Note that no organoid-derived cells could form prostaspheres in PrEGM.

Neither the prostates nor the prostaspheres contain Lgr5-expressing cells

Emerging evidence has indicated the coexistence of quiescent and active adult stem cells in mammals (54). The leucine-rich repeat containing G-protein-coupled receptor 5 (*Lgr5*) has been reported to be expressed in many active, but not quiescent, tissue stem cells (55,56). To determine whether prostaspheres contained *Lgr5*$^{+}$ cells, RT-PCR was employed to detect *Lgr5* expression at the mRNA level in primary prostate cells and first generation prostaspheres. The results showed that prostaspheres had no detectable *Lgr5* expression although primary prostate cells exhibited a very low level of *Lgr5* expression (Fig. 2.5A). In contrast, β-catenin expression was comparable between primary prostate cells and prostaspheres. Consistently, no cells in prostaspheres derived from *Lgr5*$^{EGFP\text{-}CreERT2}$/*ROSA26*^{LacZ} mice were *LacZ* positive with or without administration of 4-OHT to activate *Cre*^{ERT2} (Fig. 2.5B). This further confirmed there were no *Lgr5* expressing cells in prostaspheres. Lineage tracing with *Lgr5*$^{EGFP\text{-}CreERT2}$/ *ROSA26*^{LacZ} reporter alleles *in vivo* failed to demonstrate progeny derived from *Lgr5*-expressing cells in the prostate (Fig. 2.5C). Combined with FACS analyses, RT-PCR data also showed that *Lgr5* was only expressed in stromal cells, but not epithelial cells (Fig. 2.5D). This indicate that unlike other active tissue SCs, active P-bSCs do not express *Lgr5*.

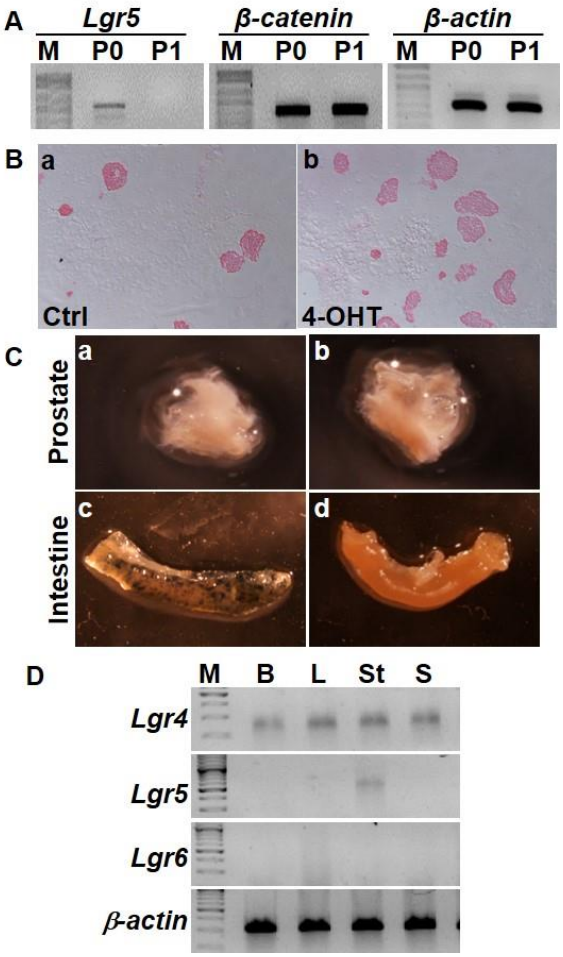

Fig. 2. 5. Lgr5 is not expressed in prostate epithelial cells and prostaspheres.

A. RT-PCR analyses of the indicated genes in primary prostate cells (P0) and 1st generation prostaspheres (P1). **B**. Prostaspheres derived from *Lgr5*$^{EGFP/CreERT2}$;*Rosa*^{lacZ} prostate were treated with 4-OHT treatment, wholemount stained with X-gal, and then sectioned. **C**. Wholemount X-Gal staining of prostates and intestines from *Lgr5*$^{EGFP/CreERT2}$;*Rosa*^{lacZ} mice with or without tamoxifen administration. Noted that the blue *LacZ* staining is visible in intestine, but not in prostate. **D.** RT-PCR analyses of *Lgr4*, *Lgr5*, and *Lgr6* expression in primary prostate cells fractioned by FACS and prostaspheres. β-actin was used as a loading control. P0, primary prostate cells; P1, 1st generation prostaspheres; M, molecular weight markers; B, basal cells; L, luminal cells; St, stromal cells; S, spheres derived from basal cells.

Discussion

Prostasphere culture has been widely used for study and quantitation of self-renewal activity of both human and mouse P-SCs (19,29,30). However, the utility of this system has been questioned due to the fact that most of the cells in the prostaspheres are primarily CK5+ basal cells, but lack NKX3.1^{+} cells or their products. The two recent studies based on organoid culture shows that the resulting organoids differ significantly from prostate spheres, in that they retain both basal and luminal epithelia layers and preserve androgen-responsiveness. However, in our study, we for the first time demonstrated that P-bSCs were also capable of forming organoids. In contrast, the organoid-forming cells were not able to form prostaspheres. Therefore, the results reveal that P-bSCs represent stem cells in the prostate, which can give rise to both luminal and basal stem cells. The results indicate that the sphere culture system is a useful and reliable *in vitro* culture system to preserve prostate basal stem cell stemness.

Adult stem cells are highly heterogeneous, including both quiescent stem cells and active stem cells. *K5$^{H2B/GFP}$* has been used in various studies to identify quiescent stem cells across different tissues as hair follicles and mouse incisors. (53,57). Lgr5, which is an active stem cell marker, is expressed in a variety of intact tissues or during wound healing (55,56,58-60). In this study, we identified the slow-cycling quiescent stem cells by using both BrdU long-term dye retention and tracking in *K5$^{H2B/GFP}$* mouse prostates and prsotaspheres that retained GFP over the long term. However, we were unable to detect Lgr5 positive cells in the

prostate and prostaspheres. This does not completely rule out the existence of active stem cells in the prostate and prostaspheres. It is possible that the prostate contains $Lgr5^+$ cells after injury, like the liver and the pancreas, in which only injury causes the emergence of an $Lgr5^+$ organoid-forming epithelial progenitor population.

A recent novel barcoding technology by keeping track of cancer cells has provided insights into the presence of rare drug resistant pre-existing cancer cell populations that arise by selection in response to therapeutic challenge (61). This small population of cells that are drug resistant is very similar to cancer stem cells. Relapse of some malignancies has been attributed to emergence of cancer stem cells. It has been reported that upon induction by loss of tumor suppressor genes, both P-bSCs and P-lSCs can be tumorigenic (15,40). Therefore, understanding how to manipulate these two types of P-SCs to undergo differentiation and remain silent will provide new avenues to retrain prostate cancer progression and relapse.

CHAPTER III

TYPE 2 FIBROBLAST GROWTH FACTOR RECEPTOR SIGNALING IS REQUIRED FOR STEMNESS AND PREVENTS DIFFERENTIATION OF BASAL COMPARTMENT STEM CELLS

Introduction

The fibroblast growth factor (FGF) family consists of 22 genes encoding structurally related proteins, among them 18 are tyrosine kinase receptor binding ligands. Based on sequence homology, FGFs can be further divided into seven subfamilies: FGF1-2, FGF4-6, FGF3/7/10/22, FGF8/17/18, FGF9/16/20, FGF11/12/13/14, and FGF19/21/23. Among them, FGF11-14 are not transmembrane tyrosine kinase receptor binding ligands, and FGF19/21/23 are endocrine messengers which work systematically in the body. The remaining FGFs signal through autocrine or paracrine mechanisms locally in various tissues. FGF regulates a broad spectrum of biological activities by activating the transmembrane tyrosine kinases encoded by four highly homologous genes, denoted *Fgfr1*, *Fgfr2*, *Fgfr3*, *and Fgfr4*, in partnership with heparin sulfate proteoglycans or α-klotho or β-klotho. FGFRs consist of diverse splice variants that vary in both extracellular ligand-binding and the intracellular kinase domains (62,63). Activation of FGFRs triggers its autophosphorylation followed by FGFR substrate 2 (FRS2) phosphorylation that is associated with it and recruitment of phospholipase-Cγ (PLCγ) (64,65). FRS2 has two isoforms, FRS2α and FRS2β.

FRS2α, which together with additional recruited adaptors and downstream signaling molecules, links multiple intracellular signaling pathways, including the mitogen-activated protein kinase/extracellular signal-regulated kinase (MAPK/ERK) and phosphinositide 3-kinase (PI3K)/AKT pathways (66,67).

In the prostate, FGF ligands and receptors are partitioned between epithelial and mesenchymal compartments and mediate the communication between the two compartments, either directionally specific or reciprocally. Aberrant expression and activation of the FGF signaling axis is associated with many diseases ranging from developmental disorders and cancer, which will be discussed in Chapter IV (68). Ablation of *Fgfr2* in mouse prostatic epithelial precursor cells compromises bud formation, branching morphogenesis, growth, and acquisition of androgen-dependency of the prostate (45), whereas conditional ablation of *Frs2α* only impairs prostate branching morphogenesis and growth (69).

The FGF signaling axis regulates a wide range of processes in embryonic development, stem cell maintenance, and differentiation. FGF2 is required for sustaining self-renewal and pluripotency of human embryonic stem cells (hESCs) (70). FGF4 stimulation of Erk1/2 is an autoinductive stimulus for pluripotent embryonic stem cells to exit self-renewal and commit to lineage differentiation (71). Precise regulation of Fgfr expression is required during hESC specification (72). FGF signaling has also been implicated in a variety of tissue stem cell activities, including neural stem cells (73), bone marrow mesenchymal stem cells (74), and hematopoietic stem cells (75). Studies from

our group have shown that the FGF signaling axis prevents differentiation of cardiac stem cells (76) and dental epithelial stem cells (77). Disruption of FGF signaling leads to premature differentiation of cardiac progenitor cells. However, thus far, the roles of FGF signaling in P-SC self-renewal and differentiation are still elusive. It has been reported that paracrine stimulation of prostate basal/stem cells with FGF10 results in multifocal adenocarcinoma (78). FGF7 (KGF) has also been shown to suppress α2β1 integrin function and promotes differentiation of the transient amplifying population in human prostatic epithelium (79).

Herein we report that FGF signaling mediated by FGFR2/FRS2α-dependent pathways plays a critical and specific role in self-renewal and differentiation of P-bSCs. Inhibition of FGF signaling impairs P-bSC self-renewal and induces its differentiation. Tissue specific ablation of *Fgfr2* with the $P63^{CreERT2}$ driver in prostaspheres or adult mice prostate reduces numbers of P-bSC. P63-positive basal cells are capable of giving rise to all epithelial lineages during prostate postnatal development (52). Conditional knockout of *Fgfr2* in P63-positive basal cells in neonatal mouse prostate significantly compromises its postnatal development. Our results indicate that FGFR2 in P63-expressing cells is critical for P-bSC self-renewal and differentiation both *in vivo* and *in vitro* and provides a novel avenue for control of P-bSC self-renewal by manipulation of FGF signaling.

Materials and Methods

Animals

Mice were housed under the Program of Animal Resources of the Institute of Biosciences and Technology in accordance with the principles and procedure of the Guide for the Care and Use of Laboratory Animals. All experimental procedures were approved by the Institutional Animal Care and Use Committee. Mice carrying loxP-flanked *Frs2α, Fgfr1, Fgfr2* alleles, and the *Nkx3.1^{cre}* and *P63^{CreERT2}* knock-in alleles were bred and genotyped as described (42-46). Prostate tissues were harvested for the described analyses after the animals were euthanized by CO_2 suffocation.

Inducible gene ablation

For inducible gene ablation, mice bearing *Fgfr1$^{f/f}$ P63^{CreERT2}*, *Fgfr2$^{f/f}$ P63^{CreERT2}*, *Fgfr1/2$^{f/f}$ P63^{CreERT2}*, and its wildtype counterpart alleles were administrated with tamoxifen (20 mg/ml stock solution in corn oil, Sigma) at 100 mg/kg. For *in vitro* ablation, cells bearing the aforementioned alleles were treated with 4-hydroxytamoxifen (Sigma, diluted in alcohol at a stock concentration of 5 mM) at the indicated concentrations.

Prostasphere culture

The conditions for culturing and passaging prostate spheres were adapted by modification of published procedures (29). Briefly, prostates dissected from 6- to

8-week-old male mice were minced with a pair of steel scissors, followed by incubating with 1 mg/ml collagenase (Sigma) in 10 ml DMEM with 10% FBS at 37°C for 90 minutes. Cells were washed with PBS, further digested with 0.25% trypsin/EDTA for 10 minutes at 37°C, and passed several times through a 25-gauge syringe. After inactivation of trypsin by FBS, cells were passed through a 40-μm cell strainer, washed with DPBS (Sigma) and counted. Prostate cells ($3x10^4$) were suspended in 50 μl of the prostate epithelial growth medium (PrEGM) (Lonza, Walersville) and then mixed with Matrigel (BD Biosciences) at a ratio of 1:1. The cell mixtures were plated around the rim of wells in a 12-well plate and allowed to solidify at 37°C for 30 minutes. Then, 1 ml of PrEGM was added to each well, and the medium was replenished every other day. After plating for 8-10 days, the spheres with a diameter over 60 μm were scored. To harvest the spheres, the Matrigel was digested by incubation in 1 ml of 1 mg/ml dispase solution (Life Technologies, Grand Island, NY) at 37°C for 30 minutes, followed by centrifugation. To subculture the spheres, the pellets were digested with 1 ml of 0.05% trypsin/EDTA (Invitrogen) for 5 minutes at 37°C. After inactivation of trypsin by FBS, the cells were passed through a 40-μm filter, counted by a hemocytometer, and replated. FGF7 or FGF10 was added to the cell culture medium at a final concentration of 10 ng/ml. 4-OHT was added to the cell culture medium at a final concentration of 500 nM.

Flow cytometry and cell sorting

Dissociated single prostate cells were stained with FITC-conjugated anti CD31, CD45, and Ter119 antibodies (eBioscience), PE-conjugated anti-Sca-1 antibody (eBioscience), and Alexa 647-conjugated anti CD49f antibody (Biolegend). All antibody incubations, washes, and flow cytometric analyses were performed in cell sorting buffer (2% FBS in PBS). Fluorescence-activated cell sorting was conducted on a BD FACSAria I SORP, and cells were sorted into DMEM+20% FBS. Primary antibody labeling for cell sorting was conducted by incubation for 20 minute on iced with antibody dilution according to manufacturer's suggestions in a volume of 100 µl per 10^5-10^8 cells in cell sorting buffer. The cells were washed in 1 ml ice-cold cell sorting buffer, resuspended in 0.5 ml cell sorting buffer, and analyzed.

Histology

Prostaspheres were fixed with 4% paraformaldehyde-PBS solution for 30 minutes. The fixed spheres were pelleted and mixed with Histogel. After solidifying at room temperature, the Histogel pellets were serially dehydrated, embedded in paraffin, and sectioned as described (29). For general histology, slides were re-hydrated and stained with hematoxylin and eosin (H&E). For immunostaining, the antigens were retrieved by boiling in citrate buffer (pH 8.0) for 20 minutes. The source and concentration of primary antibodies are: mouse anti-p63 (1:150 dilution) from Santa Cruz (Santa Cruz, CA), rabbit anti-

phosphorylated ERK (1:200 dilution), rabbit anti-phosphorylated AKT (1200 dilution), mouse anti-Ki67 (1:200 dilution), rabbit anti-β-Catenin (1:200 dilution), and anti-cleaved-Caspase 3 (1:200 dilution) from Cell Signaling Technology. The ExtraAvidin Peroxidase System (Sigma) and fluorescence-conjugated secondary antibodies (Invitrogen) were used to visualize specifically bound antibodies. For the immunofluorescence staining, the nuclei were counter stained with To-Pro 3 before being observed under a confocal microscope (Zeiss LSM 510).

Western blotting

Prostaspheres were homogenized in RIPA buffer (50 mM Tris-HCl buffer pH 7.4, 1% NP40, 150 mM NaCl, 0.25% Na-deoxycholate, 1 mM EGTA, 1 mM PMSF), and the extracted proteins were harvested by centrifugation. Samples containing 30 μg proteins were separated by SDS-PAGE and electroblotted onto PVDF membranes for Western analyses with the indicated antibodies. The dilutions of the antibodies are: anti-phosphorylated ERK1/2, 1:1000; anti-phosphorylated AKT, 1:1000; anti-ERK1/2, 1:1000; and anti-AKT, 1:1000 (Cell Signaling Technology). After being washed with TBST buffer to remove nonspecific antibodies, the membranes were then incubated with the horseradish peroxidase conjugated rabbit antibody at room temperature for 1 hour. The specifically bound antibodies were visualized by using the ECL-Plus

chemoluminescent reagents. The films were scanned with a densitometer for quantitation.

RNA expression

Total RNA was isolated from prostaspheres using the TRIzol RNA isolation reagents (Life Technologies). The first-strand cDNAs were reverse transcribed from the RNA template using SuperScript III reverse transcriptase (Invitrogen, Carlsbad, CA) and random primers according to manufacturer's protocols. Real-time PCR analyses were carried out using the Fast SYBR Green Master Mix (Life Technologies) as instructed by the manufacturer. Relative abundances of mRNA were calculated using the comparative threshold (CT) cycle method and were normalized to β-actin as the internal control. The mean±sd among at least three individual experiments are shown.

Statistical analysis

Statistical analysis was performed using the two tailed t test, with significance set to $P<0.05$. Error bars indicate standard deviation.

Results

FGF signaling promotes prostasphere formation

The FGF7/10-FGFR2 signaling axis is important in prostate development and maintenance of tissue homeostasis in the prostate (45,80,81). To determine whether FGF signaling was required for prostasphere formation, FGF7 or FGF10 was added to the culture medium at a concentration of 10 ng/ml. Both FGF7 and FGF10 significantly increased the number and size of prostaspheres (Fig. 3.1A). This indicated that FGF signaling promoted prostasphere formation and growth of individual spheres.

To determine which FGFR isoform mediates FGF signaling, we employed RT-PCR analyses to examine the expression of FGFR isoforms in prostaspheres and primary prostate cells. The results revealed that *Fgfr1* and *Fgfr2* were expressed in prostaspheres and primary prostate cells; *Fgfr3* and *Fgfr4* were detectable only in the primary prostate cells (Fig. 3.1Ba).

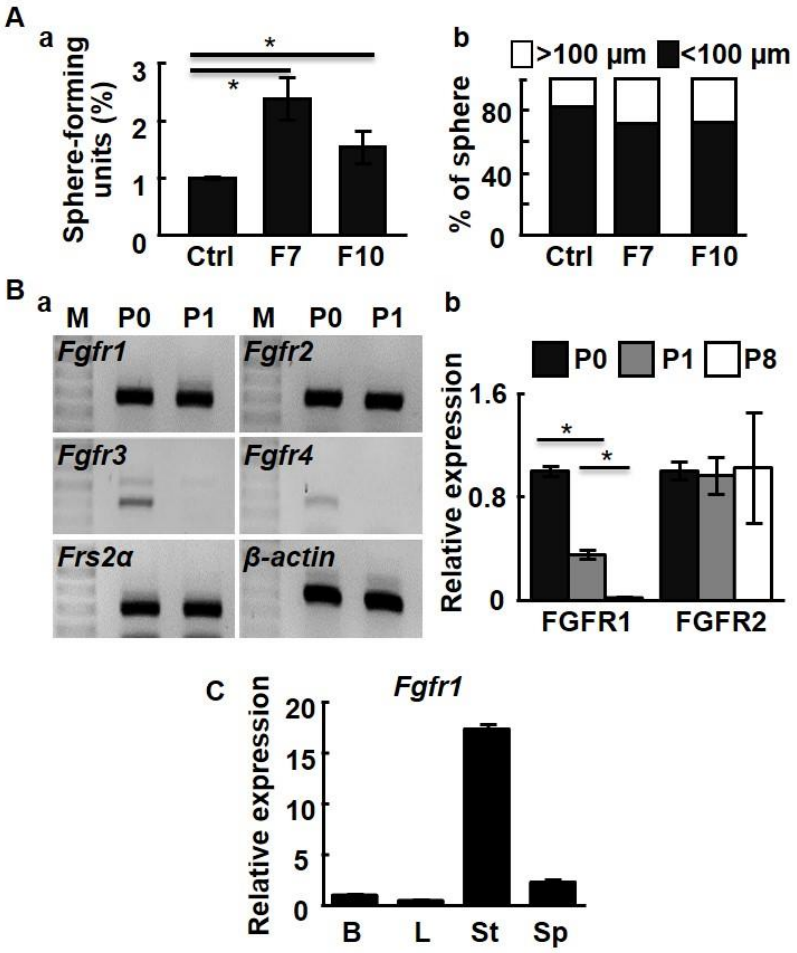

Fig. 3. 1. FGF promotes prostasphere formation and growth.

A. FGF7 (F7) or FGF10 (F10) was added to the culture medium (10 ng/ml). Sphere numbers per 100 cells were calculated (a) and sphere sizes (b) were measured at day 10. **B.** RT-PCR (a) and real-time RT-PCR (b) analyses of the indicated gene expression in primary prostate cells (P0) and prostaspheres of the 1st (P1) and 8th (P8) generations. **C.** Real-time RT-PCR analyses of *Fgfr1* expression in primary prostate cells and prostaspheres. M, DNA molecular weight markers; B, basal epithelial cells; L, luminal epithelial cells; St, stromal cells, Sp, prostasphere cells; *, P≤0.05.

In addition, *Frs2α,* an adaptor protein required for the FGFR to activate ERK and PI3K/AKT pathways, was also expressed in prostaspheres (Fig. 3.1Ba). While *Fgfr2* expression remained stable in primary, P1 and P8 prostaspheres, *Fgfr1* expression was reduced in P8 prostaspheres (Fig. 3.1Bb). Real time RT-PCR analyses of primary prostate cells showed that *Fgfr1* was predominantly expressed in stromal cells (Fig. 3.1C). However, basal cells and prostaspheres also had a trace amount of *Fgfr1* expression.

Inhibition of FGF signaling impairs self-renewal of prostaspheres

To determine whether FGF signaling was critical in prostasphere formation, spheres were treated with FGFR tyrosine kinase inhibitor 341608. The results showed that prostasphere formation was suppressed by 341608 (Fig. 3.2A). Real-time RT-PCR analyses revealed that the inhibitor concurrently increased expression of CK18 and AR and decreased expression of P63 (Fig. 3.2B), suggesting a transition from basal to luminal cells. To further test the role of FGFR signaling in basal cell maintenance, we treated the $K5^{H2B/GFP}$ reporter-bearing prostate spheres with FGFR inhibitors. The GFP^{+} cells were reduced in the inhibitor group (Fig. 3.2C). This indicated that inhibition of FGF signaling in prostasphere cells led to loss of CK5 expression, suggesting that the cells underwent differentiation.

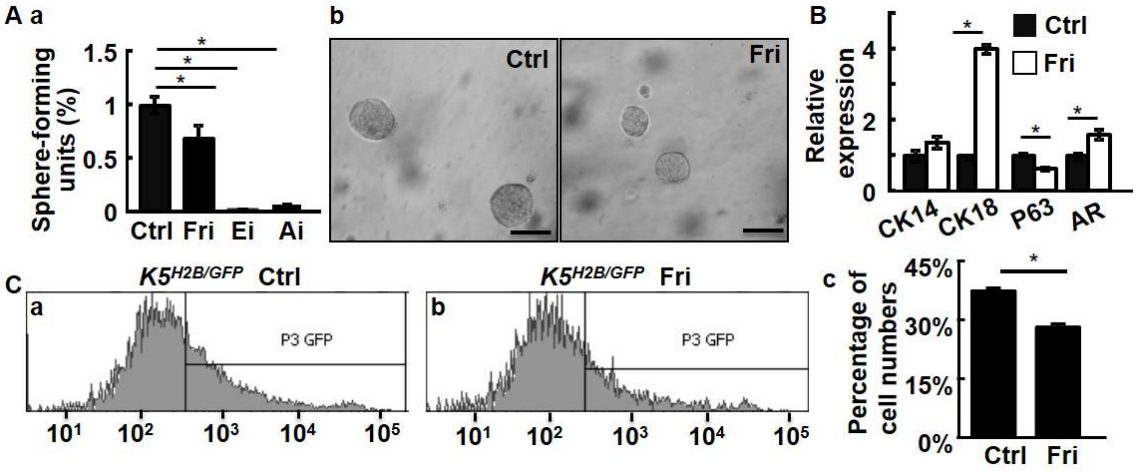

Fig. 3. 2. Inhibition of FGF signaling suppresses prostasphere formation.

A. Prostasphere cultures were carried out with or without the indicated inhibitor for 6 days. Spheres with a diameter greater than 60 μm were scored (a). Representative spheres were shown in b. **B.** Real-time RT-PCR analyses of the indicated genes expression in prostaspheres with or without treating with 500 nM FGFR inhibitors. **C.** *K5*$^{H2B/GFP}$ spheres were treated with 500 nM FGFR inhibitors and GFP positive cells were detected by FACS (a&b). The quantitative data are shown in panel c. **D.** The prostasphere cultures were treated with 500 nM FGFR inhibitor and phosphorylation of ERK and AKT was analyzed with Western blot (a) or immunostaining (b) analyses. **E.** Prostaspheres were cultured with or without 10μm ERK or AKT inhibitors. Rev indicates that the inhibitors were removed 6 days later. Representative pictures are shown in panel a and real-time RT-PCR analyses of the indicated genes expression are shown in panel b. **F.** Panel a, primary *Frs2*α^{cn} and *Frs2*$\alpha^{f/f}$ prostate cells were cultured in Matrigel and the spheres were quantitated at day 10. Panel b, prostate cells prepared from *Frs2*α^{cn} prostate were cultured in the presence of absence of 10 ng/ml FGF7 or FGF10. The sphere numbers were scored at day 10. Panel c. Total RNA extracted from *Frs2*$\alpha^{f/f}$ or *Frs2*α^{cn} prostates were subjected to real time RT-PCR of the indicated genes. Panel d, FACS analyses showing reduced P-bSCs in individual prostate lobs of *Frs2α*^{CN} prostates. AP, anterior prostate; VP, ventral prostate; DLP, dorsolateral lobes; Ctrl, solvent control; Ai, AKT inhibitor; Ei, ERk inhibitor; Fri, FGFR inhibitor; pERK, phosphorylated ERK; pAKT, phosphorylated AKT; AR, androgen receptor; WT, *Frs2α*$^{f/f}$; CN, *Frs2α*^{CN}; Data are normalized with α-actin loading control and expressed as mean±sd from triplicate samples; *, P≤0.05.

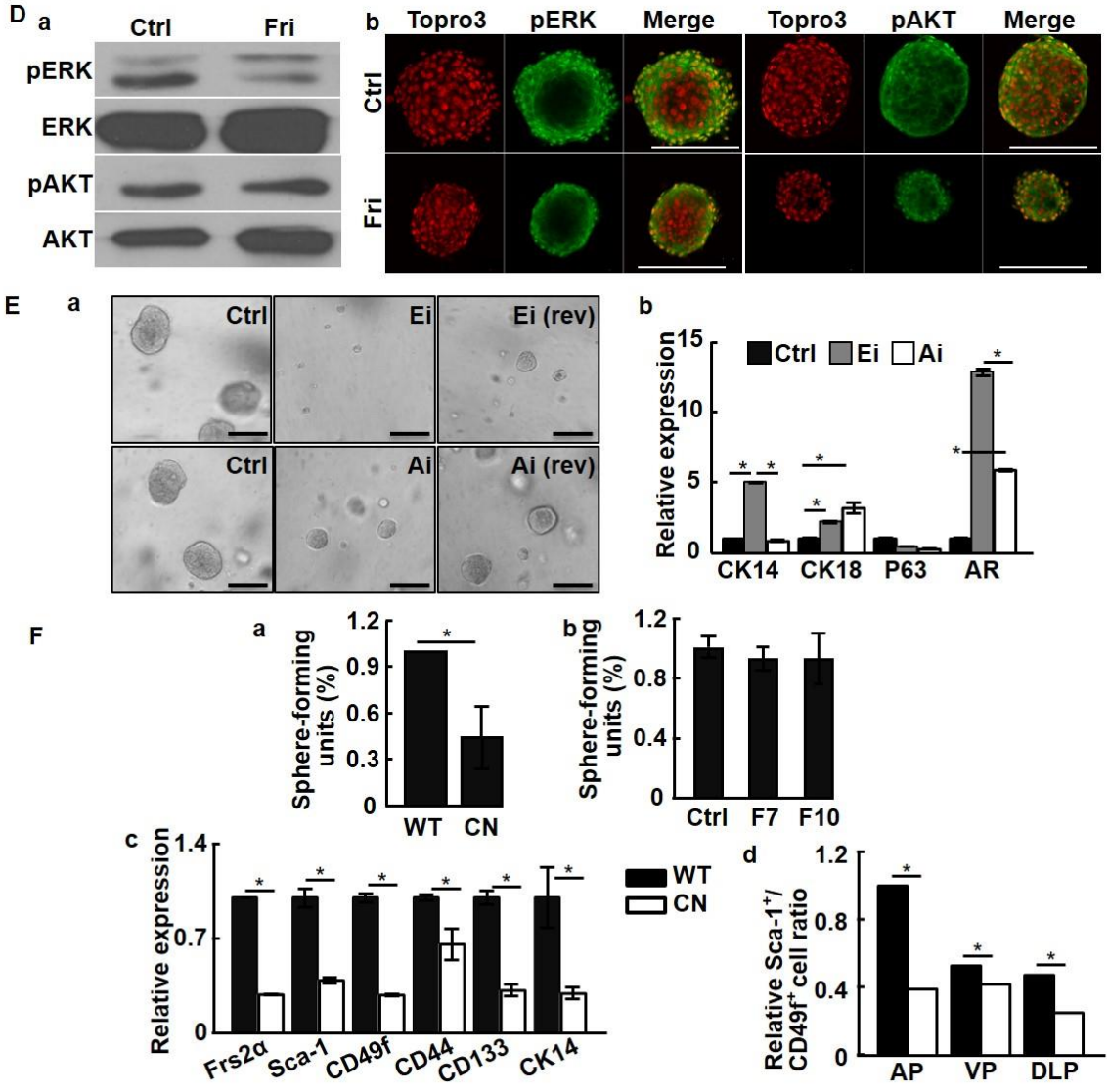

Fig. 3.2. Continued.

We then employed Western blot and immunostaining analyses to determine whether activation of the ERK or PI3K/AKT pathway, the two major signaling pathways downstream of the FGFR, was affected by FGFR inhibition in prostasphere (Fig. 3.2D). Both analyses revealed that only phosphorylated ERK, but not phosphorylated AKT, was compromised by FGFRi treatment (Fig. 3.2D). To further clarify whether the two pathways contributed to prostasphere growth, SL327, an ERK inhibitor (ERKi), or LY294002, an AKT inhibitor (AKTi) was added to the sphere culture medium for 6 days. The results indicated that both ERKi and AKTi suppressed prostasphere growth (Fig. 3.2Ea). This was despite the fact that inhibition of FGFR signaling did not reduce phosphorylation of AKT. Interestingly, withdrawal of AKTi, but not ERKi, partially restored sphere formation. This suggested that the effect of AKTi on prostasphere suppression was reversible while that of ERKi was irreversible. The result was consistent with a previous report that suppressing AKT signaling compromised proliferation of prostate sphere-forming cells without affecting cell survival (82). However, both pathways had pro-differentiation functions in prostaspheres (Fig. 3.2Eb).

FRS2α is an adaptor bridging FGFR tyrosine kinases and downstream signaling pathways. To determine whether FRS2α was required for prostasphere formation, *Frs2*α alleles were tissue-specifically ablated in prostate epithelial cells using *Nkx3.1*^{Cre} as described (83). Ablation of *Frs2α* significantly reduced the sphere forming activity of primary prostate cells (Fig. 3.2Fa). In addition, FGF7 and FGF10 failed to promote sphere forming activity in *Frs2*α null cells,

suggesting that FRS2α was required for FGF7/10 to promote prostasphere formation and growth (Fig. 3.2Fb). RT-PCR analyses further demonstrated that ablation of *Frs2α* reduced expression of stem cell markers in the prostate, including Sca-1, CD49f, CD44, and CD133, as well as the basal cell characteristic CK14 (Fig. 3.2Fc). Furthermore, Sca-1^+/$CD49f^+$ cells were reduced in all the lobes of *Frs2α* null prostates (Fig. 3.2Fd).

Ablation of FGF signaling specifically in P63-expressing cells suppresses prostasphere formation

Since sphere-forming cells expressed basal cell characteristic P63, and P63-expressing cells were capable of giving rise to all cell types in the spheres, we then investigated whether FGFR1 and FGFR2 in $P63^+$ basal cells played a role in prostasphere formation. Prostaspheres derived from mice bearing $P63^{CreERT2}$ and either *Fgfr1* floxed ($Fgfr1^{f/f}$), or *Fgfr2* floxed ($Fgfr2^{f/f}$), or both ($Fgfr1/2^{f/f}$) were treated with 4-OHT to delete the $Fgfr1^{f/f}$ and/or $Fgfr2^{f/f}$ alleles. PCR analyses showed that the floxed sequences were deleted in the cells bearing $Fgfr1^{f/f}/P63^{CreERT2}$, $Fgfr2^{f/f}/P63^{CreERT2}$, and $Fgfr1/2^{f/f}/P63^{CreERT2}$ alleles (Fig. 3.3A), which are hereafter designated as $Fgfr1^{bKO}$, $Fgfr2^{bKO}$, and $Fgfr1/2^{bKO}$, respectively. The results showed that deleting *Fgfr2* or both *Fgfr1* and *Fgfr2* reduced sphere-forming activities, indicating that intact *Fgfr2* alleles were required for prostasphere formation (Fig. 3.3Ba).

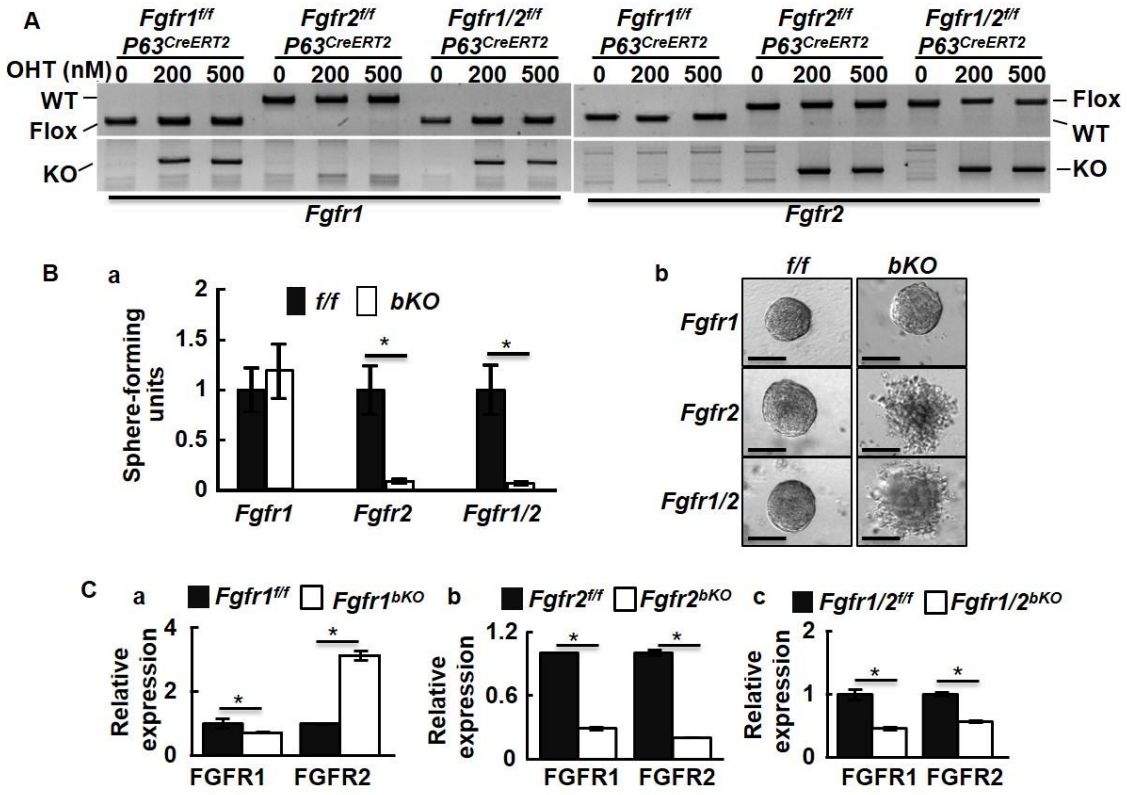

Fig. 3. 3. FGFR2 signaling is required for prostasphere formation.

A. PCR analyses of gene ablation in prostaspheres. **B.** Prostaspheres were cultured in the presence of absence of 4-hydroxytamoxifen to induce gene ablations. Relative sphere forming unites were calculated (a) and morphology of the spheres were shown (b). **C.** Real-time RT-PCR analyses of *Fgfr1* and *Fgfr2* expression in the indicated cells with or without 4-hydroxytamoxifen treatment. OHT, 4-hydroxytamoxifen; *, P≤0.05; data shown represents means ± sd from three mice.

Deleting *Fgfr1* alone did not affect prostasphere formation. In addition, deleting *Fgfr2,* or both *Fgfr1 and Fgfr2,* but not *Fgfr1,* at day 1 of primary culture impaired sphere integrity (Fig. 3.3Bb). Real-time RT PCR revealed that ablation of *Fgfr1* resulted in elevated *Fgfr2* expression. In contrast, the deletion of*Fgfr2* in prostaspheres caused the concomitant decline of *Fgfr1* expression (Fig. 3.3C).

FGFR2 signaling in P-bSCs upregulates the Wnt pathway and suppresses apoptosis

Wnt signaling enhances the self-renewal of prostate basal/stem cells and promotes expansion of "triple positive" ($CK5^+$, $CK8^+$, $p63^+$) prostate progenitor cells (84). The basal progenitor cells have high Wnt signaling activity that is positively correlated with the basal cells number (85). Interestingly, ablation of *Fgfr1* in p63-expressing cells increased, while ablation of *Fgfr2* reduced, β-catenin levels as shown by qPCR (Fig. 3.4Aa) and immunofluorescence staining (Fig. 3.4Ba). We reported earlier similar results in dental epithelial stem cells (77). Together with the data that *Fgfr2* expression was increased in *Fgfr1* ablated cells (Fig. 3.3C), the results indicated that FGFR2 enhanced Wnt signaling and enhanced self-renewal of P-bSCs.

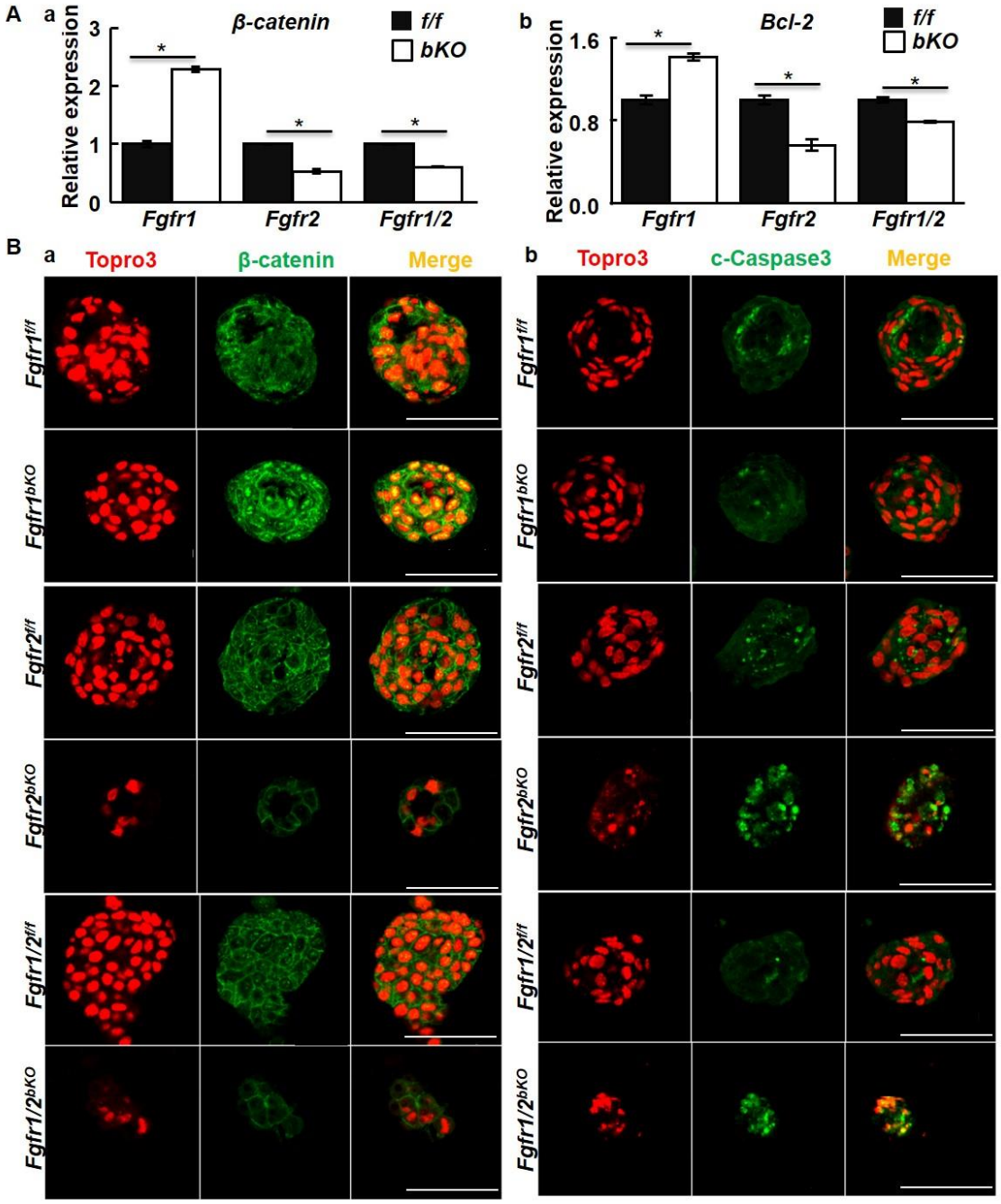

Fig. 3. 4. FGFR2 signaling in P-bSCs upregulates the Wnt pathway and suppresses apoptosis.

A. The indicated prostaspheres treated with 4-hydroxytamoxifen at day 2 after inoculation were harvested at day 10. Expression of *β-catenin* or *Bcl-2* was assessed by real-time RT-PCR. **B.** Immunostaining with anti-β-catenin or anti-c Caspase 3 antibodies for the same spheres. Ctrl, solvent control; OHT, 4-hydroxytamoxifen; c-Caspase3, cleaved caspase 3; *, P≤0.05.

Real-time RT PCR and immunofluorescence staining showed that expression of BCl-2 was decreased (Fig. 3.4Ab) while cleaved Caspase 3 was increased upon *Fgfr2* deletion or *Fgfr1/2* double deletion (Fig. 3.4Bb), indicative of augmented cell apoptosis in the spheres.

Thus, the results suggested that loss of FGFR2 signals promoted P-bSC apoptosis. Although both were induced by the loss of FGFR2 signaling, whether the loss of stemness and commitment to apoptosis have a causal link needs to be further investigated.

FGFR2 is required for maintenance of basal cell homeostasis in adult prostates

To assess the effect of ablation of *Fgfr1* or *Fgfr2* in basal cells in the adult prostate, mice carrying *Fgfr1*$^{f/f}$*-P63*^{CreERT2}, *Fgfr2*$^{f/f}$*-P63*^{CreERT2}, or *Fgfr1/2*$^{f/f}$*-P63*^{CreERT2} alleles were treated with tamoxifen for 5 consecutive days. Real-time RT-PCR analyses showed that expression of *Fgfr1* and *Fgfr2* in the dissociated basal cells was reduced a week later (Fig. 3.5A). Prostate cells were dissociated and basal and luminal cell populations were analyzed with a cell sorter (Fig. 3.5B).

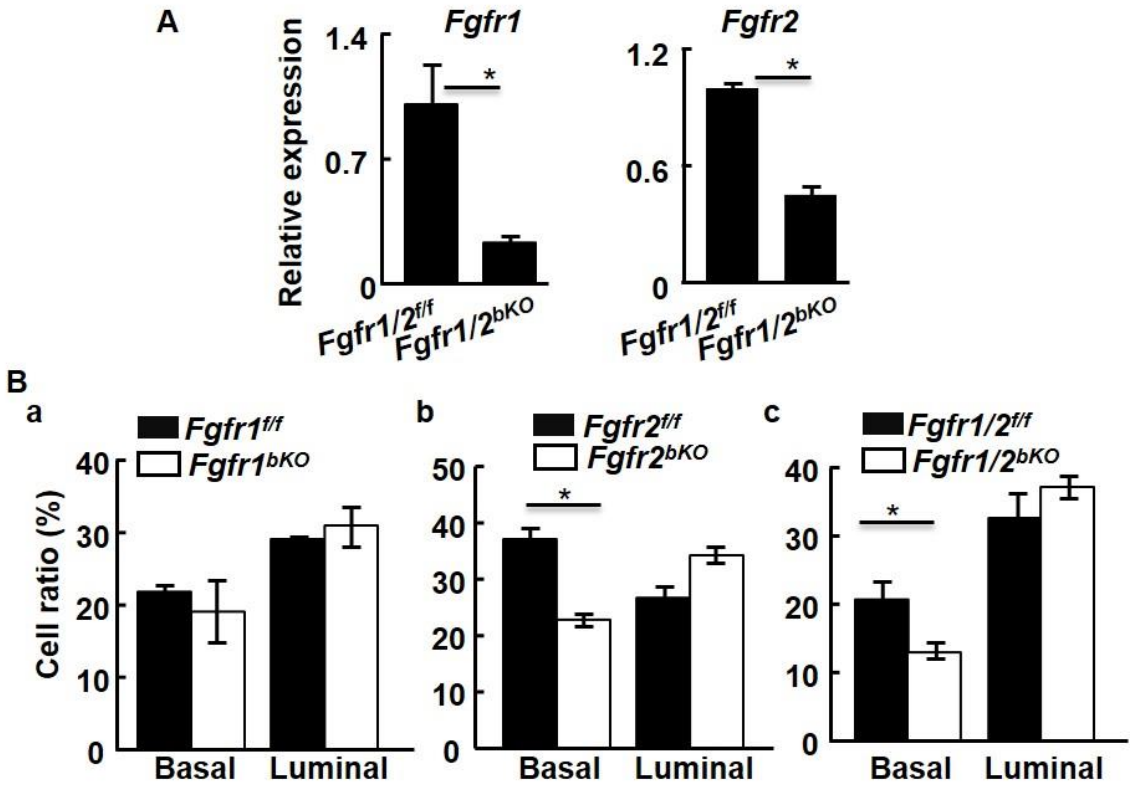

Fig. 3. 5. FGFR2 is required for maintaining basal cell homeostasis in the adult prostate.

A&B. The indicated mice were injected I.P. with tamoxifen for 5 consecutive days at the age of 8 weeks. The prostates were harvested a week later and isolated basal cells were subjected to RT-PCR analyses (A) or FACS analyses for cellular compositions (B). **C**. Immunostaining of $P63^{+}$ cells in the indicated prostate with or without tamoxifen injection. Representative pictures from three mice were shown. **D**. Sphere-forming analyses of FACS-fractionated basal cells from mice with the indicated genotype. F/F. homozygous floxed alleles; bKO, basal cell specific knock out; data represent means ± SD from three mice; *, P≤0.05.

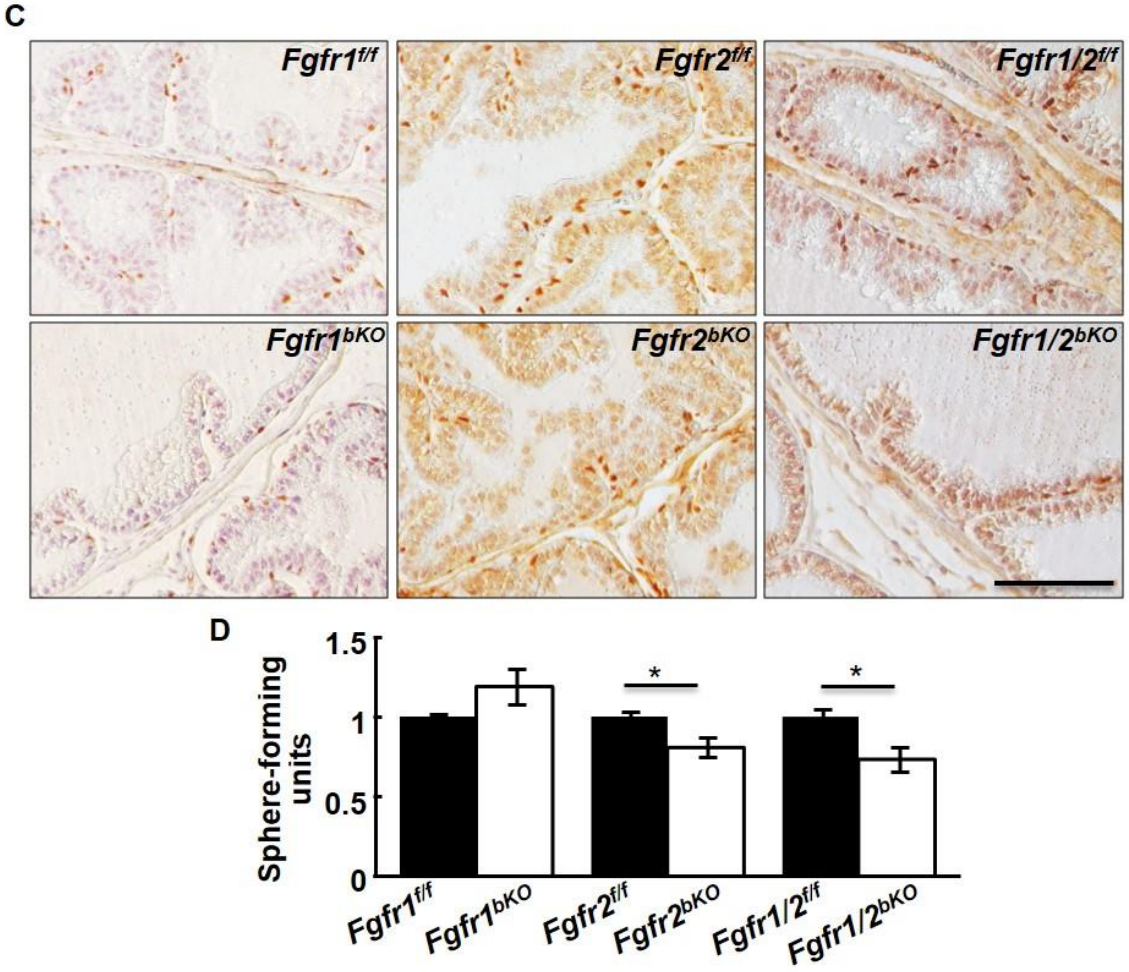

Fig. 3.5. Continued.

Deletion of both *Fgfr1* and *Fgfr2* reduced the number of basal cells by 38% and increased luminal cells by 14%. The total number of stromal cells remained the same. Ablation of *Fgfr2* also alone caused a similar decrease of 39% in basal cells while luminal cells increased by 28%. The single ablation of *Fgfr1* had no

impact on cellular composition of the prostate. P63 mmunostaining further confirmed the reduction in basal cells in *Fgfr2* or *Fgfr1/2* conditional knockout adult prostates (Fig. 3.5C). Furthermore, the sphere-forming activity of *Fgfr2* or *Fgfr1/Fgfr2* double deleted basal cells was impaired (Fig. 3.5D). Together, the results suggested that ablation of *Fgfr2*, but not *Fgfr1*, *in vivo* impaired basal cell homeostasis and enhanced basal-to-luminal cell differentiation. Thus, modulation of FGF signaling in adult basal/progenitor cells can be a determinant in specification of cell lineage.

Disruption of Fgfr2 in P63 expressing cells perturbs prostate morphogenesis

To investigate whether FGF signaling in P63-expressing cells contributed to prostate development, two-week-old mice bearing *Fgfr1/P63*^{CreERT2}, *Fgfr2/P63*^{CreERT2}, or *Fgfr1/2/P63*^{CreERT2} alleles were injected I.P. with tamoxifen to activate the Cre recombinase. Ablation of *Fgfr2* reduced the size of the prostate by 20% at 6 weeks of age (Fig. 3.6A). In addition, the complexity of epithelial enfolding and the ductal network were also reduced (Fig. 3.6B). Consistent with our *in vitro* sphere assay data, ablation of *Fgfr2* in prostates *in vivo* induced apoptosis, as shown by the reduction of anti-apoptotic protein Bcl-2 expression (Fig. 3.6C).

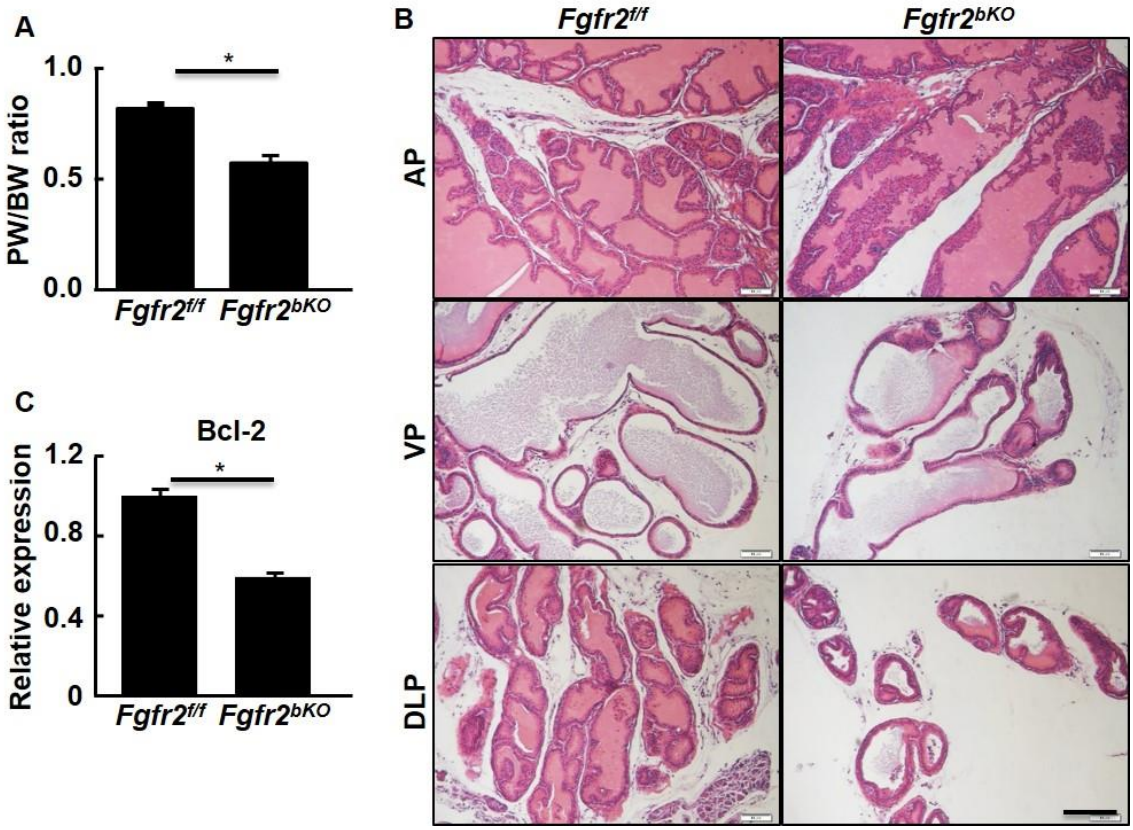

Fig. 3. 6. Disruption of Fgfr2 in P63 expressing cells perturbs prostate morphogenesis.

A. Prostate versus body weight ratio showing ablation of *Fgfr2* in basal cells compromised prostate growth. **B.** Prostate tissues from 6-week-old mice were dissected, sectioned and H&E stained. **C**. Real time RT-PCR analyses showing reduced expression of *Bcl-2* in *Fgfr2*^{bKO} prostate. **D**. Immunostaining showing reduced P63^{+} basal cells (a) and Ki67^{+} proliferating cells (c) in *Fgfr2*^{bKO} prostate. Average cell numbers calculated from three samples were shown in panels b and d, respectively. **E.** Prostate sections of 6-week-old *Fgfr1/2*^{bKO} mice were immunostained with anti-Ki67 antibodies and the Ki67 positive cells were quantitated. **F.** Sphere-forming efficiency of the indicated primary prostate cells was analyzed. Average numbers of positive cells were calculated from 3 individuals and expressed as mean ± sd. *, P≤0.05

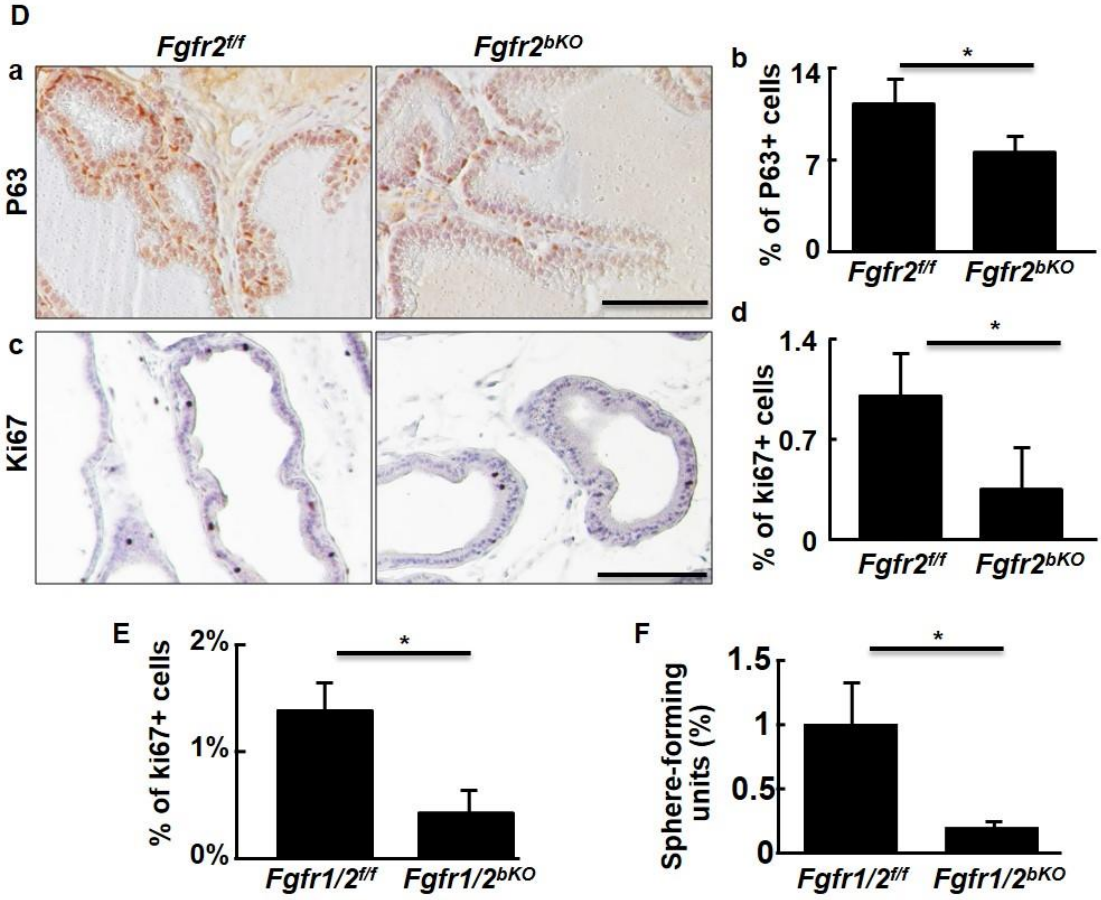

Fig. 3.6. Continued.

The *Fgfr2*^{bKO} prostate also had reduced basal cells and proliferating cells, as demonstrating by P63 and Ki67 immunostaining, respectively (Fig. 3.6D).

Similarly, double ablation of *Fgfr1* and *Fgfr2* also reduced cell proliferation in developing prostate (Fig. 3.6E), as well as decreased prostasphere-forming P-bSCs (Fig. 3.6F). Ablation of *Fgfr1* alone in basal cells had no effect (data not

shown). The results demonstrated that FGFR2 in p63^{+} basal cells was required for prostate development. The results are in line with our previous reports that ablation of *Fgfr2*, but not *Fgfr1* in prostate progenitor cells impairs prostate branching morphogenesis (45,86).

Discussion

Prostasphere culture is a method for study and quantitation of self-renewal of both human and mouse P-bSCs (19,29,30). In this report, we showed that FGF signals mediated by the FGFR2-FRS2α pathway were required for prostasphere formation, growth, and maintenance. This indicates that FGF signals mediated by the FGFR2 isotype in particular are required for self-renewal and maintenance of P-bSCs. In addition, we also demonstrated that FGFR2 signaling was required for maintenance of basal cell homeostasis in the prostate. Unlike the prostasphere culture that is suitable for P-bSCs, the recently reported organoid culture methods are suitable for luminal P-lSCs (34,41). Interestingly, constitutive activation of Notch signaling improves the sphere-forming activity of luminal cells under the same sphere culture condition (82). The hierarchy of the two P-SC populations and whether FGF signaling has similar roles in P-bSCs and P-lSCs remains to be characterized

Chapter II has already shown the cellular differentiation from common progenitor cells, specifically P63-expressing prostate basal stem cells, to daughter basal

cells and luminal cells. In this study, FGFR2 in P63-expressing cells safeguards prostate basal cell self-renewal, as well as ensures the proper differentiation from basal cells to luminal cells. Adult mouse prostate basal cells and luminal cells are independently self-sustained in their native microenvironment. However, external insults, such as inflammation, alters the differentiation program of basal cells. Acute prostatitis induces the differentiation of basal cells to luminal cells (87). Conditional ablation of Pten in prostate basal cells also promotes basal-to-luminal differentiation (39). Our study shows that conditional knockout of FGFR2 in prostate P63-expressing basal cells promotes basal-to-luminal differentiation.

FGFR1 and FGFR2 have different roles in prostate development (45,86) as well as in prostate cancer development. FGFR1 activation initiates early stages of tumor development while FGFR2 generally is associated with inhibition of tumor growth (88-90). Down-regulation of FGFR2 is associated with malignant progression in human prostate (91). Our data shows that down-regulation of FGFR2 prompts the differentiation from basal to luminal cells. FGFR2 may be among prostate cancer susceptibility genes in tumors fueled by basal stem cells due to lack of differentiation.

CHAPTER IV

OVEREXPRESSION OF FGF9 IN PROSTATE EPITHELIAL CELLS AUGMENTS REACTIVE STROMA FORMATION AND PROMOTES PROSTATE CANCER PROGRESSION

Introduction

The prostate consists of epithelial and stromal compartments separated by a basement membrane. Cells in the two compartments maintain active two-way communication through paracrine mechanisms in which ligands and receptors are partitioned between the two compartments (92,93). These precisely balanced reciprocal communications are critical for preserving tissue homeostasis. It is well documented that the accumulation of somatic mutations in epithelial cells is able to cause adenocarcinoma. Prostate carcinoma cells are surrounded by a complex microenvironment, called prostate reactive stroma, which includes extracellular matrix (ECM), diffusible growth factors and cytokines, and a variety of non-epithelial cell types. The tumor microenvironment also has a profound influence on the development and progression of carcinomas (94) and PCa is no exception. Tumor-associated reactive stroma emerges as early as the formation of pre-malignant prostatic intraepithelial neoplasia (PIN), and arises due to modulation of a large spectrum of cell signaling, either due to stimuli from epithelial cells or intrinsic genetic or epigenetic changes (95-99). Prostate reactive stroma promotes PCa progression

by supporting tumor cell proliferation, inducing a fibroblastic phenotype, remodeling the extracellular matrix, and augmenting metastasis (95).

Fibroblast growth factor (FGF) signaling is essential for prostate development and prostate tissue homeostasis (45,83). Deregulation of FGF signaling has been implicated in developmental disorders and tumorigenesis in various tissues (68). Extensive evidence shows that abnormal expression of FGF or FGFR isoforms and activation of the FGF/FGFR signaling axis are associated with PCa development and progression (83,90,100-104). Amplification of the *Fgfr1* gene is frequently found in human PCa (105). The acquisition of ectopic expression of FGFR1 in tumor epithelial cells stands out as the most frequent change among FGFR isotypes (106-109). Forced expression of constitutively active FGFR1 or multiple FGF ligands has been shown to induce prostate lesions in mouse models (78,89,90,110-115). Ablation of *Fgfr1* or *Frs2*α significantly reduces mouse PCa development and progression induced by T antigens (83,86). However, how aberrant FGF signals contribute to PCa progression is still not fully understood.

Accumulating evidence supports a role for FGF9 in PCa progression and metastasis. Previous studies have shown that FGF9 mediates osteogenesis induced by androgen receptor-negative human PCa cells (110). In addition, FGF9-positive PCa shows higher risk of biochemical recurrence (116). In spite of the correlation between FGF9 and PCa progression and bone metastases, whether overexpressed FGF9 initiates prostate tumorigenesis is still elusive. To

study whether FGF9 overexpression contributes to PCa initiation and progression, transgenic mice expressing FGF9 in prostate epithelial cells were generated and crossed with the TRAMP mouse model. Forced expression of FGF9 in the prostate led to PIN in a time dependent manner. Furthermore, it augmented the formation of reactive stroma and accelerated PCa progression in TRAMP mice. Both *in vivo* and *in vitro* data showed that activation of c-Jun-dependent TGF-β1 expression in prostate stromal cells by FGF9 constituted a paracrine loop that contributed to PCa progression. Moreover, in silico analyses of the TCGA database demonstrated that expression of FGF9 was correlated with that of TGF-β1 and its downstream effectors. Together, the results support a mechanism by which FGF9 overexpression in PCa contributes to PCa progression and metastasis.

Materials and Methods

Animals

All animals were housed in the Program for Animal Resources of the Institute of Biosciences and Technology, and were handled in accordance with the principles and procedures of the Guide for the Care and Use of Laboratory Animals. All experimental procedures were approved by the Institutional Animal Care and Use Committee. Mice carrying the *FGF9* and the TRAMP transgenes were bred and genotyped as described (69). Primers are, FGF9 forward:

CTTTGGCTTAGAATATCCTTA; FGF9 reverse: AGTGACCACCTGGGTCAGTCC; TRAMP forward: CCGGTCGACCGGAAGCTTCCA CAAGT; TRAMP reverse: CTCCTTTCAAGACCTAGAAGGTCCA. Prostate tissues and metastatic tumors were harvested after the animals were euthanized by CO_2 asphyxiation. Nude mice were purchased from Charles River Laboratory and maintained in standard conditions according to the Institutional Guidelines.

Generation of transgenic mice

The full-length rat FGF9 cDNA including the Kozak sequence was amplified by PCR using rat FGF9 cDNA as the template. After digestion with BamHI and EcoRV, the PCR product was subcloned into the pBluescript SK vector and sequenced. The insert was excised with the two restriction enzymes and cloned into the SSI vector (89). The ARR2PB-FGF9 transgene was excised with BssHII restriction enzyme and purified for pronuclear microinjection. Fertilized eggs were collected from FVB females and pronuclei were injected with the ARR2PB-FGF9 DNA construct. Injected eggs were transferred into pseudo-pregnant Swiss/Webster females for full-term development. Genomic DNA was purified from tails of founder mice at day 7 after birth and screened by PCR.

Histology

Prostates were dissected and sectioned for histological analyses as previously described (45,69). Hematoxylin and Eosin staining, immunohistochemical

analyses, and in situ hybridization were performed on 5-µm sections mounted on Superfrost/Plus slides (Fisher Scientific, Pittsburgh, PA). Antigens were retrieved by incubation in citrate buffer (10 mmol/L) for 20 minutes at 100 °C or as suggested by antibody manufacturers. The sources and concentrations of primary antibodies used are: anti-α-smooth muscle actin (1:1) from Sigma (St Louis, MO); anti-Vimentin (1:200), anti-E-cadherin (1:200) from Cell Signaling Technology; anti-androgen receptor (1:200) from Santa Cruz; anti-CD31 (1:200) from Abcam; anti-Ki67 (1:500) from Novus Biologicals. For immunofluorescence, the specifically bound antibodies were detected with FITC-conjugated secondary antibodies and visualized on a Zeiss LSM 510 Confocal Microscope. For immunohistochemical staining, specifically bound antibodies were detected with biotinylated anti-Rabbit IgG or biotinylated anti-mouse IgG antibodies (Vector labs). The signal was enhanced using the VECTASTAIN ABC system and visualized with a VECTOR NovaRED Substrate kit. Prostate lesion grading was performed as described (17,117).

Isolation of primary stromal cells

Prostates were dissected and single primary prostate cells were obtained as described (118). Briefly, prostates dissected from 4 to 8-month-old male mice were minced with steel scissors, followed by incubation with 1 mg/ml collagenase (Sigma) in 10 ml DMEM with 10% FBS at 37 °C for 90 minutes. Cells were washed with PBS and further digested with 0.25% trypsin/EDTA for 10 minutes at 37 °C. After inactivation of trypsin by FBS, cells were passed

through a 40-μm cell strainer, washed with DPBS (Sigma) and seeded in 10-cm cell plates. After overnight incubation at 37 ^{o}C, the unattached cells were removed and only attached stromal cells remained in culture. Both mouse primary prostate stromal cells and human prostate stromal HPS-19I cells were cultured as described (95).

Luciferase assay

A pGL3 plasmid containing the full-length TGF-β1 promoter region (119) was kindly provided by Dr. Zhengxin Wang, University of Texas MD Anderson Cancer Center. Luciferase assay was done following the instructions of dual-luciferase reporter assay system (Promega).

Immunoblotting

Dissected prostate tissues or prostate cancer cells were homogenized in RIPA buffer (50 mM Tris-HCl buffer pH 7.4, 1% NP40, 150 mM NaCl, 0.25% Na-deoxycholate, 1 mM EGTA, and 1 mM PMSF). Extracted soluble proteins were harvested by centrifugation. Samples containing 50 μg proteins were separated by SDS-PAGE and electroblotted onto PVDF membranes for Western Blotting analysis with the indicated antibodies. The dilutions of the antibodies are: anti-cJun, 1:1000; anti-Slug, 1:1000; anti-TGFβ1, 1:1000; anti-pSmad2/3: 1:1000; and anti-β-Actin, 1:3000. Specific bands were visualized using the ECL-Plus chemoluminescent reagents. The films were scanned with a densitometer and the bands were quantified using Image J software (NIH).

Gene expression

For *in situ* hybridization, paraffin-embedded tissue sections were rehydrated, followed by 10 µg/ml protease K digestion for 15 minutes at room temperature. After prehybridization at 65 °C for 2 hours, the hybridization was carried out by overnight incubation at 65 °C with 1 µg/ml digoxigenin-labeled RNA probes for the FGF9 transgene. Nonspecifically bound probes were removed by washing three times with 0.1X DIG washing buffer at 65 °C for 30 minutes. Specifically bound probes were detected by an alkaline phosphatase-conjugated anti-digoxigenin antibody (Roche, Indianapolis, IN).

For real-time RT-PCR analyses, total RNA was extracted from prostates using the TRIzol RNA isolation reagents (Life Technologies). The first-strand cDNAs were reverse transcribed from 1 µg RNA templates using the SuperScript III reverse transcriptase (Invitrogen, Carlsbad, CA) and random primers according to manufacturer's protocols. Real-time RT-PCR analyses were carried out using the Fast SYBR Green Master Mix (Life Technologies) as instructed by the manufacturer.

Chromatin immunoprecipitation (ChIP) assays

For the ChIP experiments, extracts were prepared from primary prostate stromal cells. ChIP assays were carried out with the EZ-Magna ChIP Kit (Millipore, Billerica, MA) according to the manufacturer's protocols. The following set of real-time PCR primers specifically for the c-Jun binding regions on the TGF-β1

promoter was used: TGFβ1-Forward: GGCTGCATCTCCAAGCATT and TGFβ1-Reverse: GGTTCTCATCTCCCACTCACTC.

Results

Overexpression of FGF9 disrupts prostate tissue homeostasis in an expression level- and time-dependent manner

To determine whether FGF9 overexpression caused prostate lesions, we generated 8 strains of ARR2PBi-FGF9 transgenic mice, in which expression of FGF9 in prostate epithelial cells was driven by the ARR2PB composite probasin promoter as described (89). Among them, TG5 and TG12 highly expressed the FGF9 transgene; TG3, TG8, and TG9 expressed the transgene at moderate levels; and TG1, TG2, and TG10 expressed the transgene at low levels (Fig. 4.1A). The Fgf9 expression level in TG12 was shown in Fig. 4.1B. Around the age of 3-8 months, the mice suffered penis protrusion (Fig. 4.1C) and the prostate was fused with the seminal vesicles (Fig. 4.1Da). H&E staining revealed that the prostate developed severe hyperplasia in both stromal (Fig. 4.1Db) and epithelial compartments (Fig. 4.1Dc). Since both TG5 and TG12 that expressed FGF9 at high levels were infertile, the line TG8 with moderate expression levels of FGF9 was chosen for the following studies and hereafter is designated as F9TG.

A

Founder	TG1	TG2	TG3	TG5	TG8	TG9	TG10	TG12
Expression level	L	L	M	H	M	M	L	H
Fertile	Y	Y	Y	N	Y	N	Y	N

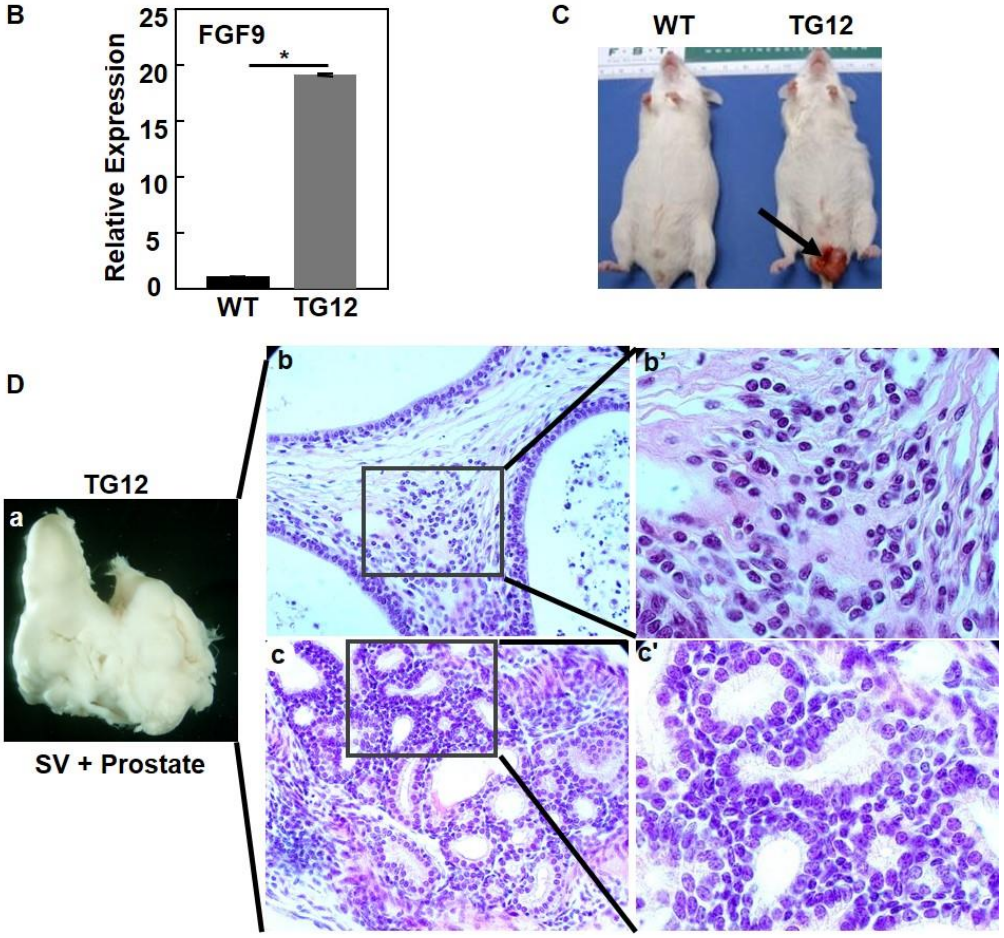

Fig. 4. 1. Overexpression of FGF9 leads to fusion of the prostate and seminal vesicles.

A. Generation of FGF9 transgenic founders. Expression of the transgene was examined with RT-PCR analysis. Note that the two high expressers were infertile. **B**. Agarose gel electrophoresis of PCR products showing expression levels of the FGF9 transgene. **C**. Real time RT-PCR analyses of FGF9 expression in TG12 founder prostate. **D**. TG12 founder developed a penis protrusion. **E**. Fusion of the prostate with seminal vesicles in TG12 founder. **F.** H&E staining showing hyperplasia in both stromal and epithelial compartments. L, low expression level; M, moderate expression level; H, high expression level; WT, wildtype; SV, seminal vesicles.

In situ hybridization demonstrated that the *Fgf9* mRNA was highly expressed in the prostate epithelium of F9TG mice (Fig 4.2A). In contrast, expression of endogenous *Fgf9* mRNA was below the detection limit under the same condition. Real-time RT-PCR analyses showed that the expression level of *Fgf9* in F9TG prostate was 30 fold higher than that of non-transgenic littermates. No apparent difference was observed in the histology and tissue size between F9TG and control prostates at young adult stages. However, mild hyperplasia was detected in the ventral prostates of 8-month-old F9TG mice (Fig. 4.2B). At 11 months of age, F9TG prostates displayed anomalies ranging from multifocal hyperplasia to low grade PIN, with atypical larger cells with irregular hyperchromatic nuclei. At 18 months, F9TG prostates (n=4) progressed to high-grade PIN and invasive carcinoma as shown by the loss of the boundary between epithelium and stroma compartments (Fig. 4.2B). Highly pleomorphic atypical cells arranged in a cribriform pattern were observed in the lumen. Extracellular matrix remodeling and stromal hypercellularity was notable adjacent to the invasive carcinoma. In contrast, WT prostates only showed a few mild hyperplasia lesions. Quantified analyses of 18-month-old mice showed that F9TG prostates developed more prostate lesions, ranging from low grade PIN, high grade PIN, to invasive carcinoma, than control prostates (Fig. 4.2C). Compared with the control prostate, cells in the F9TG prostate were more proliferative (Fig. 4.2D&E). At 11 months of age, F9TG prostates possessed nearly four times as many proliferating epithelial cells as control prostates.

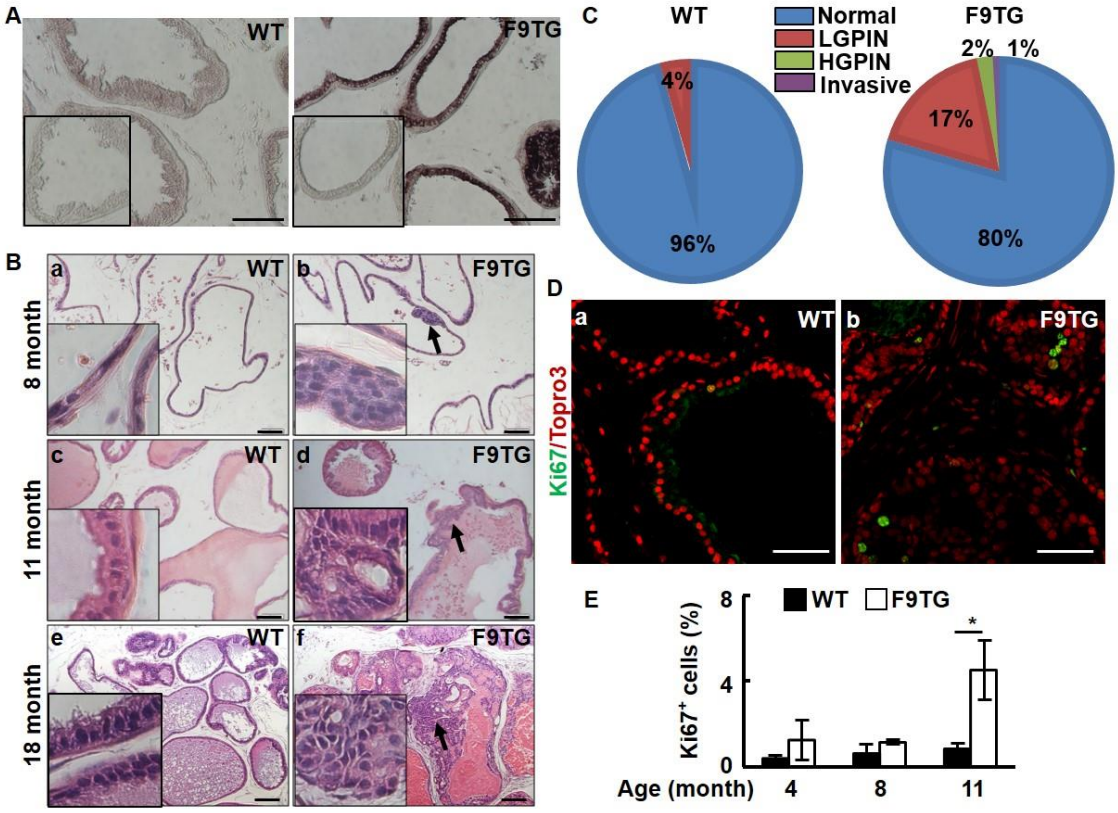

Fig. 4. 2. Forced expression of FGF9 in prostatic epithelial cells disrupts prostate tissue homeostasis.

A. In situ hybridization demonstrates expression of *Fgf9* mRNA in mouse prostate. Inserts are negative control using sense probes. **B**. H&E staining demonstrating prostate lesions in F9TG prostates at 8 months, 11 months, and 18 months. Arrows indicate hyperplasia, LGPIN, and HGPIN. Inserts are high magnification views from the same slides. **C**. Quantitation of the histology of 18-month-old WT and F9TG prostates. N=4 per group. **D.** Immunostaining of Ki67 showing proliferating epithelial cells in 11-month-old WT and F9TG prostates. **E**. Quantitation of Ki67 positive cells in F9TG and control prostates at the indicated ages. **F**. Ki67 staining showing proliferating cells in the stromal compartment. **G**. Immunohistochemical or immunofluorescence analysis with antibodies against androgen receptor, E-cadherin, α-smooth muscle actin, or CD3 of 18-month-old WT and F9TG prostates. WT, wild type; F9TG, FGF9 transgenic mice; HGPIN, high grade prostatic intraepithelial neoplasia; LGPIN, low grade prostatic intraepithelial neoplasia; F9TRAMP, FGF9tg/TRAMP bigenic mice; scale bars, 50 μm.

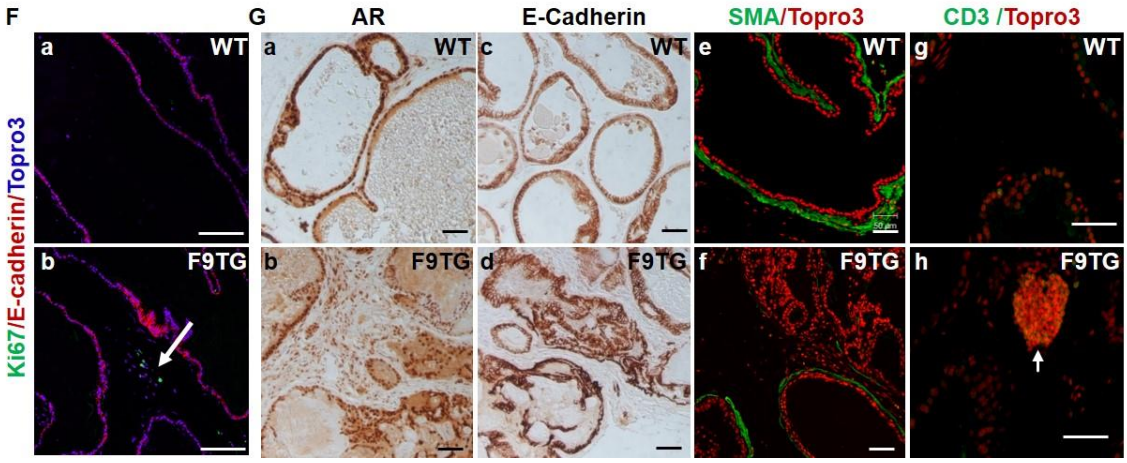

Fig. 4.2. Continued.

Moreover, stromal proliferation became prominent as shown by the Ki67 staining of the cells that did not expressed E-cadherin (Fig 4.2Fa,b). Both androgen receptor (Fig. 4.2G,b) and E-cadherin (Fig. 4.2Gc,d) expressions in F9TG prostates appeared to be similar to that of control prostates. However, the smooth muscle-like stromal cells were reduced adjacent to the high-grade PIN lesions (Fig. 4.2Ge,f). Clusters of CD3 positive cells were particularly notable in the stromal region of F9TG prostates (Fig. 4.2Gg,h), indicating the presence of T lymphocyte infiltrations. Together, the data suggest that overexpressing FGF9 disrupts prostate tissue homeostasis in both epithelial and stromal compartments.

Overexpressed FGF9 promoted initiation and progression of TRAMP tumors

To determine whether overexpression of FGF9 contributed to PCa initiation and progression, F9TG mice were crossed with TRAMP mice to generate FGF9/TRAMP bigenic mice (hereafter designated as F9TRAMP). *In situ* hybridization (Fig. 4.3A) and real-time RT-PCR (Fig. 4.3B) analyses revealed that FGF9 was highly expressed in the epithelium of the F9TRAMP prostate. F9TRAMP mice had a median survival time of 218 days, which was shorter than that of TRAMP mice that had a median survival time of 234 days. Although similar at early ages, the average weight of F9TRAMP prostates (n=13) was heavier than that of TRAMP prostates (n=10) at the age of 6 months or older (Fig. 4.3C). Since the majority of lesions in the TRAMP prostate were initiated in ventral prostate (17), H&E staining was carried out to analyze the lesion development in F9TRAMP ventral prostates at the ages of 3, 4, and 6 months (Fig. 4.3D). Apoptotic bodies were prominent in 4-month F9TRAMP ventral prostates. Cribriform architecture was seen in 6-month-old TRAMP ventral prostates, while F9TRAMP mice already developed poorly differentiated prostate cancer, composed of sheets of cells with little or no glandular formation. To quantitate the lesion development, the standardized prostate lesion grading system (17,117) was employed to assess the severity of the lesions at the ages of 3 and 6 months (Fig. 4.3E). The F9TRAMP prostates had more high-grade lesions in both groups than the TRAMP prostates. About 54% of the F9TRAMP

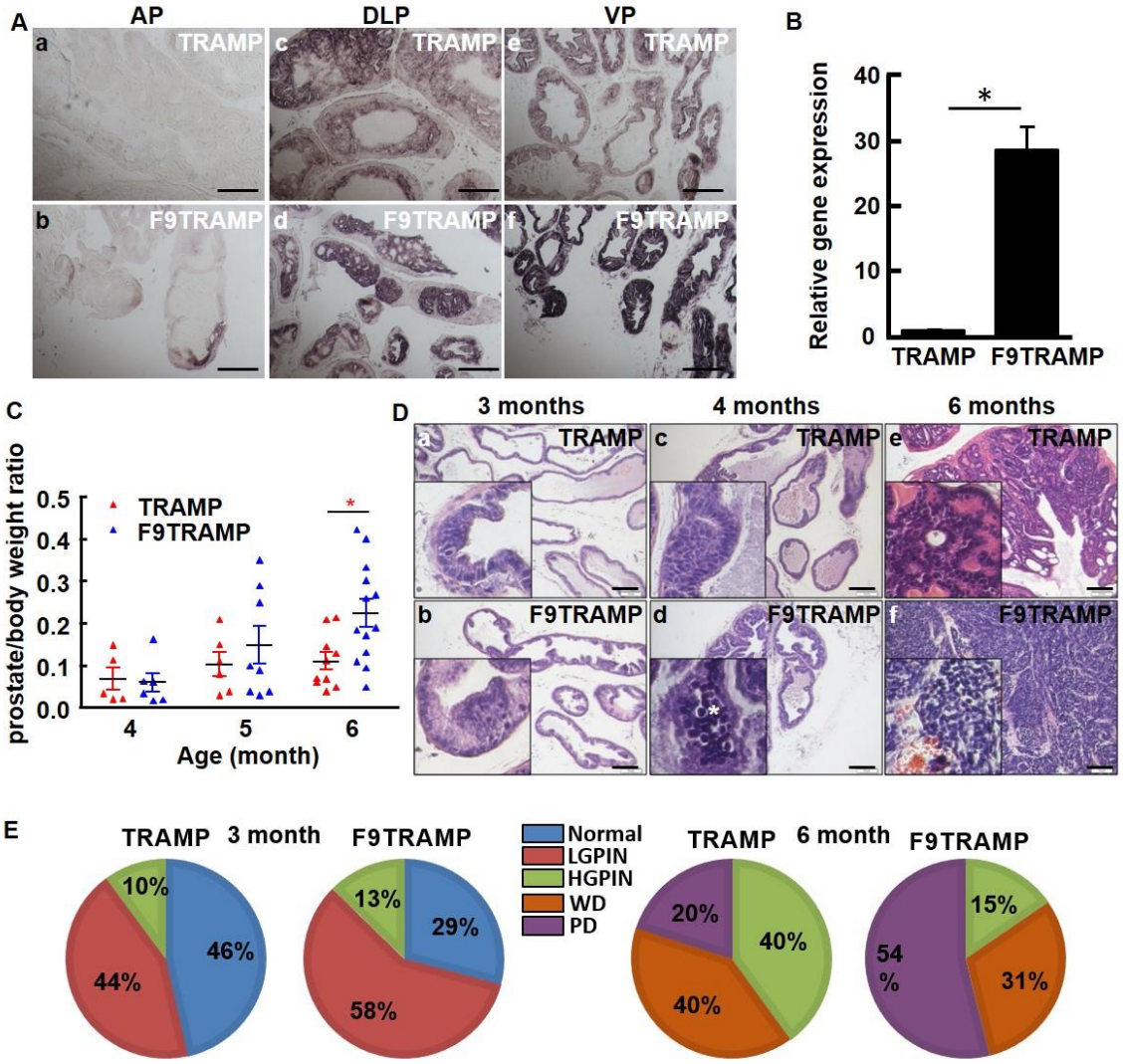

Fig. 4. 3. Overexpression of FGF9 in prostatic epithelial cells promotes PCa progression in mice.

A. In situ hybridization showing expression of *Fgf9* mRNA in mouse prostates. **B.** Real-time RT-PCR analyses of *Fgf9* expression in TRAMP and F9TRAMP prostates at 4 months. **C.** H&E staining of TRAMP and F9TRAMP prostates at the ages of 3, 4, and 6 months. **D.** Statistical analysis of prostate/body weight ratio of TRAMP and F9TRAMP prostates at the ages of 4, 5, and 6 months. **E.** Quantitative analyses of prostate lesions of TRAMP and F9TRAMP mice at the age of 3 or 6 months. N=5 per group. **F.** Immunostaining comparing AR, P63, and Ki67 expression in TRAMP and F9TRAMP prostates. Statistical analyses of proliferating cells in TRAMP and F9TRAMP prostates at the indicated ages. Scale bars, 50 μm

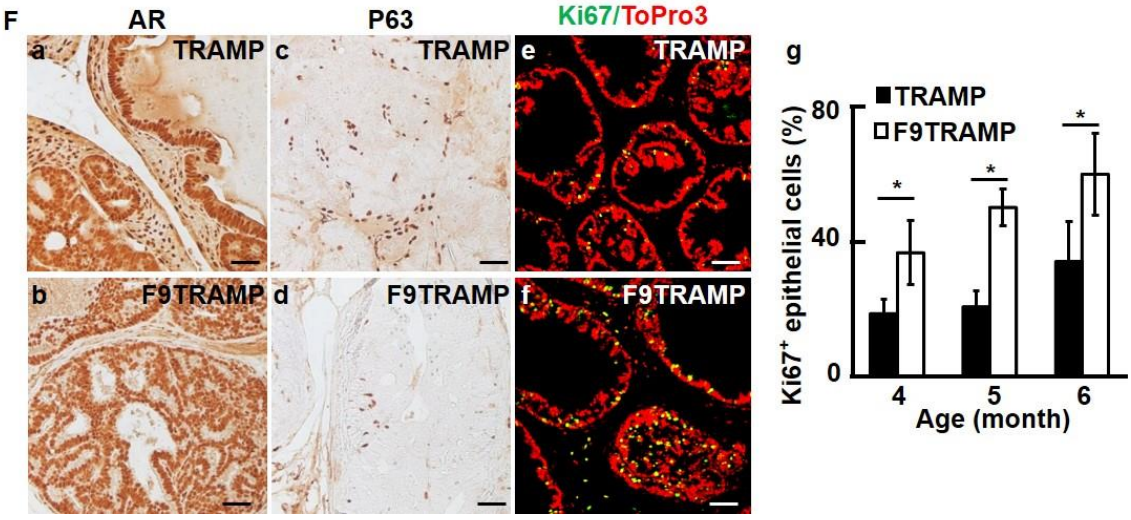

Fig. 4.3. Continued.

prostate had poorly differentiated (PD) carcinomas, while only 20% TRAMP mice developed PD carcinomas at 6 months. No obvious defect was observed in AR expression and localization in the F9TRAMP prostate (Fig. 4.3Fa,b). However, the number of P63-expressing basal cells was reduced in F9TRAMP prostates (Fig. 4.3Fc,d), which was consistent with the notion that basal cells were diminished in PCa (120,121). Moreover, cells in the F9TRAMP prostate were more proliferative than in the TRAMP prostate (Fig. 4.3Fe-g).

Overexpression of FGF9 promoted metastasis of TRAMP prostate tumors

To determine whether F9TRAMP tumors were more metastatic, we then examined the metastatic tumors in F9TRAMP and TRAMP mice at the times of sacrifice. The metastasis-free curve showed that F9TRAMP mice (n=54) developed metastases earlier than TRAMP mice (n=39) (Fig. 4.4A). Moreover, the frequency of metastasis was higher in F9TRAMP mice than in TRAMP mice at all inspection times. *In situ* hybridization showed that *Fgf9* mRNA was expressed in metastatic PCa cells in both F9TRAMP and TRAMP mice but not adjacent non-cancerous tissues (Fig. 4.4Ba,b). The metastatic PCa cells in both mice expressed AR and T-antigens (Fig. 4.4Cc-f). Intriguingly, most of the metastatic tumors were positive for synaptophysin staining and negative for P63 staining (Fig. 4.4Cg-j). This indicates the presence of neuroendocrine differentiation in metastatic tumors, which is frequently observed in advance human PCa.

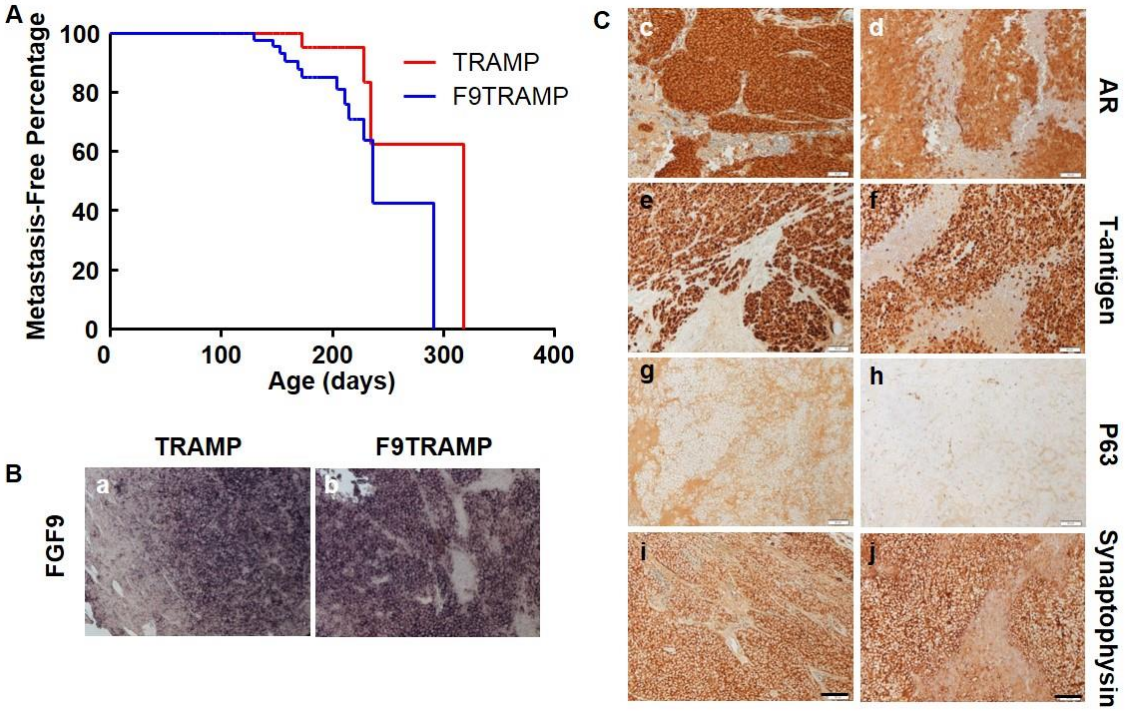

Fig. 4. 4. Overexpression of FGF9 promotes PCa metastasis in mice.

A. Kaplan-Meier analysis of metastasis-free time in TRAMP and F9TRAMP mice. **B**. In situ hybridization showing *Fgf9* expression in lymph node metastases of F9TRAMP and TRAMP tumors. **C.** Immunostaining of the indicated proteins in lymph node metastases of F9TRAMP and TRAMP tumors. Scale bars, 50 μm.

TRAMP-C2 cells are derived from TRAMP tumors and express *Fgf9* at a moderate level. To further characterize the role of FGF9 in prostate tumorigenesis, expression of *Fgf9* in TRAMP-C2 cells was depleted by infecting the cells with lentivirus bearing shRNA specific for *Fgf9* mRNA (Fig. 4.5A). The cells were then mixed with mouse urogenital sinus mesenchymal cells and grafted in the flanks of nude mice. Eight weeks after the implantation, tumor

grafts were excised for analysis. The graft size of the FGF9 depleted group was smaller than that of the control group (Fig. 4.5B). Although no significant difference in general histology between the two groups was detected (Fig. 4.5C a,b), depletion of FGF9 compromised cell proliferation in the graft (Fig. 4.5Cc,d). In addition, the FGF9-depleted grafts had fewer CD31 positive endothelial cells than the control group, indicating compromised angiogenesis in the FGF9 depleted graft (Fig. 4.5Ce,f), which was in agreement with a previous report that FGF9 induces VEGF-A expression in PCa (122). Interestingly, immunostaining with anti-F4/80 antibodies revealed that depletion of FGF9 reduced macrophage infiltration in TRAMP-C2 grafts (Fig. 4.5Cg,h), implying a role of epithelial-expressed FGF9 in reactive stroma formation and microenvironmental remodeling. Trichrome staining revealed that the stroma of F9TRAMP prostates exhibited extensive collagen deposition, which is indicative of reactive stroma (Fig. 4.5D). In addition, the well-organized smooth muscle layer surrounding the epithelial cells became fragmented with more vimentin-positive fibroblast-like cells (Fig. 4.5E). Consistently, the F9TG prostates also exhibited a disrupted stromal compartment (Fig. 4.2Ff). Together, the results indicate that overexpression of FGF9 is important for growth and metastasis of PCa, in part by modulating the tumor microenvironment.

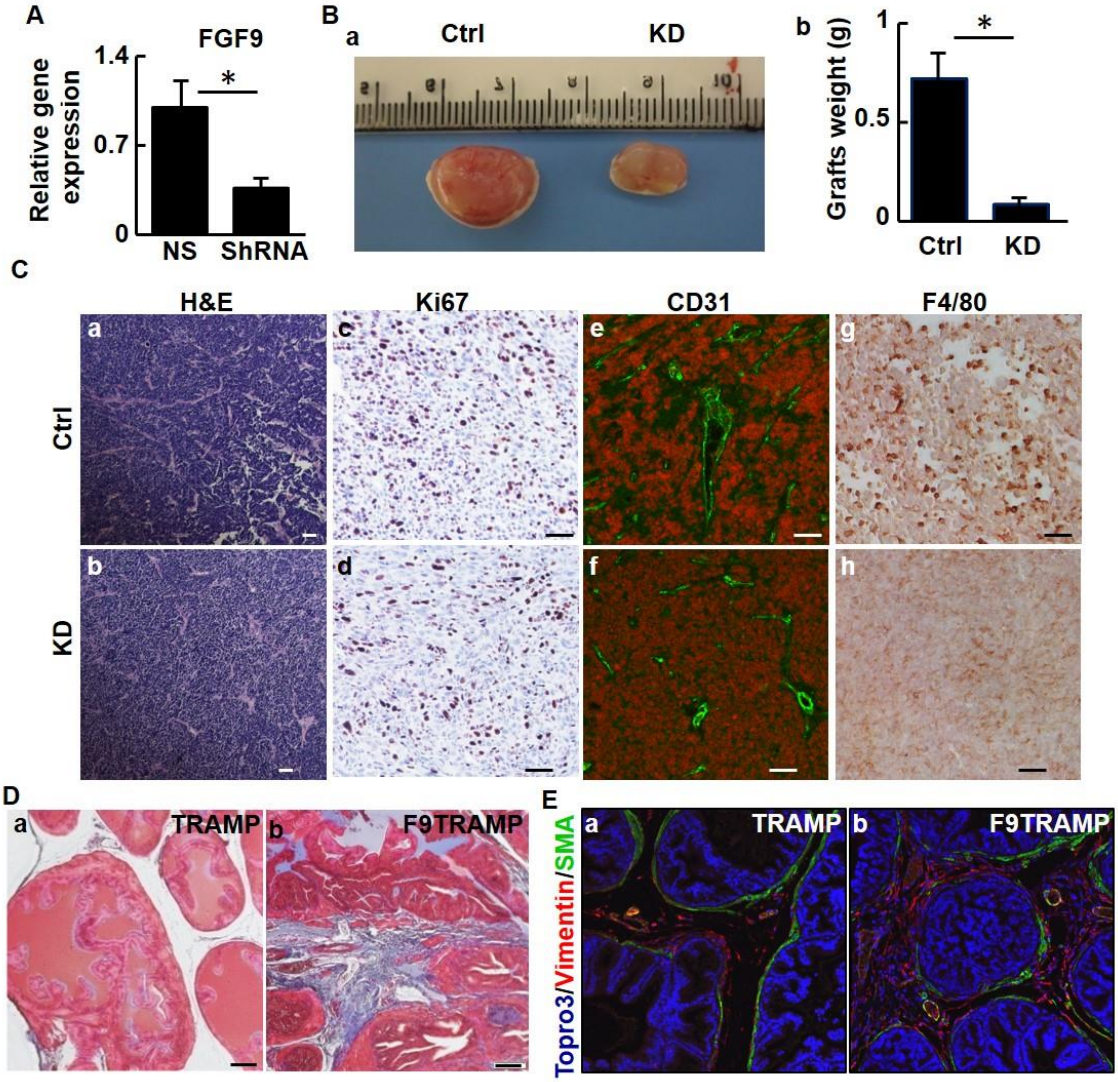

Fig. 4. 5. Depletion of FGF9 suppresses tumorigenicity of TRAMP tumor cells.

A. Real-time RT-PCR analyses for *Fgf9* expression in TRAMP-C2 cells and FGF9 depleted TRAMP-C2 cells. **B.** Subcutaneous grafts of TRAMP-C2/UGM cells with or without FGF9 depletion. Graft weight is mean ± sd from 3 grafts per group. **C.** H&E and immunostaining of graft sections with the indicated antibodies. **D.** Masson Trichrome staining of prostate sections of 4-month-old TRAMP or F9TRAMP mice, demonstrating excessive collagen deposition in the stromal compartment of F9TRAMP mice. **E.** Co-staining of α-smooth muscle actin and vimentin in 4-month-old TRAMP and F9TRAMP prostates. UGM, urogenital mesenchymal cells; Ctrl, control; KD, knockdown; Scale bar, 50 μm.

FGF9 promoted the reactive stroma by modulating TGFβ1 signaling

To investigate how FGF9 overexpression contributes to the two-way communication between the epithelium and the stroma in human PCa, LNCaP cells were forced to express FGF9 by transfection (Fig. 4.6A). The transfected cells were separated into high FGF9-expressing cells ($FGF9^{high}$) and low FGF9-expressing cells ($FGF9^{low}$) groups by limited dilution (Fig. 4.6A). The cells were then cocultured with or without HPS-19I human prostate stromal cells in a transwell migration assay, in which the stromal cells were seeded in the bottom chamber and LNCaP in the upper chamber (Fig. 4.6B). After incubation for 24 hours, LNCaP cells that migrated *through* the membrane were stained and counted. Both $FGF9^{high}$ and $FGF9^{low}$ cells exhibited a low baseline level of migration, though $FGF9^{high}$ cells possessed a slightly higher migration rate, which was consistent with a previous report (122). However, significantly more $FGF9^{high}$ cells migrated through the membrane than $FGF9^{low}$ cells in the presence of HPS-19I cells (Fig. 4.6Be). Our results suggest that FGF9 promotes HPS-19I cells to release secretory factors that promote LNCaP cell migration.

We next examined proteins potentially affecting LNCaP migration. Expression of E-cadherin was equivalent between both LNCaP groups in the absence of HPS-19I cells. However, when they are cocultured with HPS-19I cells, $FGF9^{high}$ cells expressed E-cadherin at a lower level than did $FGF9^{low}$ cells (Fig. 4.6Ca). This suggests that overexpressing FGF9 in LNCaP cells induced HPS-19I cells

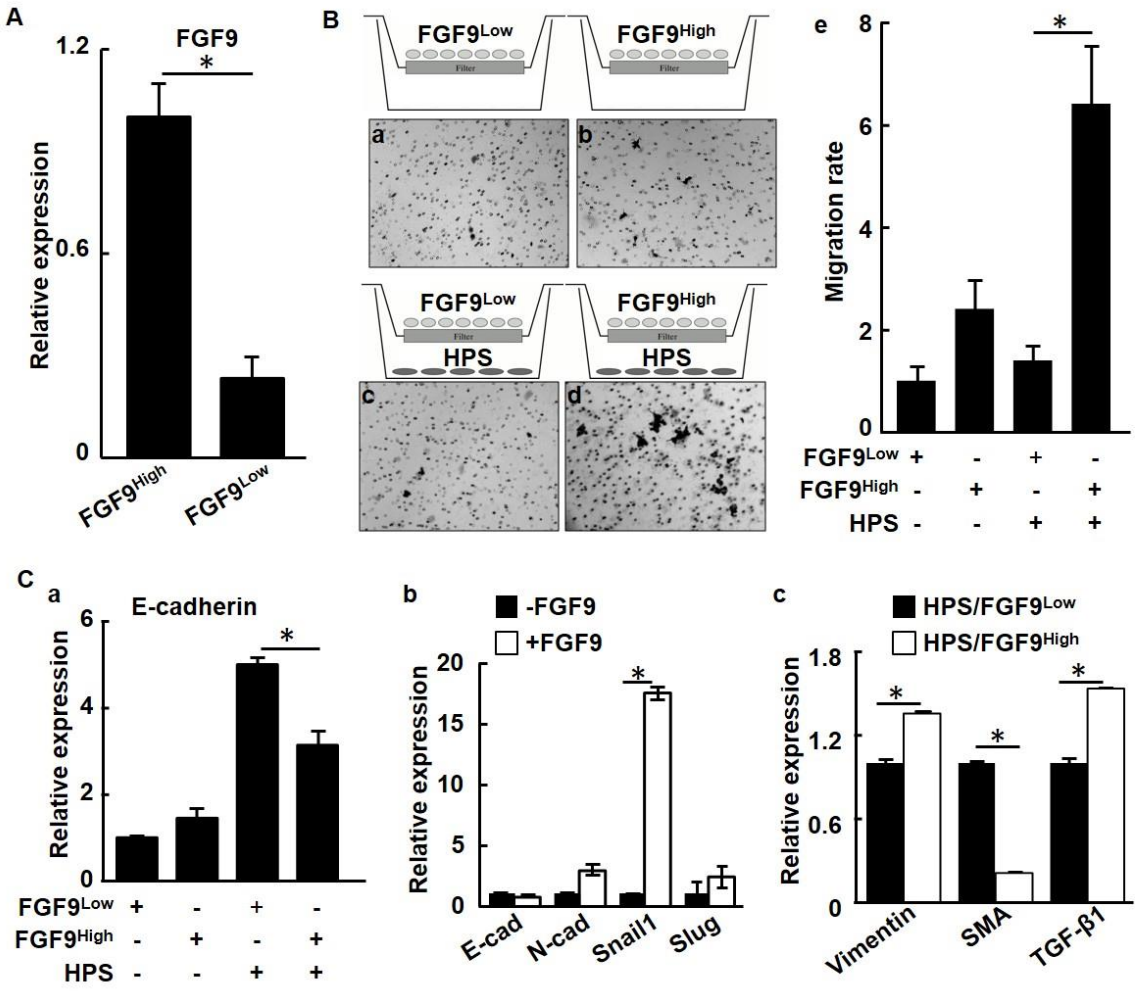

Fig. 4. 6. Overexpression of FGF9 promotes the two-way communication between PCa and stromal cells.

A. Real time RT-PCR analyses for Fgf9 expression in LNCaP cells. **B**. The indicated LNCaP cells were co-cultured with or without HPS-19I human prostate stromal cells in transwell assay. LNCaP cells migrating through the membrane were stained (panel a) and **C**. quantitated from triplicate samples and presented as mean ± sd (panel b). **D.** Real time RT-PCR analysis of LNCaP cells with or without HPS-19I cell coculture. FGF9^{high}, high FGF9-expressing LNCaP cells; FGF9^{low}, low FGF9-expressing LNCaP cells. HPS, HPS-19I human prostate stromal cells. SMA, α-smooth muscle actin.

to release factors that, in turn, promoted EMT in LNCaP cells. LNCaP cells treated with exogenous FGF9 showed an increase of Snail1 expression (Fig. 4.6Cb). Real-time RT-PCR analyses showed that coculturing with LNCaP also changed the gene expression pattern in HPS-19I cells at an FGF9 expression level-dependent manner (Fig. 4.6Cc).

Among the upregulated genes was TGFβ1, a key signaling molecule to induce reactive stroma that mediates the expression of many stromal derived factors, including FGF2, CTGF, BMP6, and IL6 (123-125). Similarly, isolated stromal cells from F9TG prostate expressed TGFβ1 at higher levels than stromal cells isolated from non-transgenic mice (Fig. 4.7Aa). In addition, treating wildtype prostate stromal cells with FGF9 increased TGFβ1 mRNA levels within 6 hours, further demonstrating the transcriptional upregulation of TGFβ1 by FGF9 (Fig. 4.7Ab). Blocking FGF receptor kinase activity with FGFR inhibitors diminished the induction effect of FGF9 on TGFβ1 expression (Fig. 4.7Ac). To further determine whether FGF9 regulated TGFβ1 expression, 293T cells were transfected with a TGFβ1 reporter carrying the TGFβ1 promoter sequence driving luciferase expression. Treating the cells with FGF9 increased expression of the reporter (Fig. 4.7B).

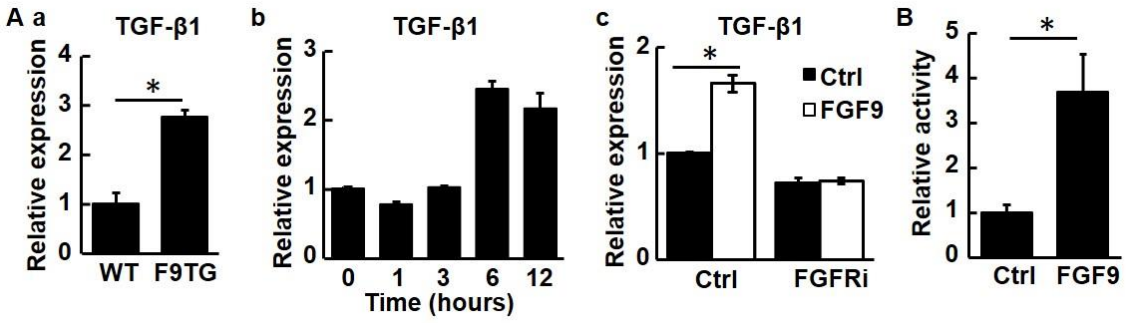

Fig. 4. 7. FGF9 promotes TGFβ1 expression in prostate stromal cells via upregulating cJun.

A. Real time RT-PCR analysis of TGFβ1 expression demonstrating upregulation of TGF-β1 expression by FGF signaling. Panel a, TGFβ1 in F9TG and wildtype prostates; panel b, mouse prostate stromal cells treated with 10 μg/ml FGF9 for the indicated time; panel c, mouse prostate stromal cells treated with vehicle control (Ctrl) or FGFR inhibitors (FGFRi) and then 10 ng/ml FGF9. **B.** Luciferase reporter assay in 293T cells showing that FGF9 stimulated TGFβ1 promoter activity. **C**. ChIP analysis showing FGF9 enhanced the binding of cJun to the TGF-β1 promoter in primary prostate stromal cells. Panel a, real time PCR analysis; panel b, agarose gel electrophoresis showing specific DNA bands. **D**. Western blot analyses of cJun and TGFβ1 expression in primary prostate stromal cells with or without FGF9 stimulation. **E.** Real time RT-PCR analysis showing that cJun downregulation in HPS-19I cells suppressed TGFβ1 expression. **F.** Real time RT-PCR analysis showing that FGFR inhibitor abrogated the induction of cJun expression by FGF9. **G.** Western blot analysis demonstrating expression of the indicated proteins in WT, F9TG, TRAMP, F9TRAMP prostates at indicated ages. **H**. Pearson correlation analysis of the TCGA dataset (downloaded from cBioPortal database) revealed a positive correlation between *FGF9* and TGFβ1 (panel a) or *vimentin* (panel b) mRNA expression in human PCa. Panel c, Pearson correlation analysis of another genome-wide study (126) revealed that the expression of FGF9 is positively correlated with TGFβ1, Twist1 and Smad2 expression. Data are mean ± sd from triplicate samples. Ctrl, control; FGFRi, FGFR inhibitor; F, F9TG; W, wildtype ;T, TRAMP; FT, F9TRAMP; *, P< 0.05.

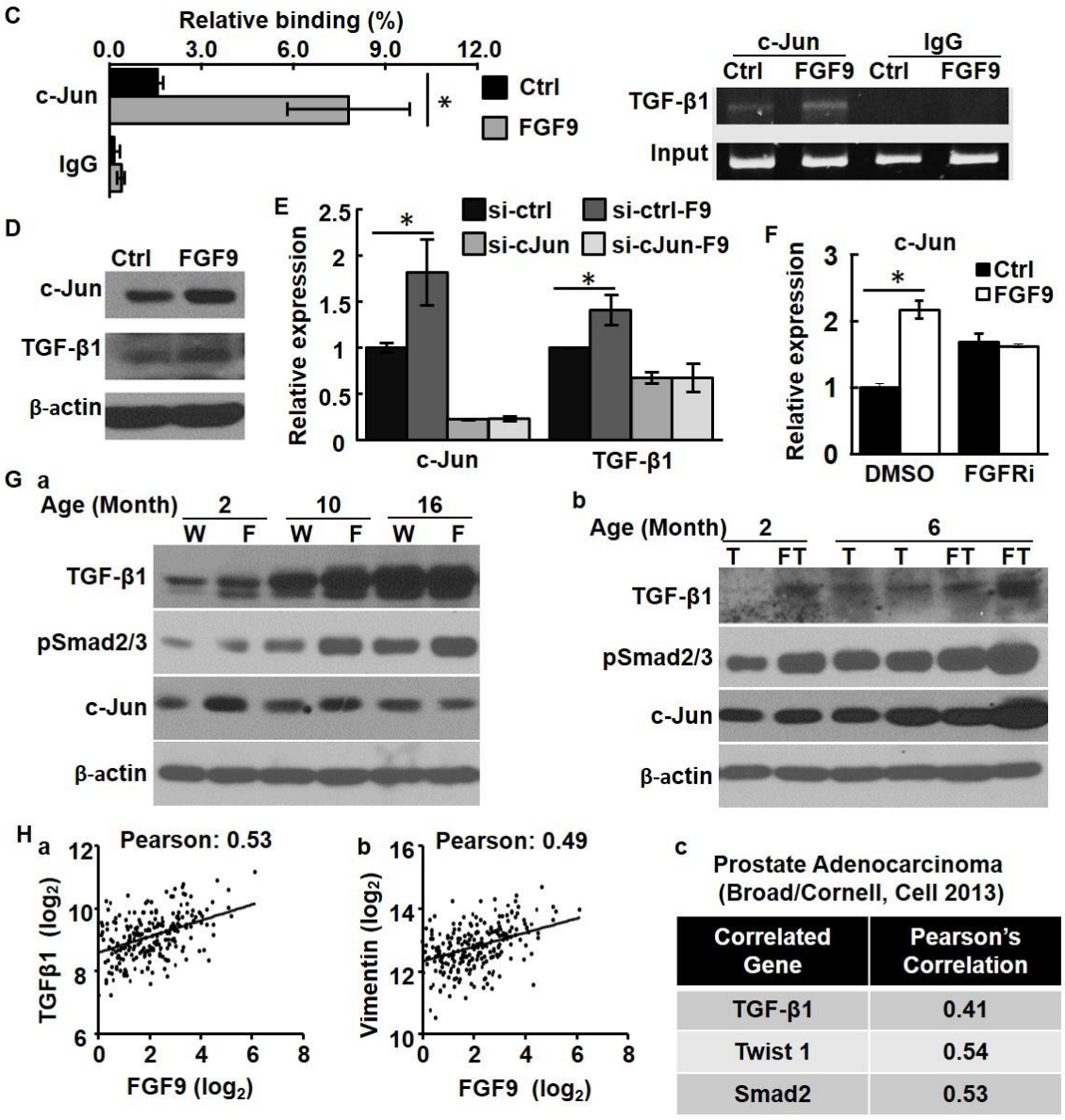

Fig. 4.7. Continued.

To identify the transcription factor(s) that mediated the induction of TGFβ1 expression by FGF9 signaling, TFSEARCH (http://diyhpl.us/~bryan/irc/protocol-online/protocol-cache/TFSEARCH.html) was used to predict the binding sites on the TGFβ1 promoter region for transcription factors that can be regulated by FGF signaling. Two c-Jun binding sites were found within a 2-kb proximal region of the TGFβ1 promoter. Treating mouse primary prostate stromal cells with FGF9 increased the binding of c-Jun to the TGF-β1 promoter (Fig. 4.7C), suggesting that c-Jun activation was involved in the regulation of TGFβ1 expression by FGF9. Moreover, FGF9 promoted both cJun and TGFβ1 expression at the protein level in mouse primary prostate stromal cells (Fig. 4.7D). In line with this finding, depletion of cJun expression by siRNA compromised the induction of TGFβ1 expression by FGF9 (Fig. 4.7E). Inhibition of FGFR activity also diminished cJun expression induced by FGF9 (Fig. 4.7F). Consistent with the *in vitro* cell culture data, both F9TG and F9TRAMP prostates exhibited a higher expression level of cJun and TGFβ1, as well as higher phosphorylated Smad2/3 levels (indicating elevated TGFβ signaling) (Fig. 4.7G). Together, our study demonstrates that overexpressing FGF9 in PCa cells induces expression of TGFβ1 via cJun in prostate stromal cells, which, in turn, promotes PCa cell migration.

To determine whether the expression level of FGF9 was correlated with TGFβ1 expression and stromal changes in human PCa, *in silico* analyses was carried out with data from the TCGA (cBioPortal) dataset. Expression of FGF9 in

human PCa was positively correlated with TGFβ1 and vimentin expression (Fig. 7Ha,b). Furthermore, in a separate dataset including genome-wide sequencing of 57 prostate tumors and matched non-cancerous tissues (126), expression of *Fgf9* was positively correlated with that of TGFβ1, Twist1, and Smad2 (Fig. 7Hc). This further indicates that FGF9 promotes EMT and reactive stroma formation in PCa.

Discussion

It has been reported that aberrantly expressed FGF9 has oncogenic and transformation activity in various human cancers, including ovarian endometrioid adenocarcinomas (127,128), ovarian cancer(129), a subset of human lung adenocarcinomas(130,131), brain tumor (132), and colon cancer cells(133). In particular, overexpression of FGF9 in human PCa predicts high bone metastasis and biochemical recurrence (110,116). Although the correlation between FGF9 and prostate cancer has been implied, how FGF9 promotes tumor epithelial-stromal interactions that contribute to PCa progression is not clear. In this study, by using *in vivo* mouse model, *in vivo* xenograft model, and molecular approach, we report that forced overexpression of FGF9 in prostate epithelial cells disrupts prostate tissue homeostasis and drives the oncogenic transformation. In the TRAMP model, FGF9 significantly expedites prostate cancer progression and metastases. It augments the formation of reactive stroma, exemplified by the collagen deposition, and an increase of vimentin positive cells. TGF-β1, a

characteristic factor in the prostate reactive stroma, is increased, concomitant with an increase of cJun. Moreover, the expression level of FGF9 is positively associated with that of cJun, TGFβ1, and Smad2 in human PCa. Together, our data provides the direct evidence that FGF9 is a causal factor of prostate cancer onset and progression. However, FGF9 alone is not sufficient to cause multi-focal invasive adenocarcinoma and metastases, thus the signals that restrain the progression remains to be uncovered.

Both F9TG and F9TRAMP prostates displayed highly proliferative epithelial cells. MAP kinase and PI3K-AKT pathways are the two major downstream signaling pathways that account for cell proliferation. To determine whether FGF9-induced signals activate the MAP kinase and PI3K-AKT pathways, prostates were harvested from TRAMP and F9TRAMP mice at 4 months of age and subjected to immunoblotting analysis of phosphorylated ERK1/2 and AKT. Phosphorylation of ERK1/2 was increased in F9TRAMP prostates. By contrast, phosphorylation of AKT were comparable between TRAMP and F9TRAMP prostates. Similarly, exogenous FGF9 phosphorylated ERK, but not AKT in human prostate cancer cell line LNCaP cells.

Our previous studies have shown the signaling from epithelial FGF9 to stromal FGFR3 potentially mediates epithelial-to-stromal communication in Dunning R3327 rat prostate tumors (134). To determine the receptors for FGF9, *Fgfr1*, *Fgfr2*, and *Fgfr1/Fgfr2/Frs2α* knockout MEF cells were stimulated with FGF9 and the cell lysate was subjected to immunoblotting. Only after triple knockout of

both FGFR1, FGFR2, and FRS2α, phosphorylation of ERK1/2 was abolished. These results suggested that FGFR1, FGFR2 and FRS2α work together to direct downstream MAPK pathway activation upon the stimulation of FGF9.

Reciprocal communication between epithelial cells and stromal cells is influential in carcinogenesis. FGF9 in the epithelial cells remodeled the tumor microenvironment and potentiated the reactive stromal response. The reactive stroma emerges due to a plethora of effectors, genetically or epigenetically, cell autonomously, or non-autonomously. The reactive stroma is a reservoir of inflammatory cells, angiogenic cells, nerve cells, smooth muscle cells, fibroblasts, extracellular matrix and cytokines. It provides a favorable environment for prostate epithelial cells to proliferate, break the epithelial barriers and metastasize to the distant organs.

Due to the close coupling between the epithelium and stroma, during prostate cancer development, changes in epithelium therefore caused abnormality in the stroma, which is further validated by our study. These stroma alterations, in turn, affect the epithelium. As shown in our study, overexpression of FGF9 induces TGFβ-1 in the stromal cells, which further either stimulate stromal cells to release other factors, such as FGF-2, CTGF, BMP6, IL6, or induce the epithelial cells to undergo epithelial mesenchymal transition. More comprehensive study will be focused on how the primed stromal cells change the cancer microenvironment.

CHAPTER V

CONCLUSIONS

Prostate cancer is the most common malignant neoplasm in men in the United States. Tens of thousands of men suffer from the disease without effective treatment. Even after initial therapy, the cancer recurs and becomes incurable. To tackle this epidemic disease, we sought out to focus on unraveling the mystery from two perspectives, prostate stem cells and the tumor microenvironment.

A rare population of cells, prostate cancer stem cells (CSCs), may play a critical role in the development and progression of PCa. Given the similarity between normal stem cells and CSCs, it is hypothesized that prostate CSCs may originate from oncogenic transformation of normal prostate stem cells. Thus understanding normal prostate stem cells is essential for insight into prostate cancer stem cells. However, where prostate stem cells reside and how prostate stem cells are regulated still needs to be deciphered. In this study, we showed that P63-expressing prostate basal stem cells (P-bSCs) represents primitive stem cells. By interrogating FGF signaling in prostate stem cells, we found type II FGFR is crucial for prostate basal stem cell self-renewal. Disrupting FGFR2 and its downstream signals promotes basal to luminal cell differentiation, thus impairs both basal cell homeostasis and prostate postnatal development.

Cancers are not just masses of malignant cells but a complex ecosystem in which many other cell type are recruited and altered. The tumor microenvironment is being increasingly recognized as a key factor in disease progression and distant metastasis. In our study, we discover that overexpression of FGF9 in prostate epithelial cells elicits high-grade PIN and invasive carcinoma. In addition, the neoplastic cells induce various changes to convert the adjacent stroma compartment into a pathological entity, i.e. reactive stroma.

Overall, our study reveals how FGF signaling regulates the homeostasis of prostate basal stem cells. This is important because deregulation of the basal stem cells is a critical biological event during prostate cancer initiation and progression. We have also uncovered that FGF signaling is essential for the growth and survival of prostate cancer, due to its profound impact on the reciprocal cross-talk between epithelial cells and stromal cells.

REFERENCES

1. McNeal, J. E. (1988) Normal histology of the prostate. *The American journal of surgical pathology* **12**, 619-633
2. McNeal, J. E. (1969) Origin and development of carcinoma in the prostate. *Cancer* **23**, 24-34
3. McNeal, J. E. (1978) Origin and evolution of benign prostatic enlargement. *Investigative urology* **15**, 340-345
4. Sugimura, Y., Cunha, G. R., and Donjacour, A. A. (1986) Morphogenesis of ductal networks in the mouse prostate. *Biology of reproduction* **34**, 961-971
5. Wu, X., Jin, C., Wang, F., Yu, C., and McKeehan, W. L. (2003) Stromal cell heterogeneity in fibroblast growth factor-mediated stromal-epithelial cell cross-talk in premalignant prostate tumors. *Cancer research* **63**, 4936-4944
6. Feinberg, A. P., Ohlsson, R., and Henikoff, S. (2006) The epigenetic progenitor origin of human cancer. *Nature reviews. Genetics* **7**, 21-33
7. Bell, D. R., and Van Zant, G. (2004) Stem cells, aging, and cancer: inevitabilities and outcomes. *Oncogene* **23**, 7290-7296
8. Woenckhaus, J., and Fenic, I. (2008) Proliferative inflammatory atrophy: a background lesion of prostate cancer? *Andrologia* **40**, 134-137

9. Logothetis, C. J., and Lin, S. H. (2005) Osteoblasts in prostate cancer metastasis to bone. *Nature reviews. Cancer* **5**, 21-28

10. Shen, M. M., and Abate-Shen, C. (2010) Molecular genetics of prostate cancer: new prospects for old challenges. *Genes & development* **24**, 1967-2000

11. Tomlins, S. A., Rhodes, D. R., Perner, S., Dhanasekaran, S. M., Mehra, R., Sun, X. W., Varambally, S., Cao, X., Tchinda, J., Kuefer, R., Lee, C., Montie, J. E., Shah, R. B., Pienta, K. J., Rubin, M. A., and Chinnaiyan, A. M. (2005) Recurrent fusion of TMPRSS2 and ETS transcription factor genes in prostate cancer. *Science* **310**, 644-648

12. Mani, R. S., Tomlins, S. A., Callahan, K., Ghosh, A., Nyati, M. K., Varambally, S., Palanisamy, N., and Chinnaiyan, A. M. (2009) Induced chromosomal proximity and gene fusions in prostate cancer. *Science* **326**, 1230

13. Clark, J. P., and Cooper, C. S. (2009) ETS gene fusions in prostate cancer. *Nature reviews. Urology* **6**, 429-439

14. Abate-Shen, C., and Shen, M. M. (2002) Mouse models of prostate carcinogenesis. *Trends in Genetics* **18**, S1-S5

15. Lawson, D. A., Zong, Y., Memarzadeh, S., Xin, L., Huang, J., and Witte, O. N. (2010) Basal epithelial stem cells are efficient targets for prostate cancer initiation. *Proceedings of the National Academy of Sciences of the United States of America* **107**, 2610-2615

16. Gingrich, J. R., and Greenberg, N. M. (1996) A transgenic mouse prostate cancer model. *Toxicol Pathol* **24**, 502-504

17. Gingrich, J. R., Barrios, R. J., Foster, B. A., and Greenberg, N. M. (1999) Pathologic progression of autochthonous prostate cancer in the TRAMP model. *Prostate Cancer Prostatic Dis* **2**, 70-75

18. Kaplan-Lefko, P. J., Chen, T. M., Ittmann, M. M., Barrios, R. J., Ayala, G. E., Huss, W. J., Maddison, L. A., Foster, B. A., and Greenberg, N. M. (2003) Pathobiology of autochthonous prostate cancer in a pre-clinical transgenic mouse model. *Prostate* **55**, 219-237

19. Rybak, A. P., He, L., Kapoor, A., Cutz, J. C., and Tang, D. (2011) Characterization of sphere-propagating cells with stem-like properties from DU145 prostate cancer cells. *Biochimica et biophysica acta* **1813**, 683-694

20. Wang, S., Gao, J., Lei, Q., Rozengurt, N., Pritchard, C., Jiao, J., Thomas, G. V., Li, G., Roy-Burman, P., Nelson, P. S., Liu, X., and Wu, H. (2003) Prostate-specific deletion of the murine Pten tumor suppressor gene leads to metastatic prostate cancer. *Cancer Cell* **4**, 209-221

21. Tuxhorn, J. A., Ayala, G. E., and Rowley, D. R. (2001) Reactive stroma in prostate cancer progression. *The Journal of urology* **166**, 2472-2483

22. English, H. F., Santen, R. J., and Isaacs, J. T. (1987) Response of glandular versus basal rat ventral prostatic epithelial cells to androgen withdrawal and replacement. *The Prostate* **11**, 229-242

23. Evans, G. S., and Chandler, J. A. (1987) Cell proliferation studies in the rat prostate: II. The effects of castration and androgen-induced regeneration upon basal and secretory cell proliferation. *The Prostate* **11**, 339-351

24. Sugimura, Y., Cunha, G. R., and Donjacour, A. A. (1986) Morphological and histological study of castration-induced degeneration and androgen-induced regeneration in the mouse prostate. *Biology of reproduction* **34**, 973-983

25. Kinbara, H., Cunha, G. R., Boutin, E., Hayashi, N., and Kawamura, J. (1996) Evidence of stem cells in the adult prostatic epithelium based upon responsiveness to mesenchymal inductors. *The Prostate* **29**, 107-116

26. Tsujimura, A., Koikawa, Y., Salm, S., Takao, T., Coetzee, S., Moscatelli, D., Shapiro, E., Lepor, H., Sun, T. T., and Wilson, E. L. (2002) Proximal location of mouse prostate epithelial stem cells: a model of prostatic homeostasis. *The Journal of cell biology* **157**, 1257-1265

27. Goldstein, A. S., Huang, J., Guo, C., Garraway, I. P., and Witte, O. N. (2010) Identification of a cell of origin for human prostate cancer. *Science* **329**, 568-571

28. Goldstein, A. S., Lawson, D. A., Cheng, D., Sun, W., Garraway, I. P., and Witte, O. N. (2008) Trop2 identifies a subpopulation of murine and human prostate basal cells with stem cell characteristics. *Proceedings of the*

National Academy of Sciences of the United States of America **105**, 20882-20887

29. Xin, L., Lukacs, R. U., Lawson, D. A., Cheng, D., and Witte, O. N. (2007) Self-renewal and multilineage differentiation in vitro from murine prostate stem cells. *Stem Cells* **25**, 2760-2769

30. Garraway, I. P., Sun, W., Tran, C. P., Perner, S., Zhang, B., Goldstein, A. S., Hahm, S. A., Haider, M., Head, C. S., Reiter, R. E., Rubin, M. A., and Witte, O. N. (2010) Human prostate sphere-forming cells represent a subset of basal epithelial cells capable of glandular regeneration in vivo. *The Prostate* **70**, 491-501

31. Leong, K. G., Wang, B. E., Johnson, L., and Gao, W. Q. (2008) Generation of a prostate from a single adult stem cell. *Nature* **456**, 804-808

32. Ousset, M., Van Keymeulen, A., Bouvencourt, G., Sharma, N., Achouri, Y., Simons, B. D., and Blanpain, C. (2012) Multipotent and unipotent progenitors contribute to prostate postnatal development. *Nature cell biology* **14**, 1131-1138

33. Wang, J., Zhu, H. H., Chu, M., Liu, Y., Zhang, C., Liu, G., Yang, X., Yang, R., and Gao, W. Q. (2014) Symmetrical and asymmetrical division analysis provides evidence for a hierarchy of prostate epithelial cell lineages. *Nature communications* **5**, 4758

34. Chua, C. W., Shibata, M., Lei, M., Toivanen, R., Barlow, L. J., Bergren, S. K., Badani, K. K., McKiernan, J. M., Benson, M. C., Hibshoosh, H., and Shen, M. M. (2014) Single luminal epithelial progenitors can generate prostate organoids in culture. *Nature cell biology* **16**, 951-961, 951-954

35. Wang, X., Julio, M. K., Economides, K. D., Walker, D., Yu, H., Halili, M. V., Hu, Y. P., Price, S. M., Abate-Shen, C., and Shen, M. M. (2009) A luminal epithelial stem cell that is a cell of origin for prostate cancer. *Nature*

36. Choi, N., Zhang, B., Zhang, L., Ittmann, M., and Xin, L. (2012) Adult murine prostate basal and luminal cells are self-sustained lineages that can both serve as targets for prostate cancer initiation. *Cancer cell* **21**, 253-265

37. Liu, J., Pascal, L. E., Isharwal, S., Metzger, D., Ramos Garcia, R., Pilch, J., Kasper, S., Williams, K., Basse, P. H., Nelson, J. B., Chambon, P., and Wang, Z. (2011) Regenerated luminal epithelial cells are derived from preexisting luminal epithelial cells in adult mouse prostate. *Molecular endocrinology* **25**, 1849-1857

38. Wang, Z. A., Mitrofanova, A., Bergren, S. K., Abate-Shen, C., Cardiff, R. D., Califano, A., and Shen, M. M. (2013) Lineage analysis of basal epithelial cells reveals their unexpected plasticity and supports a cell-of-origin model for prostate cancer heterogeneity. *Nature cell biology* **15**, 274-283

39. Lu, T. L., Huang, Y. F., You, L. R., Chao, N. C., Su, F. Y., Chang, J. L., and Chen, C. M. (2013) Conditionally ablated Pten in prostate basal cells promotes basal-to-luminal differentiation and causes invasive prostate cancer in mice. *The American journal of pathology* **182**, 975-991

40. Wang, Z. A., Toivanen, R., Bergren, S. K., Chambon, P., and Shen, M. M. (2014) Luminal cells are favored as the cell of origin for prostate cancer. *Cell reports* **8**, 1339-1346

41. Karthaus, W. R., Iaquinta, P. J., Drost, J., Gracanin, A., van Boxtel, R., Wongvipat, J., Dowling, C. M., Gao, D., Begthel, H., Sachs, N., Vries, R. G., Cuppen, E., Chen, Y., Sawyers, C. L., and Clevers, H. C. (2014) Identification of multipotent luminal progenitor cells in human prostate organoid cultures. *Cell* **159**, 163-175

42. Lin, Y., Zhang, J., Zhang, Y., and Wang, F. (2007) Generation of an Frs2alpha conditional null allele. *Genesis* **45**, 554-559

43. Trokovic, R., Trokovic, N., Hernesniemi, S., Pirvola, U., Vogt Weisenhorn, D. M., Rossant, J., McMahon, A. P., Wurst, W., and Partanen, J. (2003) FGFR1 is independently required in both developing mid- and hindbrain for sustained response to isthmic signals. *Embo J* **22**, 1811-1823

44. Yu, K., Xu, J., Liu, Z., Sosic, D., Shao, J., Olson, E. N., Towler, D. A., and Ornitz, D. M. (2003) Conditional inactivation of FGF receptor 2 reveals an essential role for FGF signaling in the regulation of osteoblast function and bone growth. *Development* **130**, 3063-3074

45. Lin, Y., Liu, G., Zhang, Y., Hu, Y. P., Yu, K., Lin, C., McKeehan, K., Xuan, J. W., Ornitz, D. M., Shen, M. M., Greenberg, N., McKeehan, W. L., and Wang, F. (2007) Fibroblast growth factor receptor 2 tyrosine kinase is required for prostatic morphogenesis and the acquisition of strict androgen dependency for adult tissue homeostasis. *Development* **134**, 723-734

46. Lee, D., Liu, Y., Liao, L., Wang, F., and Xu, J. (2014) The Prostate Basal Cell (BC) Heterogeneity and the p63-Positive BC Differentiation Spectrum in Mice *International J. of Biogical Science* **in press**

47. Bhatia-Gaur, R., Donjacour, A. A., Sciavolino, P. J., Kim, M., Desai, N., Young, P., Norton, C. R., Gridley, T., Cardiff, R. D., Cunha, G. R., Abate-Shen, C., and Shen, M. M. (1999) Roles for Nkx3.1 in prostate development and cancer. *Genes & development* **13**, 966-977

48. Shen, M. M., and Abate-Shen, C. (2003) Roles of the Nkx3.1 homeobox gene in prostate organogenesis and carcinogenesis. *Developmental dynamics : an official publication of the American Association of Anatomists* **228**, 767-778

49. Mills, A. A., Zheng, B., Wang, X. J., Vogel, H., Roop, D. R., and Bradley, A. (1999) p63 is a p53 homologue required for limb and epidermal morphogenesis. *Nature* **398**, 708-713

50. Yang, A., Schweitzer, R., Sun, D., Kaghad, M., Walker, N., Bronson, R. T., Tabin, C., Sharpe, A., Caput, D., Crum, C., and McKeon, F. (1999)

p63 is essential for regenerative proliferation in limb, craniofacial and epithelial development. *Nature* **398**, 714-718

51. Signoretti, S., Waltregny, D., Dilks, J., Isaac, B., Lin, D., Garraway, L., Yang, A., Montironi, R., McKeon, F., and Loda, M. (2000) p63 is a prostate basal cell marker and is required for prostate development. *The American journal of pathology* **157**, 1769-1775
52. Pignon, J. C., Grisanzio, C., Geng, Y., Song, J., Shivdasani, R. A., and Signoretti, S. (2013) p63-expressing cells are the stem cells of developing prostate, bladder, and colorectal epithelia. *Proceedings of the National Academy of Sciences of the United States of America* **110**, 8105-8110
53. Tumbar, T., Guasch, G., Greco, V., Blanpain, C., Lowry, W. E., Rendl, M., and Fuchs, E. (2004) Defining the epithelial stem cell niche in skin. *Science* **303**, 359-363
54. Li, L., and Clevers, H. (2010) Coexistence of quiescent and active adult stem cells in mammals. *Science* **327**, 542-545
55. Barker, N., van Es, J. H., Kuipers, J., Kujala, P., van den Born, M., Cozijnsen, M., Haegebarth, A., Korving, J., Begthel, H., Peters, P. J., and Clevers, H. (2007) Identification of stem cells in small intestine and colon by marker gene Lgr5. *Nature* **449**, 1003-1007
56. Jaks, V., Barker, N., Kasper, M., van Es, J. H., Snippert, H. J., Clevers, H., and Toftgard, R. (2008) Lgr5 marks cycling, yet long-lived, hair follicle stem cells. *Nature genetics* **40**, 1291-1299

57. Chang, J. Y., Wang, C., Jin, C., Yang, C., Huang, Y., Liu, J., McKeehan, W. L., D'Souza, R. N., and Wang, F. (2013) Self-renewal and multilineage differentiation of mouse dental epithelial stem cells. *Stem cell research* **11**, 990-1002

58. Barker, N., Huch, M., Kujala, P., van de Wetering, M., Snippert, H. J., van Es, J. H., Sato, T., Stange, D. E., Begthel, H., van den Born, M., Danenberg, E., van den Brink, S., Korving, J., Abo, A., Peters, P. J., Wright, N., Poulsom, R., and Clevers, H. (2010) Lgr5(+ve) stem cells drive self-renewal in the stomach and build long-lived gastric units in vitro. *Cell stem cell* **6**, 25-36

59. Huch, M., Bonfanti, P., Boj, S. F., Sato, T., Loomans, C. J., van de Wetering, M., Sojoodi, M., Li, V. S., Schuijers, J., Gracanin, A., Ringnalda, F., Begthel, H., Hamer, K., Mulder, J., van Es, J. H., de Koning, E., Vries, R. G., Heimberg, H., and Clevers, H. (2013) Unlimited in vitro expansion of adult bi-potent pancreas progenitors through the Lgr5/R-spondin axis. *The EMBO journal* **32**, 2708-2721

60. Huch, M., Dorrell, C., Boj, S. F., van Es, J. H., Li, V. S., van de Wetering, M., Sato, T., Hamer, K., Sasaki, N., Finegold, M. J., Haft, A., Vries, R. G., Grompe, M., and Clevers, H. (2013) In vitro expansion of single Lgr5+ liver stem cells induced by Wnt-driven regeneration. *Nature* **494**, 247-250

61. Bhang, H. E., Ruddy, D. A., Krishnamurthy Radhakrishna, V., Caushi, J. X., Zhao, R., Hims, M. M., Singh, A. P., Kao, I., Rakiec, D., Shaw, P.,

Balak, M., Raza, A., Ackley, E., Keen, N., Schlabach, M. R., Palmer, M., Leary, R. J., Chiang, D. Y., Sellers, W. R., Michor, F., Cooke, V. G., Korn, J. M., and Stegmeier, F. (2015) Studying clonal dynamics in response to cancer therapy using high-complexity barcoding. *Nature medicine*

62. McKeehan, W. L., Wang, F., and Kan, M. (1998) The heparan sulfate-fibroblast growth factor family: diversity of structure and function. *Progress in nucleic acid research and molecular biology* **59**, 135-176

63. Powers, C. J., McLeskey, S. W., and Wellstein, A. (2000) Fibroblast growth factors, their receptors and signaling. *Endocrine-related cancer* **7**, 165-197

64. Gotoh, N. (2008) Regulation of growth factor signaling by FRS2 family docking/scaffold adaptor proteins. *Cancer science* **99**, 1319-1325

65. Mohammadi, M., Honegger, A. M., Rotin, D., Fischer, R., Bellot, F., Li, W., Dionne, C. A., Jaye, M., Rubinstein, M., and Schlessinger, J. (1991) A tyrosine-phosphorylated carboxy-terminal peptide of the fibroblast growth factor receptor (Flg) is a binding site for the SH2 domain of phospholipase C-gamma 1. *Molecular and cellular biology* **11**, 5068-5078

66. Kouhara, H., Hadari, Y. R., Spivak-Kroizman, T., Schilling, J., Bar-Sagi, D., Lax, I., and Schlessinger, J. (1997) A lipid-anchored Grb2-binding protein that links FGF-receptor activation to the Ras/MAPK signaling pathway. *Cell* **89**, 693-702

67. Choi, S. C., Kim, S. J., Choi, J. H., Park, C. Y., Shim, W. J., and Lim, D. S. (2008) Fibroblast growth factor-2 and -4 promote the proliferation of bone marrow mesenchymal stem cells by the activation of the PI3K-Akt and ERK1/2 signaling pathways. *Stem cells and development* **17**, 725-736

68. Corn, P. G., Wang, F., McKeehan, W. L., and Navone, N. (2013) Targeting fibroblast growth factor pathways in prostate cancer. *Clinical cancer research : an official journal of the American Association for Cancer Research* **19**, 5856-5866

69. Zhang, Y., Zhang, J., Lin, Y., Lan, Y., Lin, C., Xuan, J. W., Shen, M. M., McKeehan, W. L., Greenberg, N. M., and Wang, F. (2008) Role of epithelial cell fibroblast growth factor receptor substrate 2alpha in prostate development, regeneration and tumorigenesis. *Development* **135**, 775-784

70. Xu, C., Inokuma, M. S., Denham, J., Golds, K., Kundu, P., Gold, J. D., and Carpenter, M. K. (2001) Feeder-free growth of undifferentiated human embryonic stem cells. *Nature biotechnology* **19**, 971-974

71. Kunath, T., Saba-El-Leil, M. K., Almousailleakh, M., Wray, J., Meloche, S., and Smith, A. (2007) FGF stimulation of the Erk1/2 signalling cascade triggers transition of pluripotent embryonic stem cells from self-renewal to lineage commitment. *Development* **134**, 2895-2902

72. Dvorak, P., Dvorakova, D., Koskova, S., Vodinska, M., Najvirtova, M., Krekac, D., and Hampl, A. (2005) Expression and potential role of fibroblast growth factor 2 and its receptors in human embryonic stem cells. *Stem Cells* **23**, 1200-1211

73. Zheng, W., Nowakowski, R. S., and Vaccarino, F. M. (2004) Fibroblast growth factor 2 is required for maintaining the neural stem cell pool in the mouse brain subventricular zone. *Dev Neurosci* **26**, 181-196

74. Eom, Y. W., Oh, J. E., Lee, J. I., Baik, S. K., Rhee, K. J., Shin, H. C., Kim, Y. M., Ahn, C. M., Kong, J. H., Kim, H. S., and Shim, K. Y. (2014) The role of growth factors in maintenance of stemness in bone marrow-derived mesenchymal stem cells. *Biochemical and biophysical research communications* **445**, 16-22

75. Itkin, T., Ludin, A., Gradus, B., Gur-Cohen, S., Kalinkovich, A., Schajnovitz, A., Ovadya, Y., Kollet, O., Canaani, J., Shezen, E., Coffin, D. J., Enikolopov, G. N., Berg, T., Piacibello, W., Hornstein, E., and Lapidot, T. (2012) FGF-2 expands murine hematopoietic stem and progenitor cells via proliferation of stromal cells, c-Kit activation, and CXCL12 down-regulation. *Blood* **120**, 1843-1855

76. Zhang, J., Liu, J., Liu, L., McKeehan, W. L., and Wang, F. (2012) The fibroblast growth factor signaling axis controls cardiac stem cell differentiation through regulating autophagy. *Autophagy* **8**

77. Chang, J. Y., Wang, C., Liu, J., Huang, Y., Jin, C., Yang, C., Hai, B., Liu, F., D'Souza, R. N., McKeehan, W. L., and Wang, F. (2013) Fibroblast growth factor signaling is essential for self-renewal of dental epithelial stem cells. *The Journal of biological chemistry* **288**, 28952-28961

78. Memarzadeh, S., Xin, L., Mulholland, D. J., Mansukhani, A., Wu, H., Teitell, M. A., and Witte, O. N. (2007) Enhanced paracrine FGF10 expression promotes formation of multifocal prostate adenocarcinoma and an increase in epithelial androgen receptor. *Cancer Cell* **12**, 572-585

79. Heer, R., Collins, A. T., Robson, C. N., Shenton, B. K., and Leung, H. Y. (2006) KGF suppresses {alpha}2{beta}1 integrin function and promotes differentiation of the transient amplifying population in human prostatic epithelium. *Journal of cell science* **119**, 1416-1424

80. Kan, M., Uematsu, F., Wu, X., and Wang, F. (2001) Directional specificity of prostate stromal to epithelial cell communication via FGF7/FGFR2 is set by cell- and FGFR2 isoform-specific heparan sulfate. *In vitro cellular & developmental biology. Animal* **37**, 575-577

81. Lu, W., Luo, Y., Kan, M., and McKeehan, W. L. (1999) Fibroblast growth factor-10. A second candidate stromal to epithelial cell andromedin in prostate. *The Journal of biological chemistry* **274**, 12827-12834.

82. Kwon, O. J., Valdez, J. M., Zhang, L., Zhang, B., Wei, X., Su, Q., Ittmann, M. M., Creighton, C. J., and Xin, L. (2014) Increased Notch signalling

inhibits anoikis and stimulates proliferation of prostate luminal epithelial cells. *Nature communications* **5**, 4416

83. Zhang, Y., Zhang, J., Lin, Y., Lan, Y., Lin, C., Xuan, J. W., Shen, M. M., McKeehan, W. L., Greenberg, N. M., and Wang, F. (2008) Role of epithelial cell fibroblast growth factor receptor substrate 2{alpha} in prostate development, regeneration and tumorigenesis. *Development* **135**, 775-784

84. Shahi, P., Seethammagari, M. R., Valdez, J. M., Xin, L., and Spencer, D. M. (2011) Wnt and Notch pathways have interrelated opposing roles on prostate progenitor cell proliferation and differentiation. *Stem cells* **29**, 678-688

85. Wang, B. E., Wang, X. D., Ernst, J. A., Polakis, P., and Gao, W. Q. (2008) Regulation of epithelial branching morphogenesis and cancer cell growth of the prostate by Wnt signaling. *PloS one* **3**, e2186

86. Yang, F., Zhang, Y., Ressler, S. J., Ittmann, M. M., Ayala, G. E., Dang, T. D., Wang, F., and Rowley, D. R. (2013) FGFR1 is essential for prostate cancer progression and metastasis. *Cancer research* **73**, 3716-3724

87. Kwon, O. J., Zhang, L., Ittmann, M. M., and Xin, L. (2014) Prostatic inflammation enhances basal-to-luminal differentiation and accelerates initiation of prostate cancer with a basal cell origin. *Proceedings of the National Academy of Sciences of the United States of America* **111**, E592-600

88. Freeman, K. W., Gangula, R. D., Welm, B. E., Ozen, M., Foster, B. A., Rosen, J. M., Ittmann, M., Greenberg, N. M., and Spencer, D. M. (2003) Conditional activation of fibroblast growth factor receptor (FGFR) 1, but not FGFR2, in prostate cancer cells leads to increased osteopontin induction, extracellular signal-regulated kinase activation, and in vivo proliferation. *Cancer research* **63**, 6237-6243

89. Jin, C., McKeehan, K., Guo, W., Jauma, S., Ittmann, M. M., Foster, B., Greenberg, N. M., McKeehan, W. L., and Wang, F. (2003) Cooperation between ectopic FGFR1 and depression of FGFR2 in induction of prostatic intraepithelial neoplasia in the mouse prostate. *Cancer research* **63**, 8784-8790

90. Acevedo, V. D., Gangula, R. D., Freeman, K. W., Li, R., Zhang, Y., Wang, F., Ayala, G. E., Peterson, L. E., Ittmann, M., and Spencer, D. M. (2007) Inducible FGFR-1 activation leads to irreversible prostate adenocarcinoma and an epithelial-to-mesenchymal transition. *Cancer cell* **12**, 559-571

91. Naimi, B., Latil, A., Fournier, G., Mangin, P., Cussenot, O., and Berthon, P. (2002) Down-regulation of (IIIb) and (IIIc) isoforms of fibroblast growth factor receptor 2 (FGFR2) is associated with malignant progression in human prostate. *The Prostate* **52**, 245-252

92. Cunha, G. R., Cooke, P. S., and Kurita, T. (2004) Role of stromal-epithelial interactions in hormonal responses. *Arch Histol Cytol* **67**, 417-434

93. Cunha, G. R., Ricke, W., Thomson, A., Marker, P. C., Risbridger, G., Hayward, S. W., Wang, Y. Z., Donjacour, A. A., and Kurita, T. (2004) Hormonal, cellular, and molecular regulation of normal and neoplastic prostatic development. *J Steroid Biochem Mol Biol* **92**, 221-236

94. Bhowmick, N. A., Neilson, E. G., and Moses, H. L. (2004) Stromal fibroblasts in cancer initiation and progression. *Nature* **432**, 332-337

95. Tuxhorn, J. A., Ayala, G. E., Smith, M. J., Smith, V. C., Dang, T. D., and Rowley, D. R. (2002) Reactive stroma in human prostate cancer: induction of myofibroblast phenotype and extracellular matrix remodeling. *Clinical cancer research : an official journal of the American Association for Cancer Research* **8**, 2912-2923

96. Barron, D. A., and Rowley, D. R. (2012) The reactive stroma microenvironment and prostate cancer progression. *Endocrine-related cancer* **19**, R187-204

97. Tuxhorn, J. A., McAlhany, S. J., Yang, F., Dang, T. D., and Rowley, D. R. (2002) Inhibition of transforming growth factor-beta activity decreases angiogenesis in a human prostate cancer-reactive stroma xenograft model. *Cancer research* **62**, 6021-6025

98. Yang, F., Strand, D. W., and Rowley, D. R. (2008) Fibroblast growth factor-2 mediates transforming growth factor-beta action in prostate cancer reactive stroma. *Oncogene* **27**, 450-459

99. Franco, O. E., Jiang, M., Strand, D. W., Peacock, J., Fernandez, S., Jackson, R. S., 2nd, Revelo, M. P., Bhowmick, N. A., and Hayward, S. W. (2011) Altered TGF-beta signaling in a subpopulation of human stromal cells promotes prostatic carcinogenesis. *Cancer research* **71**, 1272-1281

100. Thomson, A. A. (2001) Role of androgens and fibroblast growth factors in prostatic development. *Reproduction* **121**, 187-195.

101. Gowardhan, B., Douglas, D. A., Mathers, M. E., McKie, A. B., McCracken, S. R., Robson, C. N., and Leung, H. Y. (2005) Evaluation of the fibroblast growth factor system as a potential target for therapy in human prostate cancer. *British journal of cancer* **92**, 320-327

102. Abate-Shen, C., and Shen, M. M. (2007) FGF signaling in prostate tumorigenesis--new insights into epithelial-stromal interactions. *Cancer Cell* **12**, 495-497

103. Wesche, J., Haglund, K., and Haugsten, E. M. (2011) Fibroblast growth factors and their receptors in cancer. *The Biochemical journal* **437**, 199-213

104. McKeehan, W. L., Wang, F., and Luo, Y. (2009) *The fibroblast growth factor (FGF) signaling complex. Handbook of Cell Signaling*, 2dn ed., Academic/Elsevier Press, New York

105. Taylor, B. S., Schultz, N., Hieronymus, H., Gopalan, A., Xiao, Y., Carver, B. S., Arora, V. K., Kaushik, P., Cerami, E., Reva, B., Antipin, Y., Mitsiades, N., Landers, T., Dolgalev, I., Major, J. E., Wilson, M., Socci, N. D., Lash, A. E., Heguy, A., Eastham, J. A., Scher, H. I., Reuter, V. E., Scardino, P. T., Sander, C., Sawyers, C. L., and Gerald, W. L. (2010) Integrative genomic profiling of human prostate cancer. *Cancer Cell* **18**, 11-22

106. Giri, D., Ropiquet, F., and Ittmann, M. (1999) Alterations in expression of basic fibroblast growth factor (FGF) 2 and its receptor FGFR-1 in human prostate cancer. *Clinical cancer research : an official journal of the American Association for Cancer Research* **5**, 1063-1071.

107. Ozen, M., Giri, D., Ropiquet, F., Mansukhani, A., and Ittmann, M. (2001) Role of fibroblast growth factor receptor signaling in prostate cancer cell survival. *Journal of the National Cancer Institute* **93**, 1783-1790

108. Devilard, E., Bladou, F., Ramuz, O., Karsenty, G., Dales, J. P., Gravis, G., Nguyen, C., Bertucci, F., Xerri, L., and Birnbaum, D. (2006) FGFR1 and WT1 are markers of human prostate cancer progression. *BMC cancer* **6**, 272

109. Wang, J., Stockton, D. W., and Ittmann, M. (2004) The fibroblast growth factor receptor-4 Arg388 allele is associated with prostate cancer initiation and progression. *Clinical cancer research : an official journal of the American Association for Cancer Research* **10**, 6169-6178

110. Li, Z. G., Mathew, P., Yang, J., Starbuck, M. W., Zurita, A. J., Liu, J., Sikes, C., Multani, A. S., Efstathiou, E., Lopez, A., Wang, J., Fanning, T. V., Prieto, V. G., Kundra, V., Vazquez, E. S., Troncoso, P., Raymond, A. K., Logothetis, C. J., Lin, S. H., Maity, S., and Navone, N. M. (2008) Androgen receptor-negative human prostate cancer cells induce osteogenesis in mice through FGF9-mediated mechanisms. *The Journal of clinical investigation* **118**, 2697-2710

111. Wang, F., McKeehan, K., Yu, C., Ittmann, M., and McKeehan, W. L. (2004) Chronic activity of ectopic type 1 fibroblast growth factor receptor tyrosine kinase in prostate epithelium results in hyperplasia accompanied by intraepithelial neoplasia. *The Prostate* **58**, 1-12

112. Song, Z., Powell, W. C., Kasahara, N., van Bokhoven, A., Miller, G. J., and Roy-Burman, P. (2000) The effect of fibroblast growth factor 8, isoform b, on the biology of prostate carcinoma cells and their interaction with stromal cells. *Cancer research* **60**, 6730-6736.

113. Giri, D., Ropiquet, F., and Ittmann, M. (1999) FGF9 is an autocrine and paracrine prostatic growth factor expressed by prostatic stromal cells. *Journal of cellular physiology* **180**, 53-60.

114. Polnaszek, N., Kwabi-Addo, B., Peterson, L. E., Ozen, M., Greenberg, N. M., Ortega, S., Basilico, C., and Ittmann, M. (2003) Fibroblast growth factor 2 promotes tumor progression in an autochthonous mouse model of prostate cancer. *Cancer research* **63**, 5754-5760

115. Valta, M. P., Tuomela, J., Bjartell, A., Valve, E., Vaananen, H. K., and Harkonen, P. (2008) FGF-8 is involved in bone metastasis of prostate cancer. *International journal of cancer. Journal international du cancer*

116. Teishima, J., Shoji, K., Hayashi, T., Miyamoto, K., Ohara, S., and Matsubara, A. (2012) Relationship between the localization of fibroblast growth factor 9 in prostate cancer cells and postoperative recurrence. *Prostate cancer and prostatic diseases* **15**, 8-14

117. Suttie, A., Nyska, A., Haseman, J. K., Moser, G. J., Hackett, T. R., and Goldsworthy, T. L. (2003) A grading scheme for the assessment of proliferative lesions of the mouse prostate in the TRAMP model. *Toxicologic pathology* **31**, 31-38

118. Xin, L., Ide, H., Kim, Y., Dubey, P., and Witte, O. N. (2003) In vivo regeneration of murine prostate from dissociated cell populations of postnatal epithelia and urogenital sinus mesenchyme. *Proceedings of the National Academy of Sciences of the United States of America* **100 Suppl 1**, 11896-11903

119. Qi, W., Gao, S., and Wang, Z. (2008) Transcriptional regulation of the TGF-beta1 promoter by androgen receptor. *The Biochemical journal* **416**, 453-462

120. Grisanzio, C., and Signoretti, S. (2008) p63 in prostate biology and pathology. *Journal of cellular biochemistry* **103**, 1354-1368

121. Humphrey, P. A. (2007) Diagnosis of adenocarcinoma in prostate needle biopsy tissue. *Journal of clinical pathology* **60**, 35-42

122. Teishima, J., Yano, S., Shoji, K., Hayashi, T., Goto, K., Kitano, H., Oka, K., Nagamatsu, H., and Matsubara, A. (2014) Accumulation of FGF9 in prostate cancer correlates with epithelial-to-mesenchymal transition and induction of VEGF-A expression. *Anticancer research* **34**, 695-700

123. Strand, D. W., Liang, Y. Y., Yang, F., Barron, D. A., Ressler, S. J., Schauer, I. G., Feng, X. H., and Rowley, D. R. (2014) TGF-beta induction of FGF-2 expression in stromal cells requires integrated smad3 and MAPK pathways. *American journal of clinical and experimental urology* **2**, 239-248

124. Yang, F., Tuxhorn, J. A., Ressler, S. J., McAlhany, S. J., Dang, T. D., and Rowley, D. R. (2005) Stromal expression of connective tissue growth factor promotes angiogenesis and prostate cancer tumorigenesis. *Cancer research* **65**, 8887-8895

125. Yang, F., Chen, Y., Shen, T., Guo, D., Dakhova, O., Ittmann, M. M., Creighton, C. J., Zhang, Y., Dang, T. D., and Rowley, D. R. (2014) Stromal TGF-beta signaling induces AR activation in prostate cancer. *Oncotarget* **5**, 10854-10869

126. Baca, S. C., Prandi, D., Lawrence, M. S., Mosquera, J. M., Romanel, A., Drier, Y., Park, K., Kitabayashi, N., MacDonald, T. Y., Ghandi, M., Van Allen, E., Kryukov, G. V., Sboner, A., Theurillat, J. P., Soong, T. D.,

Nickerson, E., Auclair, D., Tewari, A., Beltran, H., Onofrio, R. C., Boysen, G., Guiducci, C., Barbieri, C. E., Cibulskis, K., Sivachenko, A., Carter, S. L., Saksena, G., Voet, D., Ramos, A. H., Winckler, W., Cipicchio, M., Ardlie, K., Kantoff, P. W., Berger, M. F., Gabriel, S. B., Golub, T. R., Meyerson, M., Lander, E. S., Elemento, O., Getz, G., Demichelis, F., Rubin, M. A., and Garraway, L. A. (2013) Punctuated evolution of prostate cancer genomes. *Cell* **153**, 666-677

127. Hendrix, N. D., Wu, R., Kuick, R., Schwartz, D. R., Fearon, E. R., and Cho, K. R. (2006) Fibroblast growth factor 9 has oncogenic activity and is a downstream target of Wnt signaling in ovarian endometrioid adenocarcinomas. *Cancer research* **66**, 1354-1362

128. Matsumoto-Yoshitomi, S., Habashita, J., Nomura, C., Kuroshima, K., and Kurokawa, T. (1997) Autocrine transformation by fibroblast growth factor 9 (FGF-9) and its possible participation in human oncogenesis. *Int J Cancer* **71**, 442-450

129. Schmid, S., Bieber, M., Zhang, F., Zhang, M., He, B., Jablons, D., and Teng, N. N. (2011) Wnt and hedgehog gene pathway expression in serous ovarian cancer. *International journal of gynecological cancer : official journal of the International Gynecological Cancer Society* **21**, 975-980

130. Arai, D., Hegab, A. E., Soejima, K., Kuroda, A., Ishioka, K., Yasuda, H., Naoki, K., Kagawa, S., Hamamoto, J., Yin, Y., Ornitz, D. M., and

Betsuyaku, T. (2014) Characterization of the cell of origin and propagation potential of the fibroblast growth factor 9-induced mouse model of lung adenocarcinoma. *J Pathol*

131. Ohgino, K., Soejima, K., Yasuda, H., Hayashi, Y., Hamamoto, J., Naoki, K., Arai, D., Ishioka, K., Sato, T., Terai, H., Ikemura, S., Yoda, S., Tani, T., Kuroda, A., and Betsuyaku, T. (2014) Expression of fibroblast growth factor 9 is associated with poor prognosis in patients with resected non-small cell lung cancer. *Lung Cancer* **83**, 90-96
132. Todo, T., Kondo, T., Kirino, T., Asai, A., Adams, E. F., Nakamura, S., Ikeda, K., and Kurokawa, T. (1998) Expression and growth stimulatory effect of fibroblast growth factor 9 in human brain tumors. *Neurosurgery* **43**, 337-346
133. Chen, T. M., Shih, Y. H., Tseng, J. T., Lai, M. C., Wu, C. H., Li, Y. H., Tsai, S. J., and Sun, H. S. (2014) Overexpression of FGF9 in colon cancer cells is mediated by hypoxia-induced translational activation. *Nucleic Acids Res* **42**, 2932-2944
134. Jin, C., Wang, F., Wu, X., Yu, C., Luo, Y., and McKeehan, W. L. (2004) Directionally specific paracrine communication mediated by epithelial FGF9 to stromal FGFR3 in two-compartment premalignant prostate tumors. *Cancer research* **64**, 4555-4562